

Review

Hierarchical and comparative kinetic modeling of laminar flame speeds of hydrocarbon and oxygenated fuels

E. Ranzi ^{a,*}, A. Frassoldati ^a, R. Grana ^a, A. Cuoci ^a, T. Faravelli ^a, A.P. Kelley ^b, C.K. Law ^{b,c}^a Dipartimento di Chimica, Materiali e Ingegneria Chimica, Politecnico di Milano, Piazza Leonardo da Vinci 32, 20131 Milano, Italy^b Department of Mechanical and Aerospace Engineering, Princeton University, Princeton, NJ 08544, USA^c Center for Combustion Energy, Tsinghua University, Beijing 100084, China

ARTICLE INFO

Article history:

Received 4 March 2011

Accepted 15 March 2012

Available online 21 April 2012

Keywords:

Laminar flame speed

Detailed kinetics

Hydrocarbon fuels

Reference fuels

ABSTRACT

The primary objective of the present endeavor is to collect, consolidate, and review the vast amount of experimental data on the laminar flame speeds of hydrocarbon and oxygenated fuels that have been reported in recent years, analyze them by using a detailed kinetic mechanism for the pyrolysis and combustion of a large variety of fuels at high temperature conditions, and thereby identify aspects of the mechanism that require further revision. The review and assessment was hierarchically conducted, in the sequence of the foundational C₀–C₄ species; the reference fuels of alkanes (n-heptane, iso-octane, n-decane, n-dodecane), cyclo-alkanes (cyclohexane and methyl-cyclo-hexane) and the aromatics (benzene, toluene, xylene and ethylbenzene); and the oxygenated fuels of alcohols, C₃H₆O isomers, ethers (dimethyl ether and ethyl tertiary butyl ether), and methyl esters up to methyl decanoate. Mixtures of some of these fuels, including those with hydrogen, were also considered. The comprehensive nature of the present mechanism and effort is emphasized.

© 2012 Elsevier Ltd. All rights reserved.

Contents

1. Introduction	469
2. Kinetic model and numerical method	470
3. Comparison and model predictions	472
3.1. Small hydrocarbon species	472
3.1.1. Alkanes (CH ₄ , C ₂ H ₆ , C ₃ H ₈ , n-C ₄ H ₁₀ , iso-C ₄ H ₁₀)	472
3.1.2. Alkenes (C ₂ H ₄ , C ₃ H ₆ , nC ₄ H ₈ , iso-C ₄ H ₈)	478
3.1.3. Alkynes and dienes (C ₂ H ₂ , C ₃ H ₄ , 1,3-C ₄ H ₆)	479
3.2. Large hydrocarbon species	481
3.2.1. Primary reference fuels (n-heptane and iso-octane)	481
3.2.2. Cyclo-alkanes	482
3.2.3. Heavy normal-alkanes (n-decane and n-dodecane)	483
3.2.4. Aromatics	484
3.3. Alcohols and oxygenated species	486
3.3.1. Alcohols	486
3.3.2. Oxygenated species	487
3.4. Hydrocarbon mixtures	492
3.4.1. Hydrogen addition to C ₁ –C ₃ fuel-Air mixtures	492
3.4.2. Methane/ethylene mixtures	493
3.4.3. Primary reference fuel mixtures	493
3.4.4. Other hydrocarbon mixtures	493
4. Laminar flame speeds at constant flame temperature	495

* Corresponding author. Tel.: +39 2 23993250; fax: +39 2 70638173.

E-mail address: eliseo.ranzi@polimi.it (E. Ranzi).

5. Conclusions	495
Acknowledgments	495
References	498

1. Introduction

The laminar flame speed of a combustible mixture as a function of its thermodynamic states of temperature, pressure, and composition is a rigorously defined fundamental property of this mixture, embodying and thereby manifesting the net effects of its diffusivity, exothermicity, and reactivity. Consequently, it is also the elemental unit in the description of complex combustion phenomena such as the turbulent flame structure and speed, various modes of flame front instabilities, flame extinction through heat loss and stretch, and flame stabilization.

Although extensive experiments have been conducted to measure the laminar flame speeds of a wide variety of fuels, the early efforts, see e.g. [1], were however complicated by unrecognized and thereby unquantified stretch effects, leading to considerable and systematic scatter in the reported data. It was not until the mid-1980s when Wu and Law [2] noted the importance of these stretch effects in the experimental determination of laminar flame speeds, and proposed a rational approach towards their elimination. This has led to two notable consequences: the collapse of the subsequent experimental data to a much narrower range of scatter, and the use of these values, with moderate confidence, as an additional experimental input in the development of detailed reaction mechanisms of combustible mixtures.

To illustrate the significance of the first consequence, Fig. 1 shows the maximum laminar flame speeds of methane/air mixtures at atmospheric pressure and temperature, obtained by using a variety of experimental methods [3]. It is seen that while the early measurements varied by more than ± 25 cm/s, the scatter was reduced to less than about 8 cm/s after the work of Wu and Law [2], and was further reduced to less than ± 2 cm/s recently when additional understanding was gained on the non-linear nature of stretch on the flame speed [4,5].

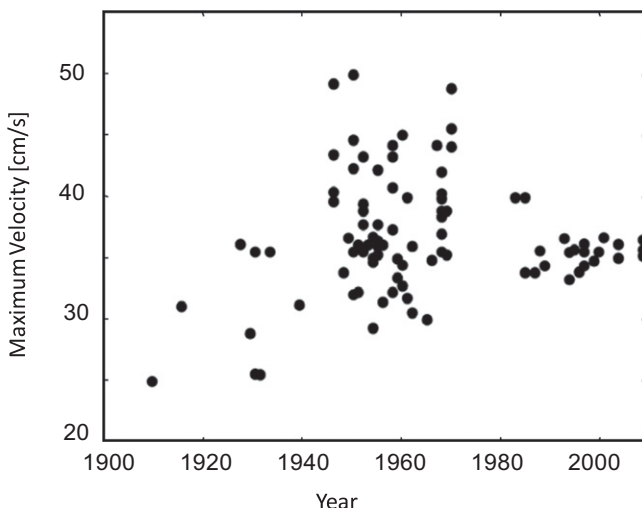


Fig. 1. Historical measurements of the maximum flame speed for methane/air mixtures at atmospheric pressure [3].

Regarding the second consequence, it is noted that the availability of accurately determined laminar flames speeds has assumed an added utility and hence significance in combustion research, as substantiated by Davis and Law [6] and Johnston and Farrell [7], in the extensive determination of their values for a wide range of fuels with stretch effects largely eliminated. Indeed, the recent enhanced activities in the experimental determination of laminar flame speeds and their use in kinetic modeling studies strongly testify to such recognition [7–17].

There are two objectives for the present work. First, it is recognized that a large body of experimental laminar flame speed data have been acquired recently for an extensive array of hydrocarbon fuels, and that the development of their reaction mechanisms has also progressed to the stage of moderate comprehensiveness. Since the last effort to assemble and review the data of laminar flame speeds was conducted almost twenty years ago [18], and since there have been substantial advance in terms of the accuracy in the acquisition of these data as well as the sophistication of the reaction mechanisms that have been developed to describe fuels oxidation, it is appropriate and timely to take stock, to consolidate them and assess the performance of the mechanisms in light of the wealth of the experimental data. Second, it is also of interest to conduct the review based on the hierarchical nature of hydrocarbon oxidation in terms of the size and functional complexity, and thereby provide guidelines for further improvement. In particular, sensitivity analysis shows that the most sensitive reactions pertinent to laminar flame speeds are largely similar for different hydrocarbons, especially for those of the same family. Nevertheless, fuel-specific reactions, such as those of chain initiation, recombination, and interactions between small radicals and stable species, also play appropriate roles. As such, comparison between experimental measurements and model predictions can identify deficiencies in the existing mechanisms, leading to further refinement.

In view of the above considerations, we have systematically collected the vast body of experimental laminar flame speeds and then compared them with calculated values, progressing from those of the small hydrocarbons to the reference species of gasoline and diesel fuels. The families of the fuels considered include alkanes, alkenes, alkynes, dienes, cyclo-alkanes, aromatics, alcohols, oxygenates, and mixtures of some of them.

It is also important to recognize that there are two major limitations in the rigor and scope of the present assessment. First, although it is reasonable to expect that while leading-order effects of stretch have been eliminated in the reported data, some degree of uncertainty may still exist in the rigor of the stretch correction, such as the accuracy of linear versus non-linear extrapolations and subtle aerodynamic effects [4]. These aspects are discussed in more detail in the Appendix. Second, in light of the various reaction mechanisms available in the literature [19–40], as a reference we shall confine the present kinetic modeling to the specific mechanism that was developed by the lead author of this paper and his associates, recognizing that this mechanism has been tested for various situations including those of low and high temperatures [41–43], and that the major kinetic pathways and the associated rate constants for various mechanisms are largely

similar anyway. We nevertheless also hasten to note that an alternate, competitively viable mechanism could have served equally well as the reference mechanism in the present assessment and comparison. This degree of flexibility basically reflects the current state of mechanism development for hydrocarbon oxidation, in that while the major elements constituting the mechanisms either appear to be largely in place or can be rationally postulated, there still exist considerable uncertainty and disagreement among these mechanisms that would affect their quantitative performance. Indeed, the attainment of quantitative predictability is a major, albeit long-term goal of fundamental combustion research at present, and its progress requires periodic, interim assessments of the state of the art, such as the present

effort, in order to identify and focus further directions and items of research. The mechanism [43,44] adopted here to evaluate and analyze the extensive amount of experimental data collected therefore provides a kinetic guideline useful to compare and unify flame speeds involving similar fuels and/or conditions from different sources.

2. Kinetic model and numerical method

The semi-detailed oxidation mechanism of hydrocarbons up to C₁₆ adopted herein [43,44], consisting of over 8000 reactions and more than 250 species, was developed based on hierarchical modularity (<http://creckmodeling.chem.polimi.it>). Thermochemical

Table 1
Sources of experimental data of laminar flame speeds.

Authors	Species investigated	Pressure (atm)	Temperature (K)	Measurement method	Ref.
Vagelopoulos and Egolfopoulos (1998)	CH ₄ , C ₂ H ₆ , C ₃ H ₈	1	298	Stagnation flow	[61]
Gu et al. (2000)	CH ₄	1, 5, 10	298, 360, 400	Spherical flame	[62]
Park et al. (2011)	CH ₄	1, 2, 4	298	Counterflow	[67]
Rozencan et al. (2002)	CH ₄	1, 2, 5, 10, 20, 40, 60	298	Spherical flame	[64]
Halter et al. (2010)	CH ₄ /H ₂ mixtures	1, 3, 5	298	Spherical flame	[66]
Kumar et al. (2008)	C ₂ H ₄	1	298, 360, 400, 470	Counterflow	[79]
Liu et al. (2010)	C ₂ H ₄ /CH ₄ mixtures	1, 2, 5	298	Spherical flame	[12]
Egolfopoulos et al. (1990)	CH ₄ , C ₂ H ₂ , C ₂ H ₄ , C ₂ H ₆ , and C ₃ H ₈	0.5, 1, 2	298	Counterflow	[59]
Bosschaart et al. (2004)	C ₁ –C ₄ alkanes	1	298	Flat burner	[8]
Jomaas et al. (2005)	C ₂ H ₂ , C ₂ H ₄ , C ₂ H ₆ , C ₃ H ₆ , C ₃ H ₈	1, 2, 5	298	Spherical flame	[65]
Hassan et al. (1998)	CH ₄ , C ₂ H ₄ , C ₂ H ₆ , C ₃ H ₈	0.5, 1, 2, 3, 4	298	Spherical flame	[60]
Davis and Law (1998)	C ₁ –C ₈ (alkane, alkenes, cycloalkane, aromatics)	1	298	Counterflow	[6]
Hirasawa et al. (2002)	C ₂ H ₄ , n-C ₄ H ₁₀ , toluene (pure and mixtures)	1	298	Counterflow	[63]
Bradley et al. (1998)	iC ₈	1, 2.5, 5, 7.5, 10	358, 400, 450	Spherical flame	[140]
Kumar et al. (2007)	nC ₇ –iC ₈	1	298, 360, 400, 470	Counterflow	[83]
Huang et al. (2004)	nC ₇ , iC ₈ , reformer gas and PRF	1	298	Counterflow	[84]
Ji et al. (2010)	C ₅ –C ₁₂ normal alkanes	1	353, 403	Counterflow	[76]
Kelley et al. (2011)	C ₅ –C ₈ normal alkanes	1, 2, 5, 10, 20	353	Spherical flame	[14]
Kelley et al. (2010)	iC ₈	1, 2, 5, 10	353	Spherical flame	[14]
Kumar et al. (2007)	nC ₁₀ –nC ₁₂	1	360, 400, 470	Counterflow	[89]
Johston and Farrell (2005)	Benzene, toluene, ethylbenzene, m-xylene, and n-propylbenzene	3	450	Spherical flame	[7]
Liu et al. (2011)	n-butanol, iso-butanol, methyl butanoate	1, 2	353	Spherical flame	[16]
Veloo and Egolfopoulos (2011)	Butanol isomers	1	343	Counterflow	[106]
Veloo et al. (2009)	Propanol isomers	1	343	Counterflow	[105]
Veloo and Egolfopoulos (2011)	Propanol isomers	1	343	Counterflow	[68]
Veloo et al. (2010)	C ₁ –C ₂ –C ₄ alcohols and alkanes	1	343	Counterflow	[17]
Burluka et al. (2010)	C ₃ H ₆ O isomers	1	298	Spherical flame	[114]
Pichon et al. (2009)	Acetone	1	298	Spherical flame	[115]
Daly et al. (2001)	Dimethyl ether	1	298	Spherical flame	[119]
Qin and Ju (2005)	Dimethyl ether	1	298	Spherical flame	[118]
Zhao et al. (2004)	Dimethyl ether	1	298	Stagnation flow	[160]
Yahyaoui et al. (2008)	Ethyl tertiary butyl ether	1	298	Spherical flame	[121]
Jerzembeck et al. (2009)	nC ₇ , iC ₈ , and PRF	10, 15, 20, 25	373	Spherical flame	[10]
Dooley et al. (2010)	Methyl formate	1	295	Spherical flame	[127]
Wang et al. (2011)	C ₄ –C ₁₀ methyl esters	1	403	Counterflow	[128]
Wu et al. (2011)	C ₂ H ₂ , C ₂ H ₄ , C ₂ H ₆ , C ₃ H ₈ with H ₂ addition	1, 5, 20	293	Spherical flame	[161]
Wu et al., 2011	Cyclohexane and mono-alkylated cyclohexane	1, 2, 5, 10, 20	353	Spherical flame	[87]
Ji et al., 2011	Benzene and alkylated benzene	1	353	Counterflow	[159]

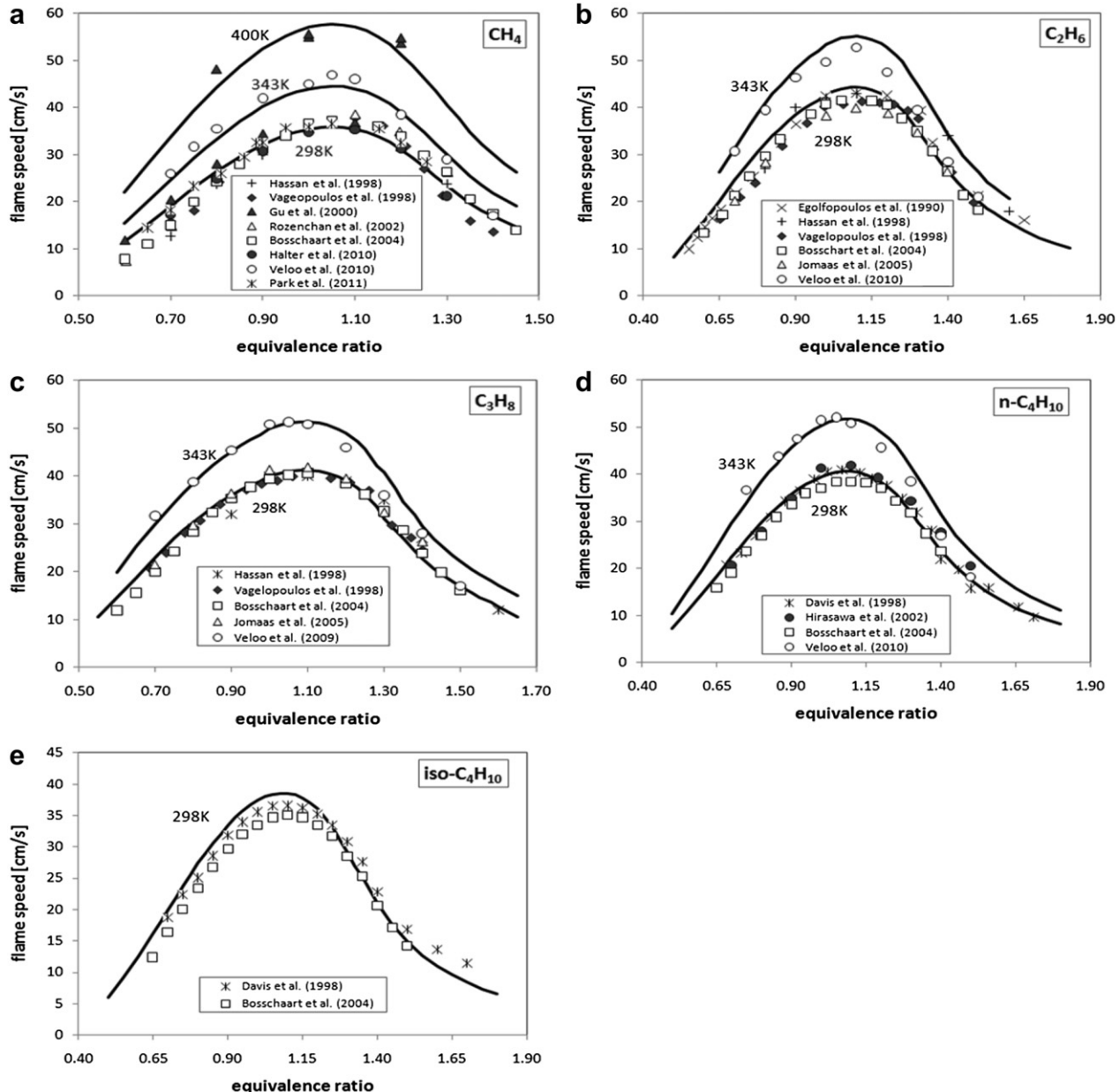


Fig. 2. Laminar flame speeds of small alkane flames in air at atmospheric pressure: (a) methane; (b) ethane; (c) propane; (d) n-butane; (e) iso-butane. See Table 1 for references of the experimental data.

data for most species were obtained from the CHEMKIN thermodynamic database [45] and from [46]. For those species whose thermodynamic data are not available in the literature, the group additive method was used to estimate these properties [47].

The complete high temperature mechanism, with thermodynamic and transport properties, is available in the CHEMKIN format as *Supplemental Materials*.

Laminar flame speeds were calculated for the steady, freely propagating, adiabatic flames in the doubly infinite domain, without radiative heat transfer while allowing for Soret diffusion. A mixture-averaged formula is used to compute multicomponent diffusion coefficients. The conservation equations with proper boundary conditions [48,49] were discretized by means of conventional finite differencing techniques with nonuniform mesh

spacing. Diffusive and convective terms use central and upwind differencing respectively.

All numerical simulations were performed with the Open-SMOKE code [50], which is an upgraded version and extension of the well-tested DSMOKE code [51]. The BzzMath 6.0 numerical library was adopted [52–54]. The mathematical model of laminar flame speed calculation results in a stiff and large system of algebraic equations, requiring particular attention to the numerical methods and solver routines. A modified global Newton method is applied to ensure complete convergence. Initial guess comes from the solution of the corresponding unsteady model solved through the BzzDAESystemSparseObject solver for banded block-tridiagonal systems.

The normalized flame speed sensitivity coefficient s_{S_L} is used instead of the raw coefficient S_{S_L} [48]:

$$S_{s_L} = \frac{\partial \ln s_L}{\partial \ln \alpha} = \frac{\alpha \partial S_L}{S_L \partial \alpha} = \frac{\alpha}{S_L} S_{s_L}$$

where s_L is the calculated mass flow rate and α the generic frequency factor.

3. Comparison and model predictions

The high temperature flame chemistry that governs the propagation of laminar flames has a hierarchical dependence on the chemistry of small fuel molecules, arising from the fuel decomposition pathways that result in small fuel fragments which in turn are oxidized in the main reaction zone of the flame. Consequently chemical kinetic mechanisms must be hierarchically validated moving from the H₂/CO mechanism [55–57]. Since Frassoldati et al. [58] have already discussed the flame speeds of the H₂ and syngas mixtures, we shall then sequentially study the following systems:

- 1) Small hydrocarbon species (alkanes, alkenes, alkynes, dienes)
- 2) Large hydrocarbon species
 - a. Linear and branched alkanes (n-heptane, n-decane, n-dodecane, iso-octane)
 - b. Cyclo-alkanes
 - c. Aromatics
- 3) Alcohols and oxygenated species
- 4) Hydrocarbon mixtures

The small hydrocarbon species investigated represent the fragments typically formed in fuel decomposition. The large hydrocarbons and alcohols are typical of the component classes found in practical fuels and emerging alternative fuels. The addition of hydrocarbon mixtures in the mechanism validation represents the chemical interaction of fuel components and decomposition products found in practical fuels.

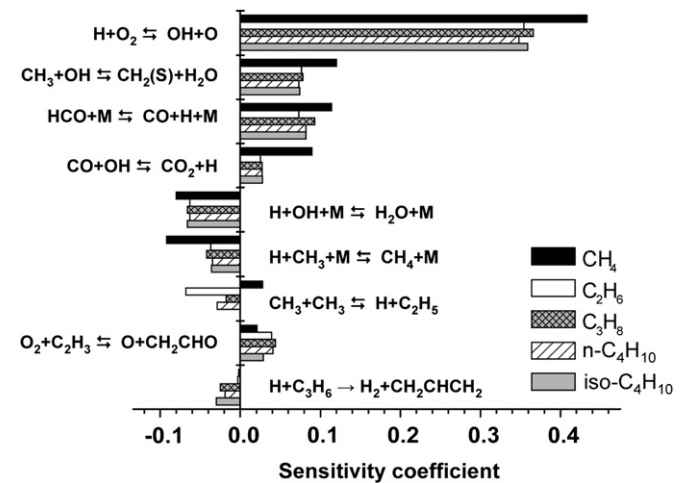
To impose an additional constraint on the kinetic model, laminar flame speeds at elevated pressures are compared where experimental data are available; noting that elevated pressure increases three-body collisions which could lead to significant changes in the dominant chemistry. Table 1 summarizes the experimental conditions collected and used in this study. The numerical values of all the experimental laminar flame speeds used in the present study are given in the **Supplemental Materials** of this paper.

3.1. Small hydrocarbon species

3.1.1. Alkanes (CH₄, C₂H₆, C₃H₈, n-C₄H₁₀, iso-C₄H₁₀)

Fig. 2 compares the experimental and calculated atmospheric laminar flame speeds of alkanes from CH₄ up to the C₄H₁₀ isomers [6,8,17,59–68]. The results show that ethane and methane respectively have the highest and lowest flame speeds, and that the branched species have lower flame speeds than the unbranched ones. The comparison can be considered to be close, with the experimental values for very rich methane flames being somewhat smaller, and those for the ethane flames being uniformly higher. The effect of the initial temperature is adequately captured. It is also noted that the experimental measurements of Veloo and Egolfopoulos [68] and Veloo et al. [17] for propane and butane peak on the lean side of other reported experimental measurements.

We next note that Babushok and Tsang [69] observed and discussed strong similarities among the alkane/air flames, and analyzed their relative sensitivity coefficients. It was demonstrated that most reactions with positive sensitivities correspond to those that produce the hydrogen atom, while negative sensitivity coefficients correspond to those consuming them. Fig. 3 shows the



sensitivity coefficients of laminar flame speeds on the reaction rate coefficients for these flames at $\Phi = 1$ and atmospheric pressure, showing that the most sensitive reactions are those associated with the H₂/CO sub-system.

Large positive coefficients are exhibited by the following reactions:



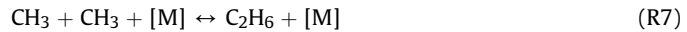
The first reaction is chain branching, hence having a positive coefficient. The second and third reactions, while chain carrying, produce the H radicals needed by the first reaction and therefore also have positive coefficients. The recombination reaction:



has a large negative coefficient due to chain termination. Furthermore, formation of the singlet methylene radical via OH and methyl radical interaction shows a positive effect for all the fuels:



The reactions:

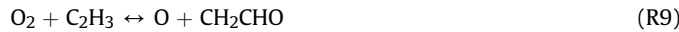


indicate negative sensitivity for both k_0 and k_∞ . The reaction:



is fuel-specific in that it promotes the reactivity of methane by forming the H and ethyl radicals (C₂H₅) from methyl recombination, while it has a large negative effect on the ethane flame by promoting the formation of the methyl radical. A similar negative effect is also observed for n-butane flames.

The branching reaction of the vinyl radical (C₂H₃) with oxygen to form the CH₂CHO radical:



has a positive impact, and is more relevant when large ethylene yields are obtained. Different reaction channels of the vinyl radical and O_2 interactions, to form acetylene and HO_2 , formaldehyde and HCO , and ketene and OH , do not show significant sensitivity coefficients for the analyzed conditions.

Successive H-abstraction reactions on propylene, formed in propane and butane flames, give rise to allyl radicals (aC_3H_5 , i.e. CH_2CHCH_2) with a negative impact on the corresponding flame speeds.

A more direct comparison of the laminar flame speeds of methane and n-alkanes at the same temperature and pressure conditions shows that the methane flame is the slowest, while the

ethane flame is the fastest one, and propane and n-butane flame speeds have intermediate reactivity and are very similar to each other. A similar reactivity behavior is also observed in high temperature shock tube ignition studies [70]. At shock tube temperatures, after the initial period of radical generation, the exponential growth in the radical pool is dominated by reaction (R1), with a sharp temperature increase. The shock experiments reported by Burcat et al. [71] for the ignition of stoichiometric mixtures of n-alkanes in oxygen/argon clearly indicate that methane ignites the slowest, ethane the fastest, and propane and n-butane have intermediate and similar reactivity. Kinetic modeling shows that methyl radicals, formed from H atom abstraction from methane, mainly lead to chain termination through reaction (R7) and thereby causes the slow ignition of methane. Ethane is most

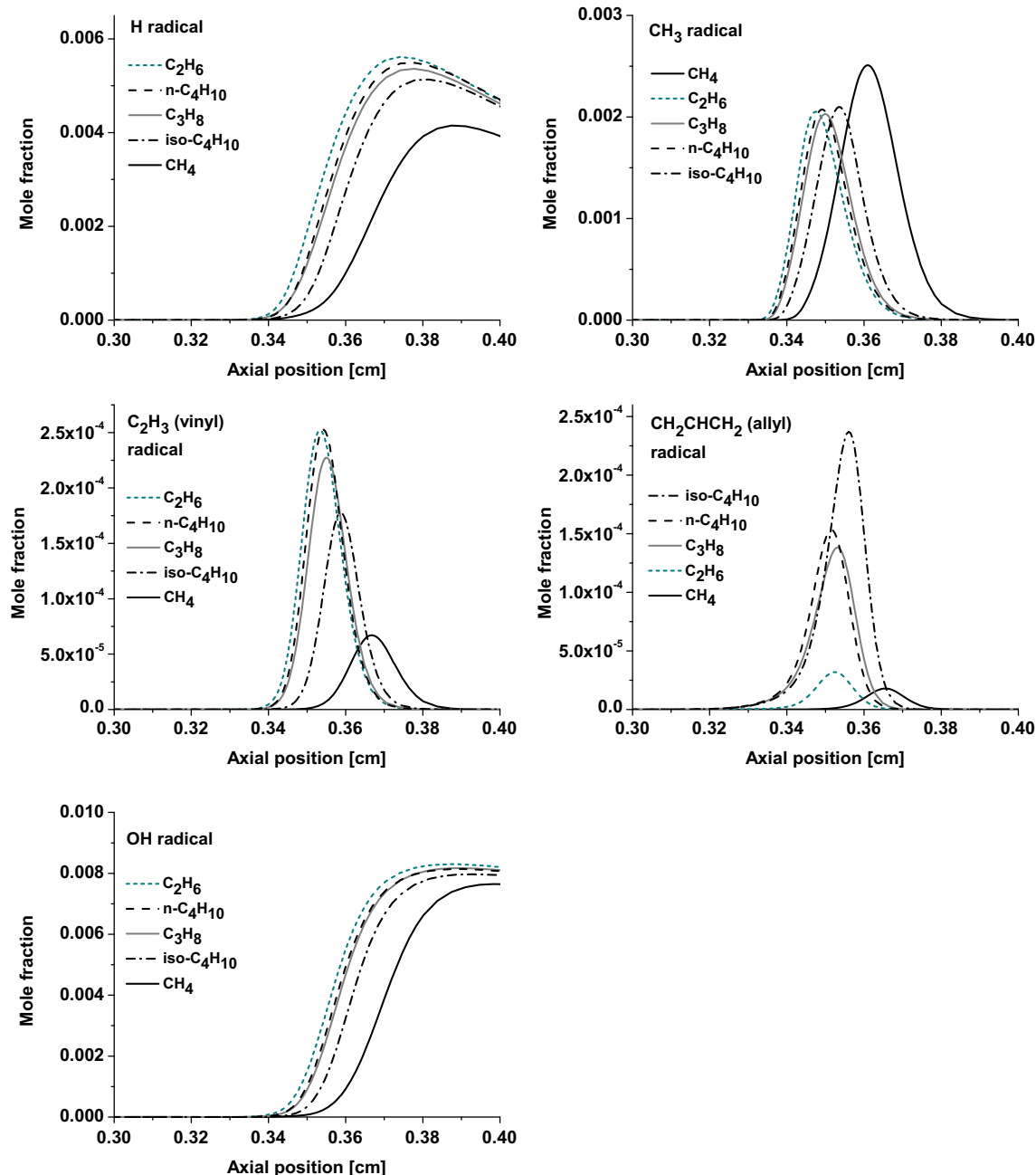
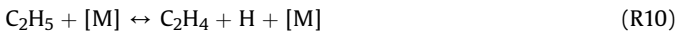
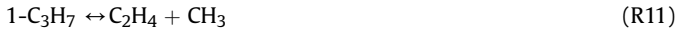


Fig. 4. Laminar air-stoichiometric flames of small hydrocarbons ($T_0 = 298 \text{ K}$, $P = 1 \text{ atm}$). Predicted profiles of relevant radicals: H, CH_3 , Vinyl, Allyl, and OH.

reactive because the ethyl radical, formed via H-abstraction from ethane, produces an H atom via the dehydrogenation reaction:



For higher n-alkanes, the different alkyl radicals produce both H and CH₃ radicals that promote chain branching through reaction (R1) and chain termination through reactions (R6) and (R7). For example, 1- and 2-propyl radicals from propane mainly decompose through:



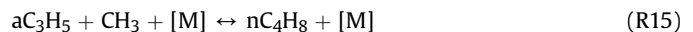
These two steps confirm that propane produces a mixture of H and CH₃ radicals, as is also the case with n-butane:



Thus, methane and ethane represent extremes of reactivity, while larger alkanes have intermediate ignition properties and reactivity due to their mixed production of H and CH₃ radicals.

The structures of the atmospheric and air-stoichiometric flames of the five small alkanes are analyzed in Fig. 4 by comparing the mole fraction profiles of the relevant radical species: hydrogen, methyl, vinyl, allyl and OH. As expected, model predictions confirm that the methane flame has the highest methyl and lowest hydrogen

radical formation, with a laminar flame speed of ~36 cm/s. Except for the methane flame, the H radical mole fractions peak from 0.005 to 0.0055 cm in different flames, while the methyl radical mole fractions are always close to ~0.002 cm, with adiabatic flame temperatures ranging from 2268 K to 2280 K. The ethane flame shows the highest H fraction and the iso-butane flame the lowest one, corresponding to the highest and lowest flame speeds, 43 cm/s and 36.5 cm/s, respectively. Vinyl and allyl radical fractions in the different flames further help to better understand the difference in laminar flame speeds. Parallel to the slightly higher H radical formation, the ethane flame is also characterized by the lowest allyl and the highest vinyl formation. The branching reaction (R9) of the vinyl radical, together with the moderate effect of the allyl recombination reactions:



further explain the highest flame speed of ethane. The similarity of propane and n-butane flame speeds agrees well with the similar concentrations of all these radicals. Finally, iso-butane produces, together with low H and vinyl concentrations, a very high concentration of allyl radical formed by the H-abstraction on propylene. In fact, the β-decomposition of the isobutyl radicals:

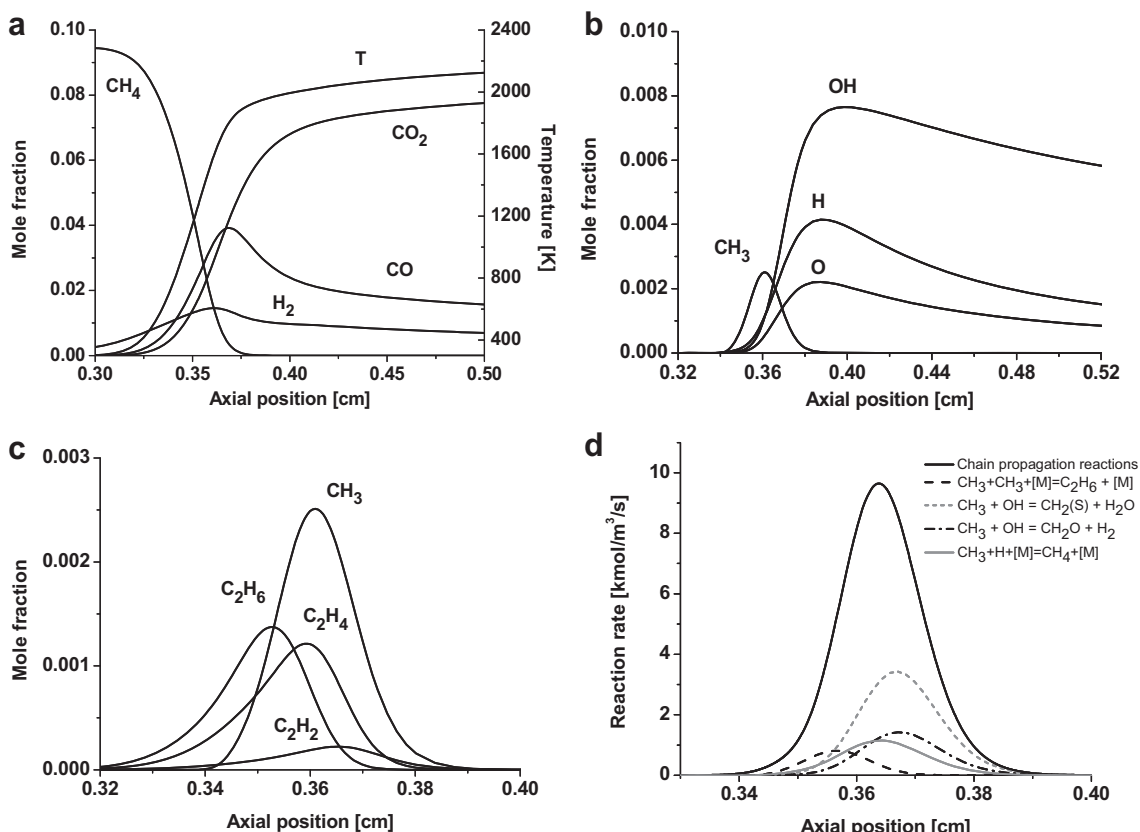


Fig. 5. Structure of the air-stoichiometric methane flame. Panels a, b and c: Structure of the flame and profiles of relevant species and radicals. Panel d: Rate of production analysis of methyl radical.

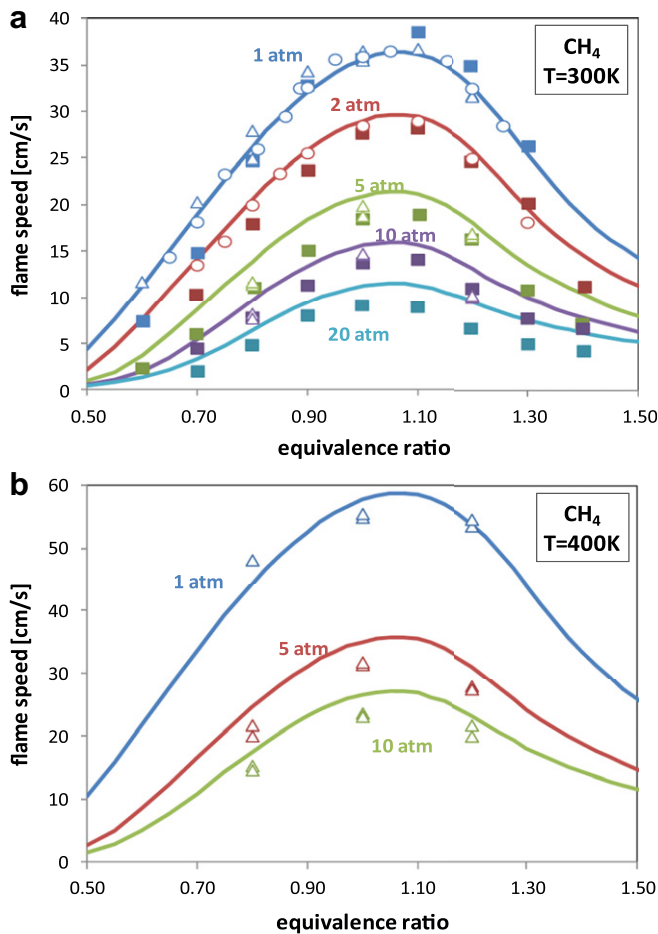


Fig. 6. Pressure effect on laminar flame speeds of CH_4 in air at 300 K and 400 K: Δ [62]; ■ [64]; ○ [67].

forms propylene and isobutene. The successive H-abstraction reactions on alkenes form resonantly stabilized allyl and methyl-allyl radicals, which participate significantly in the recombination reactions. H-abstraction reactions on n-butene mainly form the resonant but-2-en-1-yl radical ($\text{CH}_2\text{CH}=\text{CHCH}_3$: aC₄H₇), while H abstractions on isobutene form the 2-methyl-allyl radical iC₄H₇.

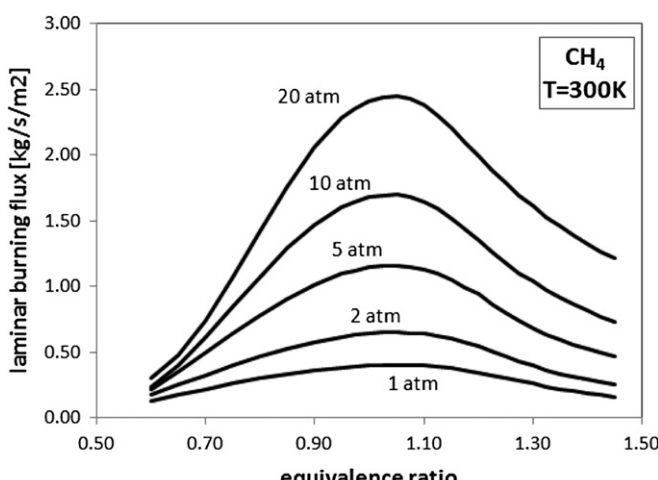


Fig. 7. Predicted laminar burning flux for methane/air mixtures at $T = 300$ K.

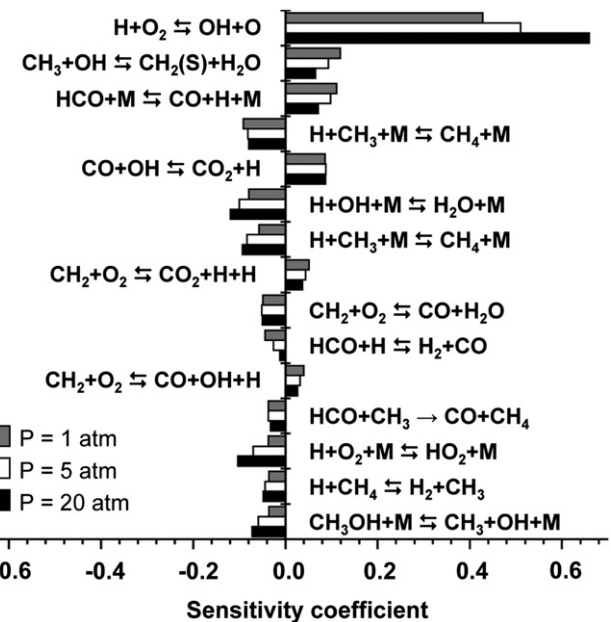


Fig. 8. Sensitivity coefficients of laminar flame speed on reaction rate coefficients, for CH_4/air flames at $\Phi = 1$ and different pressures.

Moreover, the H addition reactions on alkenes result in a scavenging effect due to the successive dealkylation reactions (R11) and (R17), hence further explain the low reactivity of iso-butane.

The different behavior of the H and OH radical profiles as compared to those of the remaining radicals deserves further consideration. Thus, Panel a of Fig. 5 shows a more complete picture of the structure of the stoichiometric methane/air flame. It is seen that CH_4 decomposition and the initial CO formation take place at the front of the flame structure, while the successive CO conversion and CO_2 formation mainly take place in the trailing portion of the flame. Once the fuel is mostly decomposed, hydrocarbon radicals disappear and only the H, OH and O radicals further propagate and complete the reaction chain (Panel b). CO conversion, through reaction (R3), is the final and slow step in the overall combustion process. Panel a also shows the temperature profile and the relevant H₂ back diffusion across the flame. Panels c and d highlight the importance of the methyl radical recombination with ethane

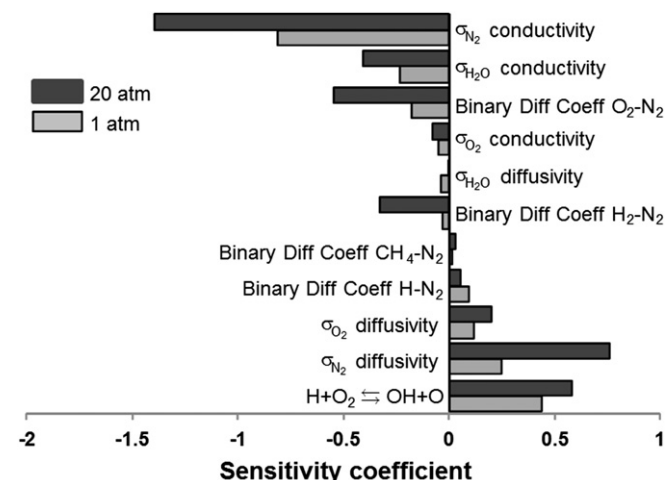


Fig. 9. Sensitivity coefficients of laminar flame speed on transport properties, for CH_4/air flames at $\Phi = 1$ and different pressures.

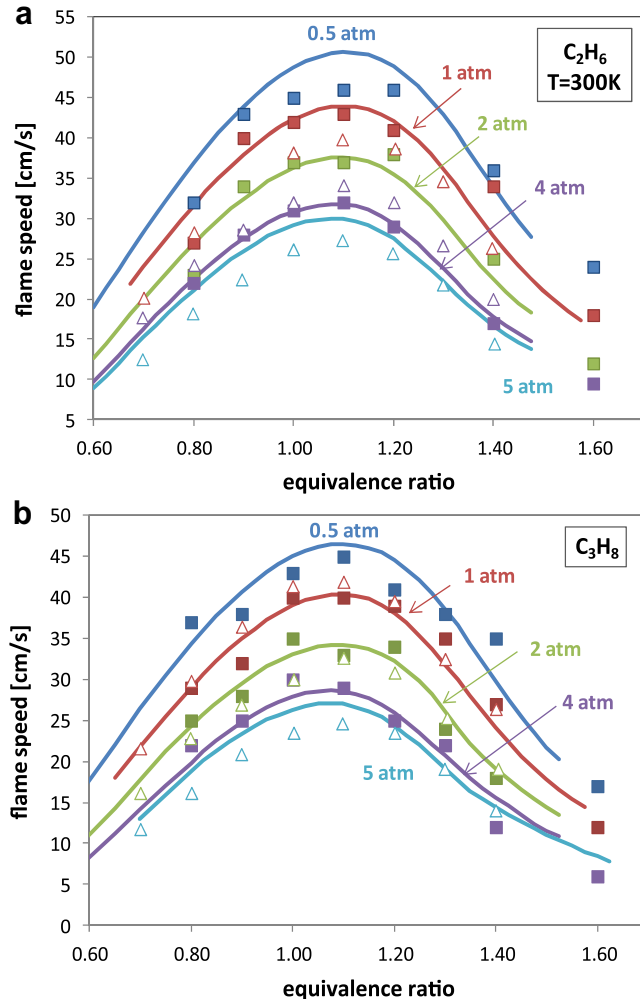


Fig. 10. Pressure effect on laminar flame speeds of C_2H_6 and C_3H_8 in air at 298 K : ■ [60]; △ [65]; ▲ [65].

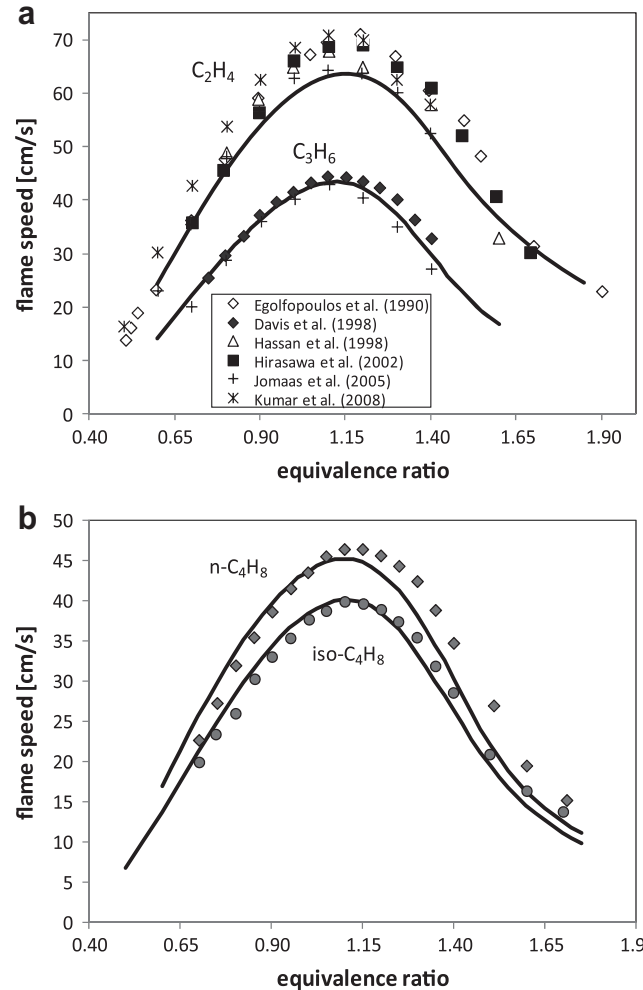


Fig. 11. Laminar flame speeds of small alkenes in air at $T_0 = 298\text{ K}$ and atmospheric pressure [6,8,59,60,65,79].

formation, as already well discussed by Warnatz [72]. The successive dehydrogenation reactions of ethane to form ethylene and acetylene are well characterized by the sequence of the peaks along the flame. The rate production analysis of Panel d indicates that the methyl radical is mostly formed via H-abstraction reactions, with the prevailing role of OH radicals, followed by H and O radicals, with similar importance. Methyl radical is then transformed by OH into the singlet methylene radical with reaction (R5) or recombines with methyl and H radicals to form ethane and methane, with reactions (R7) and (R6), respectively. The formation of formaldehyde with the reaction



is also an important oxidation path. The formaldehyde produced in reaction (R19) subsequently forms the formyl radical HCO via H abstraction, hence constituting an important contribution to the H formation.

Finally, Panel d of Fig. 5 shows that the recombination reaction (R7) is mostly effective at low temperatures, and that CH_3 interaction with OH dominates at higher temperatures where the OH concentration becomes more significant. As already observed by Law [73], this flame structure and combustion behavior is quite general for hydrocarbon fuels. The initial fuel breakdown always

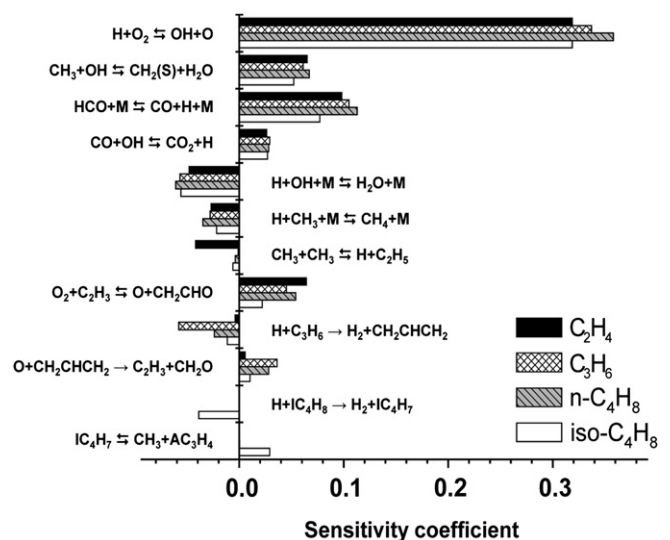


Fig. 12. Sensitivity coefficients of laminar flame speed on reaction rate coefficients, for small alkenes/air flames at $\Phi = 1$ and atmospheric pressure.

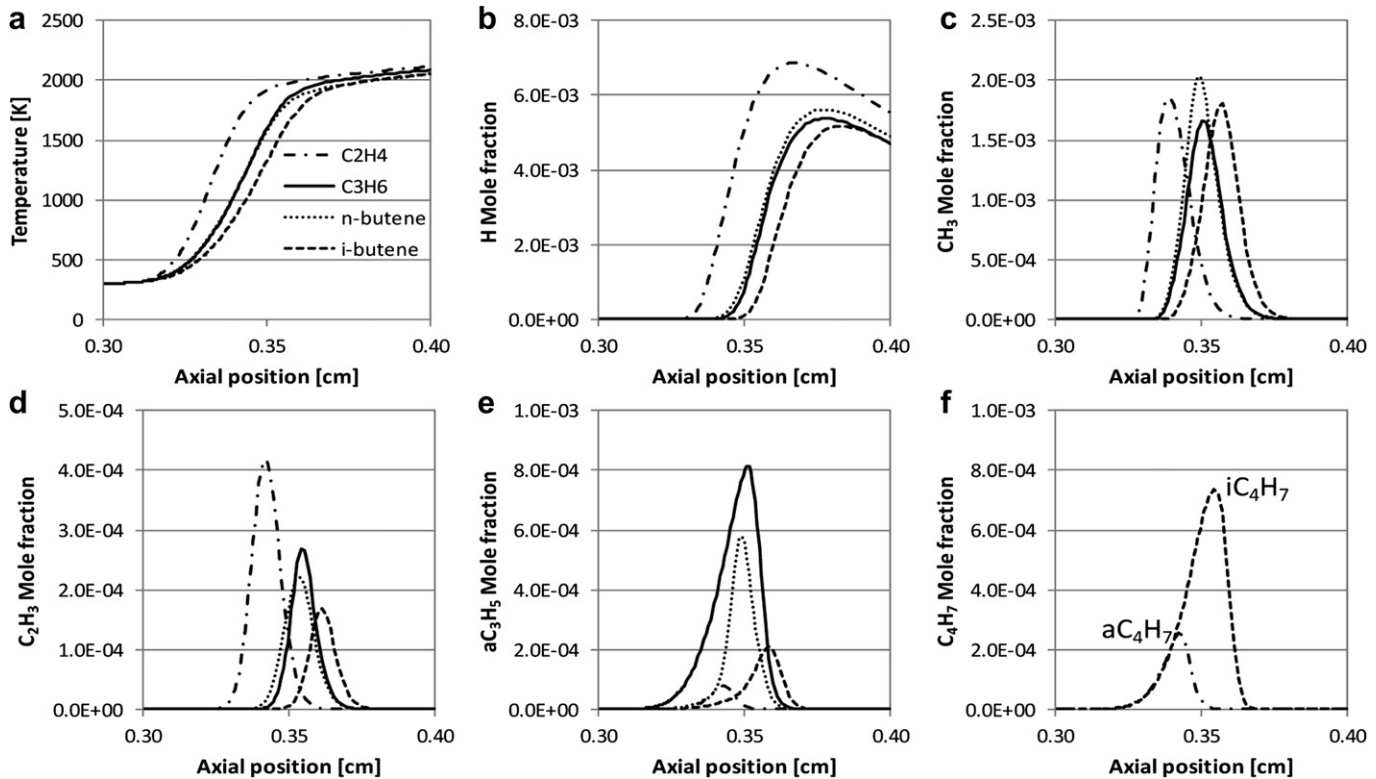


Fig. 13. Structure of the air-stoichiometric flames of small alkenes at $T_0 = 298$ K. Panel a: Temperature profiles. Panels b–f: Profiles of relevant radicals: H, CH₃, Vinyl, Allyl and Methyl-allyl.

leads to similar smaller species and radicals. The comprehensive understanding of the flame behavior and structure is then strongly hierarchical in that mechanisms for the oxidation of heavier fuels contain within them the sub-mechanisms of methane and the simpler molecules.

Fig. 6 compares the experimental laminar flame speeds of CH₄ [62,64,67] with the model predictions, at pressures up to 20 atm, showing adequate agreement. Since the relevant quantity for comparison of the kinetic effects of pressure is the laminar burning flux [73], which is the product of the upstream density and the laminar flame speed, and is the proper parameter to indicate the influence of reaction and transport, the data of Fig. 6a are re-plotted as the laminar burning flux in Fig. 7. It is seen that the laminar burning flux increases with pressure – a trend that is expected to hold for most mixtures except for the very weakly burning ones, demonstrating that the increase in density with pressure dominates over the retarding effect exerted by the increased influence of the three-body termination reactions, relative to the two-body carrying and branching reactions, as shown in the sensitivity plots of Fig. 8.

As already discussed by Westbrook and Dryer [74] as well as by Glassman and Yetter [75] regarding this pressure trend, the key chain branching reaction in any hydrogen containing system is reaction (R1). Any process that reduces the H atom concentration and any reaction that competes with (R1) for H atoms will reduce the overall oxidation rate and thereby inhibit the combustion process. In particular, the third-order reaction



competes directly with (R1) and has a stronger pressure dependence. As pressure increases, (R20) inhibits the overall reaction and reduces the flame speed. For pressures below atmospheric, (R20) does not compete effectively with (R1) and any

decrease due to (R20) is compensated by a rise in temperature and there is only a very small reduction in the flame speed. At higher pressures, however, the reduction in the flame speed with increasing pressure becomes more pronounced. Specifically, the three-body reaction (R20) competes more effectively with the two-body reaction (R1) above 1 atm, resulting in a steeper decline in the flame speed. Since the kinetic trend with pressure exists for all hydrocarbons, the same pressure effect on the laminar flame speed exists for all such fuels. The importance of the different third-order reactions is well evident in the sensitivity plots of Fig. 8.

Fig. 9 ranks the sensitivity coefficients of stoichiometric methane/air flame speeds (at 1 and 20 atm and 298 K) on the transport properties. The kinetics is represented by the most important branching reaction (R1), whilst the conductivity and diffusivity are analyzed through the collision radius. As expected, the flame propagation is very sensitive to the N₂ conductivity, followed by the diffusion coefficient of N₂ with respect to the total gas mixture; note that the negative sensitivity coefficient to the collision radius means that higher conductivity or diffusivity increase the flame speed, such that the conductivity and diffusivity decrease as the collision radius increases. The major contribution to the N₂ diffusion in the mixture originates from the O₂-N₂ binary diffusion coefficient and a significant role is also played by the H₂-N₂ binary coefficient, whilst the flame speed is not sensitive to that of CH₄-N₂. These results confirm what was already observed in Ji et al. [76]. It is also noted that even though the burning rate is more sensitive to transport properties than to kinetic parameters, the uncertainties in the transport properties are much lower than those of the kinetic parameters.

Fig. 10 compares the laminar flame speeds of C₂H₆ and C₃H₈ [60,65] at pressures from 0.5 to 5 atm. The calculation agrees relatively well with the experimental measurements of Hassan et al. [60] except for a slight overprediction of ethane at 0.5 atm. The

experimental measurements of Jomaas et al. [65] are uniformly lower than those of Hassan et al. [60] for ethane. Their measurements for propane are however within the experimental uncertainty and are seen to be both reasonably well predicted by the present mechanism, indicating that the elevated pressure chemistry is well represented.

The reader is referred to [77] and [78] for additional data on the laminar flame speeds of small alkanes and their mixtures, which show similar trends as those discussed above and as such do not need to be separately presented.

3.1.2. Alkenes (C_2H_4 , C_3H_6 , nC_4H_8 , $iso-C_4H_8$)

Fig. 11a shows the laminar flame speeds of C_2H_4 and C_3H_6 . Since the adiabatic flame temperatures of stoichiometric ethylene and propylene flames are ~ 2375 K and ~ 2345 K, respectively, the difference in the flame speeds are thus mainly of kinetic nature. Sensitivity analysis, shown in Fig. 12, reveals the importance of the reaction of the vinyl radical with oxygen in ethylene flames. The H and OH abstraction from propylene to form the resonantly stabilized allyl radicals reduces the propylene flame speed. The present mechanism shows good agreement with the outwardly propagating flame measurements of Hassan et al. [60] and Jomaas et al. [65], but underpredicts the measurements using the counterflow measurements [59,63,79]. Propylene, on the other hand, shows very good agreement with the two experimental datasets.

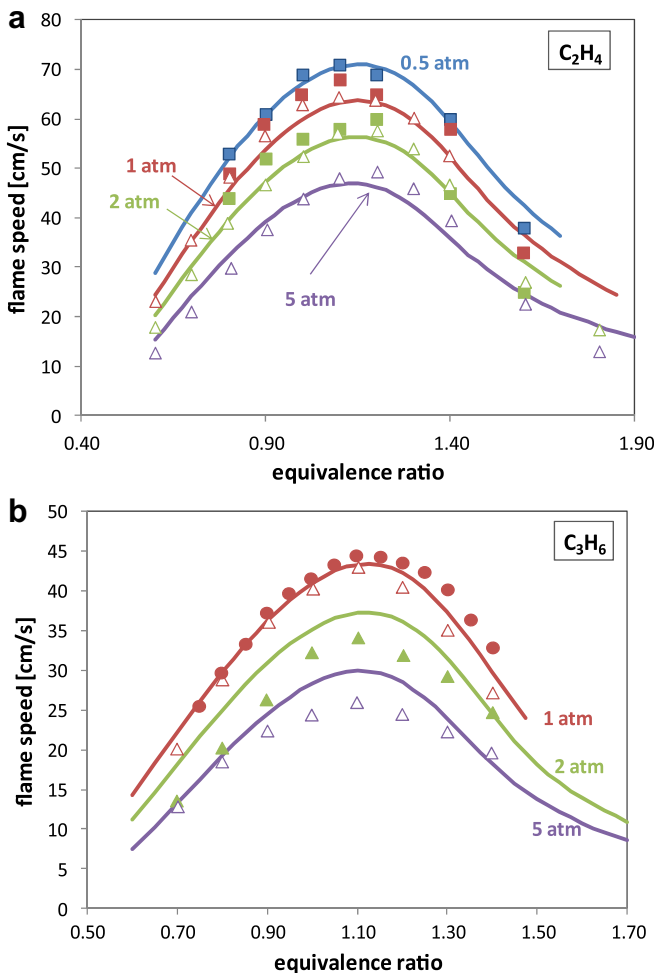


Fig. 14. Pressure effect on laminar flame speeds of C_2H_4 (panel a) and C_3H_6 (panel b) in air at 298 K: ■ [60]; △ [65]; ● [6].

Fig. 11b compares the flame speeds of nC_4H_8 and $iso-C_4H_8$; the reduced reactivity of branched species is again evident. It is seen that while the model predictions are good in lean conditions, there are deviations for 1-butene in rich conditions.

Fig. 12 shows the sensitivity coefficients of the laminar flame speeds of these alkene/air flames. One notes the positive effect of the vinyl radical in all the flames and the negative effect of the allyl radical in propylene and n-butene flames. The analysis also shows the fuel-specific 2-methyl-allyl radical reactions in isobutene flames.

Fig. 13 shows a detailed analysis of the predictions of the stoichiometric atmospheric alkenes/air flames at $T_0 = 298$ K. The flame speed of ethylene is ~ 60 cm/s while those of propylene and n-butene are close to 41 cm/s. Furthermore, the isobutene flame is the slowest, at ~ 36 cm/s, with an adiabatic flame temperature of ~ 2320 K. The H radical concentrations are in the same order as that of the flame speeds, thus confirming its role in these flames. Propylene and n-butene flames, with similar concentrations of H, CH_3 , and C_2H_3 radicals, mainly differ in the formation of allyl and methyl-allyl radicals. Specifically, the allyl radical is the primary product from H-abstraction reactions on propylene [80]:

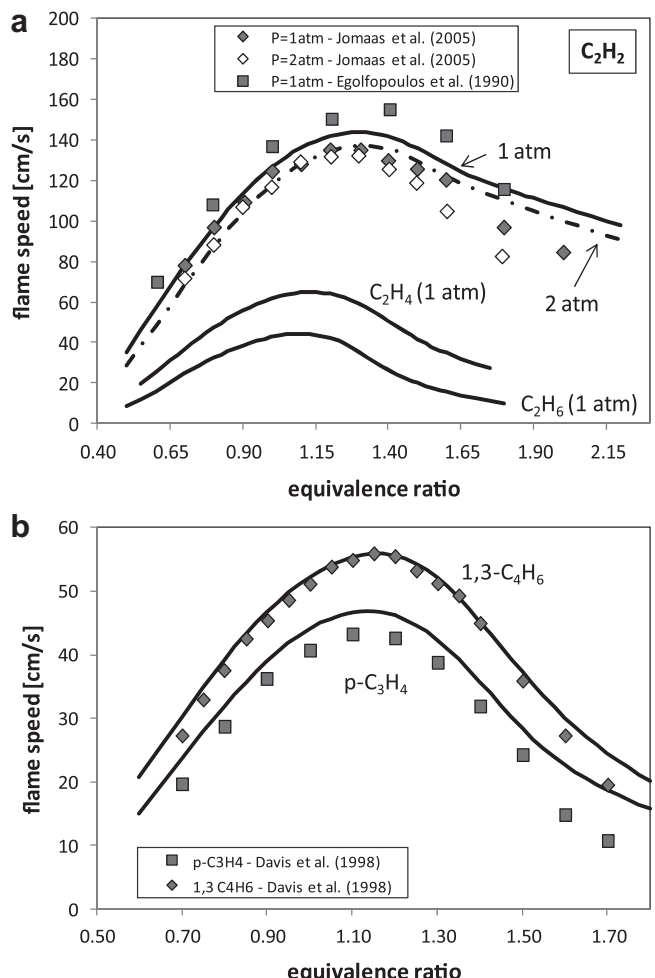


Fig. 15. Laminar flame speed of alkynes and butadiene in air at $T_0 = 298$ K and atmospheric pressure: (a) flame velocity of C_2H_2 ; (b) flame velocity of pC_3H_4 (18% oxygen in the oxidizer) and $1,3-C_4H_6$ [6,59,65].

while it is mainly the product of the initiation reaction of n-butene decomposition



Apart from the lowest H and C₂H₃ radical concentrations, the lowest reactivity of isobutene is further explained by the high concentration of the very stable 2-methyl-allyl radical (iC₄H₇), which is the primary product of the H-abstraction reaction:



The successive decomposition reaction of 2-methyl-allyl radical forms allene or the propadiene (aC₃H₄) and CH₃ radicals:



This reaction competes with the recombination reaction:



thus showing a positive sensitivity coefficient in Fig. 12.

Fig. 14a shows the laminar flame speeds of C₂H₄ at different pressures [60,65]. Further experimental data on the pressure effect on the laminar ethylene/air flames [12] are analyzed and discussed later in relation to fuel mixtures. Fig. 14b shows the laminar flame speeds of C₃H₆ at different pressures. The model agrees well with the measurements of Davis and Law [6], while consistently over predicts the measurements of Jomaas et al. [65]. This, however, does not imply that the data of the former is more accurate as the model itself could also carry some degree of inaccuracy which leads to over-predictions.

3.1.3. Alkynes and dienes (C₂H₂, C₃H₄, 1,3-C₄H₆)

Fig. 15 compares the laminar flame speeds of C₂H₂, C₂H₄ and C₂H₆. The model properly captures the different reactivities of these species. There are two sets of laminar flame speeds of acetylene at 1 atm [59,65]. These experimental data agree well in lean conditions, while they are significantly scattered for rich conditions. The predictions fall in between these two experimental datasets. The flame speeds of acetylene are more than twice those of ethylene and three times those of ethane. At atmospheric pressure and 298 K, the laminar flame speeds of their air-stoichiometric flames are 128 cm/s, 62 cm/s, and 43 cm/s, respectively, while the corresponding, adiabatic flame temperatures are ~2550 K, ~2375 K, and ~2270 K respectively. The large differences in the flame temperatures then partially explain the large variations in the flame speeds.

Fig. 16 shows a more complete picture of the flame front and radical profiles in the air-atmospheric flames of acetylene, ethylene and ethane, at 1 atm and T₀ = 298 K. The acetylene flame shows the highest hydrogen concentration and the lowest methyl radical concentration. On the contrary the ethane flame exhibits the lowest hydrogen concentration and the highest methyl radical concentration. The ethylene flame has intermediate values for both these radicals, while showing the highest concentration of the vinyl radical. The higher laminar flame speeds of C₂H₂ and C₂H₄ are further supported by the higher concentrations of the formyl and singlet methylene radicals, mainly in the acetylene flame. The highest CH₂(S) radical formation in the acetylene flame is mainly obtained through the ketenyl (HCCO) radical that is promptly formed from direct oxidation:

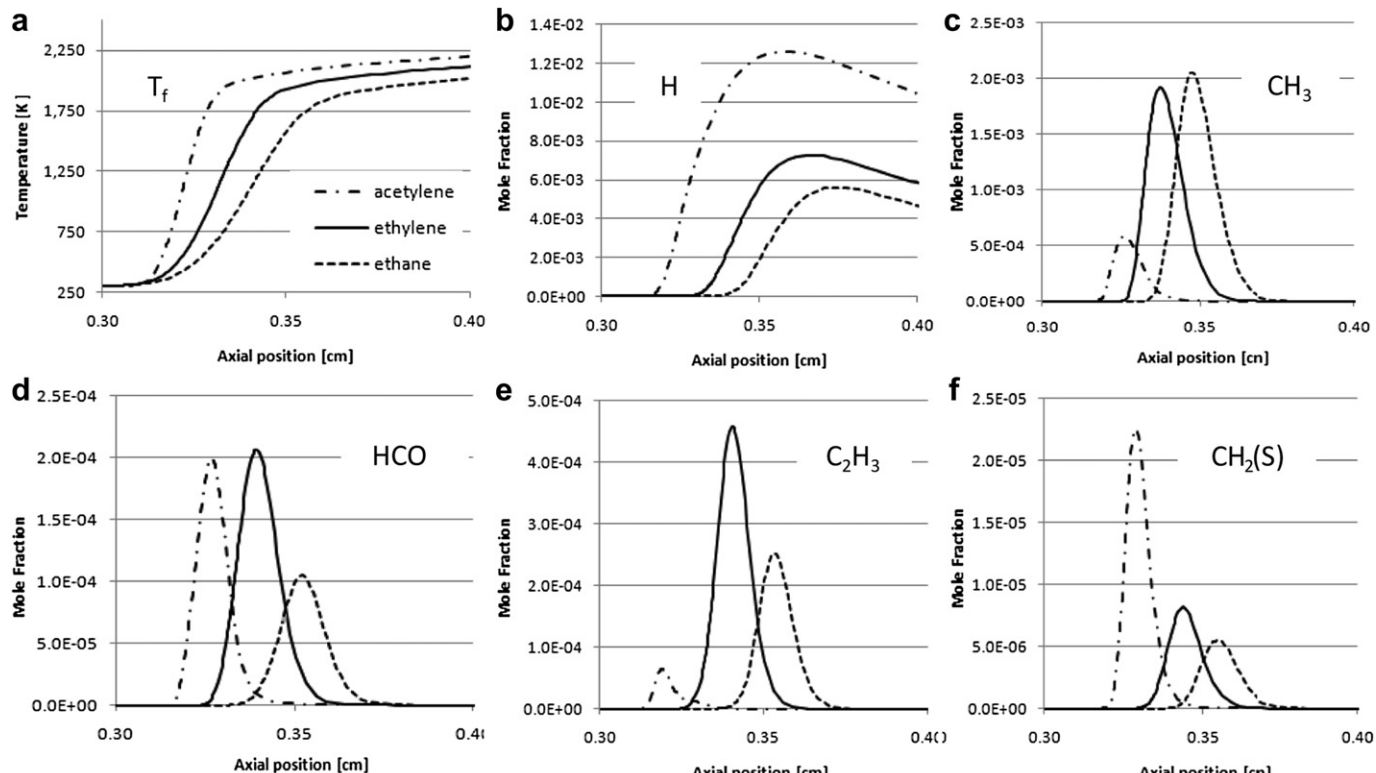
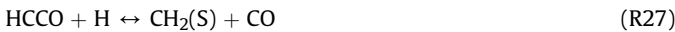
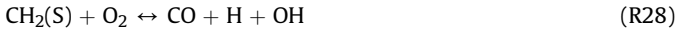


Fig. 16. Flame structure and radical profiles in the air-atmospheric flames of acetylene, ethylene and ethane, at 1 atm and T₀ = 298 K. Panel a: Temperature profiles. Panel b-f: Profiles of relevant radicals: H, CH₃, HCO, Vinyl, CH₂(S).

Then, the ketenyl radical interacts with the H radical to form the $\text{CH}_2(\text{S})$ radical:



The singlet methylene radical is highly energetic and reactive, due to the empty orbital and the lack of unpaired electrons [73]. The $\text{CH}_2(\text{S})$ radical partially reacts with O_2 forming H and OH radicals with the following propagation path:



The prevailing reaction of $\text{CH}_2(\text{S})$ forms the more stable triplet CH_2 radical, with two unpaired electrons:



Furthermore, the CH_2 radical promptly reacts with O_2 promoting the chain propagation:



These reactions explain the high HCO radical concentration in acetylene flames. The formaldehyde and formyl radical concentrations in the ethylene flame are further supported by the recombination reactions of methyl and OH radicals through (R19).

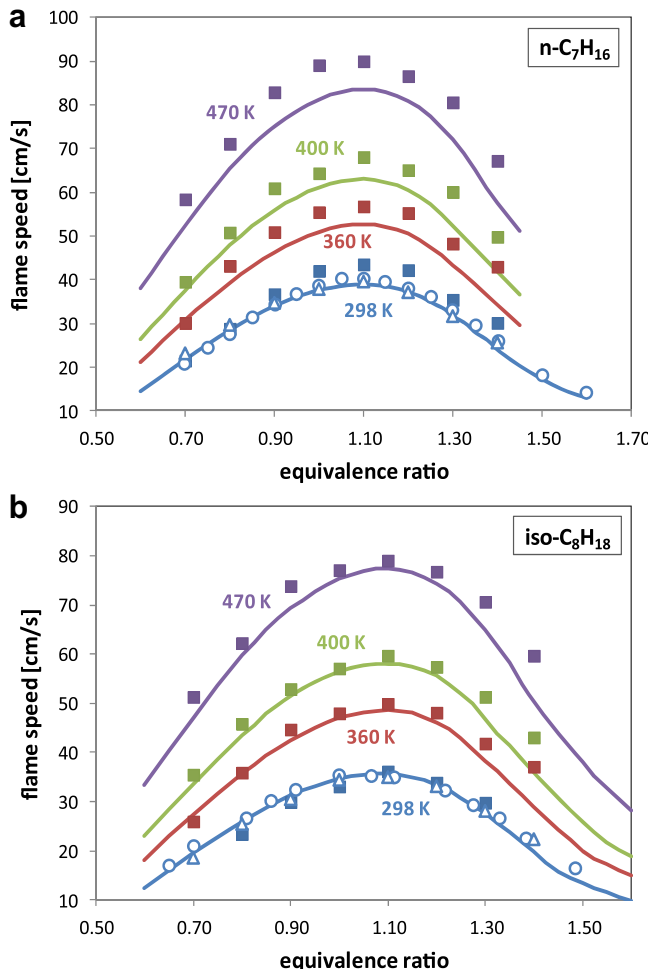


Fig. 17. Temperature effect: laminar flame speeds of n-heptane (panel a) and iso-octane (panel b) atmospheric flames in air: ■ [83]; ○ [6]; Δ [84].

Contrary to the model of [9], acetylene isomerization to singlet vinylidene:



and the successive reactions with molecular oxygen are not significant in our model, in either acetylene or ethylene flames. Fig. 15a also shows that the pressure effects on the acetylene laminar flame speed are weaker when compared with those of methane or other fuels. In agreement with the experimental measurements of Jomaas et al. [65], the model indicates that the laminar flame speed decreases with an apparent pressure exponent of about $-0.10 \sim -0.15$.

Fig. 15b shows the laminar flame speeds of pC_3H_4 and $1,3\text{-C}_4\text{H}_6$. The two fuels, however, cannot be directly compared because the propyne flame was obtained with 18% oxygen in the oxidizer. The flame speeds of $1,3\text{-C}_4\text{H}_6$ are higher than those of nC_4H_8 , while those of n-butane are the lowest. Again, these results confirm the effect of unsaturation on the flame speed. The interest in 1,3-butadiene flames is due to its role in the formation of the butadienyl radical which is a relevant precursor for the first aromatic ring formation. Model predictions confirm that, for the same carbon number, the laminar flame speeds of unsaturated species are larger than those of saturated species.

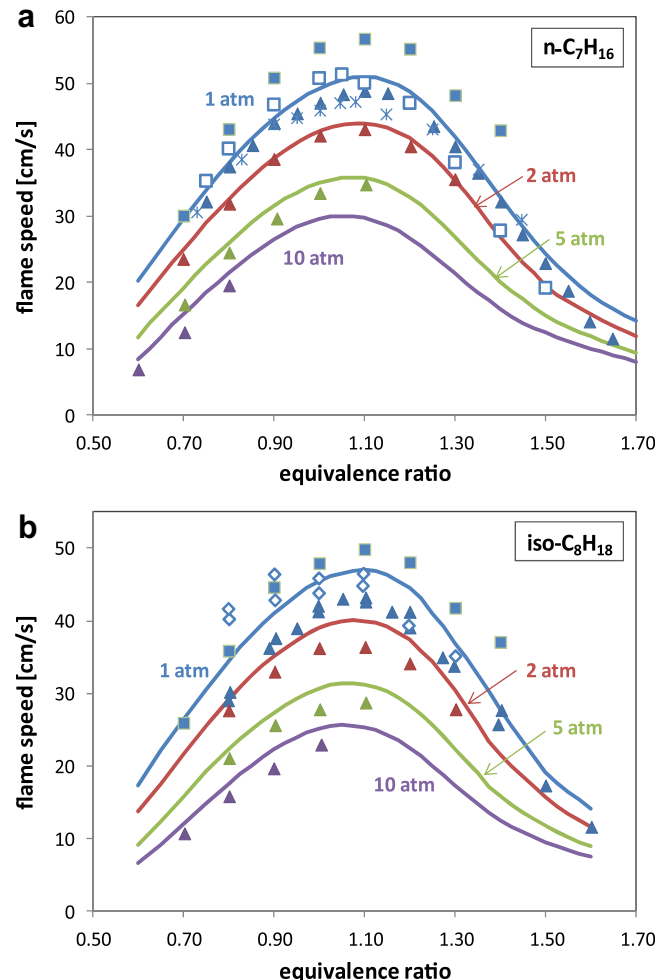


Fig. 18. Pressure effect: laminar flame speeds of n-heptane (panel a) and iso-octane (panel b) flames in air at 353 K: ■ [83]; ▲ [13]; ◇ [76]; * [11].

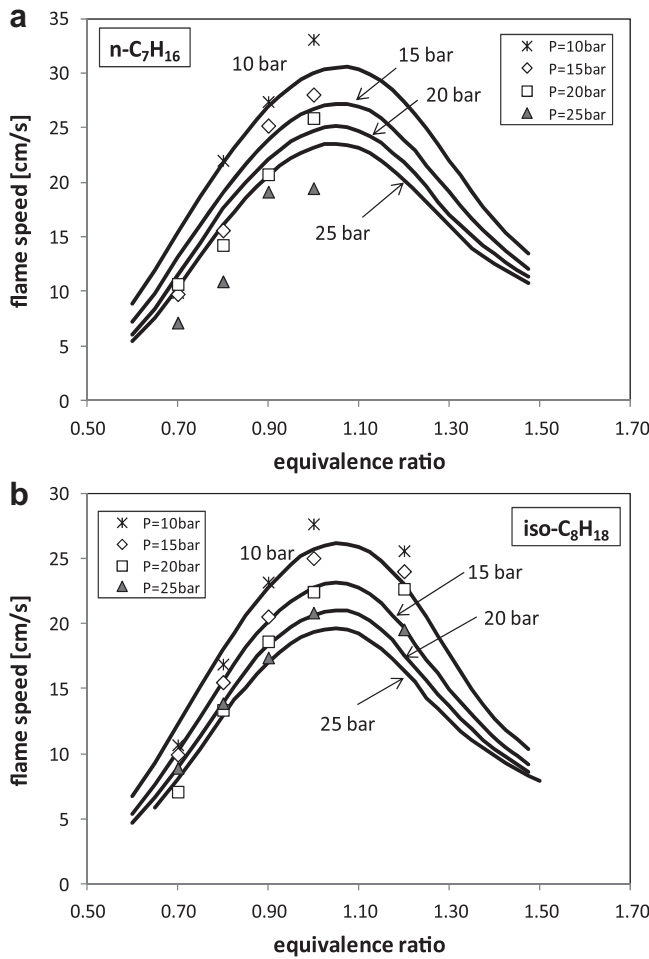


Fig. 19. Pressure effect: laminar flame speeds of n-heptane and iso-octane flames in air (20.5% O₂ vol.) at 373 K. Experimental data from [10].

3.2. Large hydrocarbon species

3.2.1. Primary reference fuels (*n*-heptane and iso-octane)

Babushok and Tsang [69] studied the flame speeds of n-heptane and noted that their sensitivity to the reactions of the C₅–C₇ species is relatively small, and the sensitive reactions are similar to those

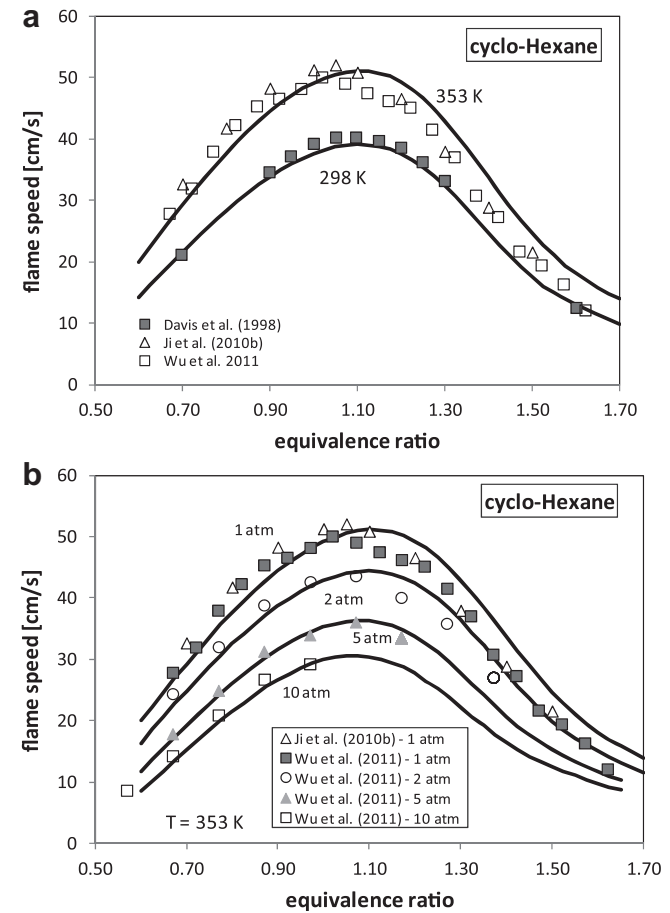


Fig. 21. Laminar flame speeds of cyclohexane. Experimental data from [6,85,87]. Panel a) Effect of initial temperature on laminar flame speed at atmospheric conditions. Panel b) Effect of pressure at 353 K.

controlling the flame speeds of C₁–C₄ hydrocarbons. Fig. 17 shows that the model predictions agree well with the experiments of Davis and Law [6] for n-heptane and iso-octane, hence further confirming the lower flame speeds of the branched species. Parallel to the large formation of methyl radicals, the reduced flame speeds of iso-octane are also due to the formation of isobutene as a major intermediate.

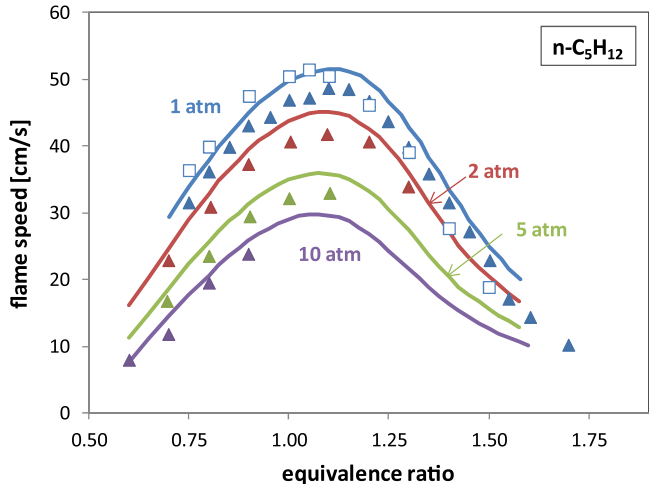


Fig. 20. Pressure effect: laminar flame speeds of n-pentane flames in air at 353 K: ▲ [14]; □ [76].

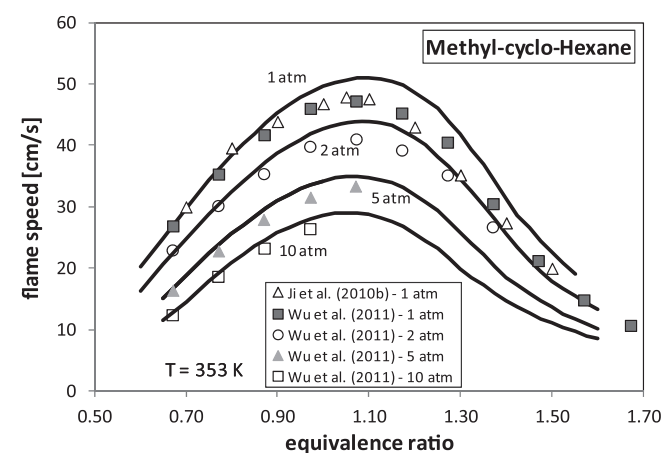


Fig. 22. Laminar flame speed of methyl-cyclo-hexane at 353 K and different pressures. Experimental data from [85] and [87].

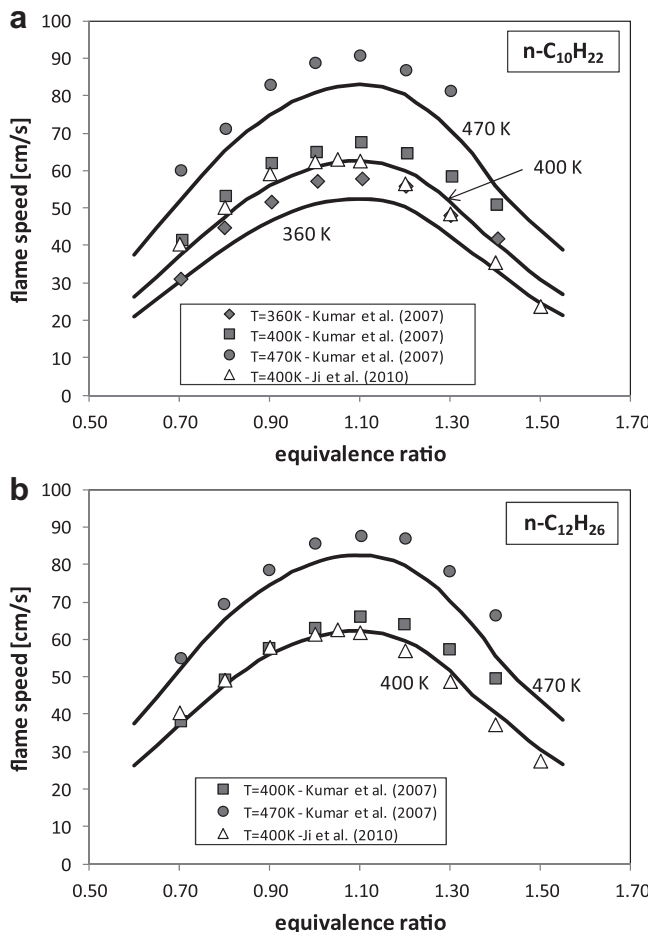


Fig. 23. Temperature effect: laminar flame speeds of n-decane and n-dodecane atmospheric flames in air: Experimental data from [89] and [76].

It is noted that n-heptane and iso-octane are the primary reference fuels used in the knock rating of gasoline through the Octane Number (ON), assuming values of 0 and 100 respectively. At low temperatures, n-heptane is more reactive and

autoignites much more rapidly (ON = 0) than the less reactive iso-octane (ON = 100). The low temperature mechanism leading to autoignition not only is different from that of the high temperature, but is itself also differentiated for n-heptane and iso-octane through the isomerization reactions of peroxy radicals, which are very sensitive to the hydrocarbon fuel structure [81,82]. Specifically, the total rate of the isomerization reactions of the peroxy radicals increases with the linear structure of n-heptane, because of the large number of six- and seven membered transition state rings and the high percentage of loose secondary C-H bonds. On the contrary, this rate is lower in iso-octane, due to the lower possibility to form low-energy transition state rings and to the large percentage of the primary H atoms which are difficult to be abstracted [70].

Fig. 18 shows the effect of pressure on the laminar flame speeds of n-heptane and iso-octane [13]. While the relative values of these predictions agree well with the experimental measurements, i.e. the model properly captures the pressure effect, a systematic overprediction of about 2 cm/s for both fuels under all conditions is also observed.

We note in passing that the results of Kumar et al. [83] are systematically and substantially higher than those of Davis and Law [6], Huang et al. [84] and Ji et al. [76]. While the cause of such a discrepancy has yet to be identified, it is prudent to be discriminative when comparing the results of [83] to other experimental or computational data.

Figs. 19 and 20 respectively show the pressure effect on the laminar flame speeds of the primary reference fuels as well as n-pentane. A comparison between Figs. 18 and 20 confirms, experimentally and computationally, that the laminar flame speeds of n-pentane and n-heptane, as well as their flame structures, are very similar.

3.2.2. Cyclo-alkanes

Figs. 21 and 22 compare the experimental [6,85] and calculated laminar flame speeds of cyclohexane at 298 K and 353 K and methyl-cyclohexane at 353 K, respectively. According to the observation of Ji et al. [85], cyclohexane/air flames propagate somewhat faster than alkylated cyclohexane/air flames. Flames of different mono-alkylated cyclohexane compounds, from methyl-cyclo-hexane to n-butylcyclohexane, were found to have similar laminar flame speeds, suggesting that the different alkyl groups have a secondary effect on flame propagation. Based on the analysis of the model results [86], the lower propagation rates of mono-alkylated cyclohexane flames are attributed to the greater production of propene and allyl and the increased H-atom scavenging by the C3 intermediates. Very recent measurements of laminar flame speeds of cyclohexane, methyl-cyclohexane and ethyl-cyclohexane at atmospheric and elevated pressures up to 20 atm [87] show the following trend for the flame speeds: cyclohexane > n-hexane > alkyl-cyclohexane at all pressures, with the difference being ~10% at high pressures. On the basis of simulations [87] with the JetSurF 2.0 mechanism [86], it is shown that the relative high reactivity of cyclohexane is mainly due to the fact that it substantially decomposes into butadiene and forms less propylene and chain-terminating C3 intermediates. Moreover, because of the presence of the alkyl group and a tertiary C-atom, alkyl-cyclohexane decomposes to a more balanced distribution of intermediates, which bring their reactivity close to that of n-hexane, confirming these different butadiene and propylene formations from different fuels.

Additional data on atmospheric laminar flame speeds of n-propyl-cyclohexane determined using a spherical bomb are given in [88].

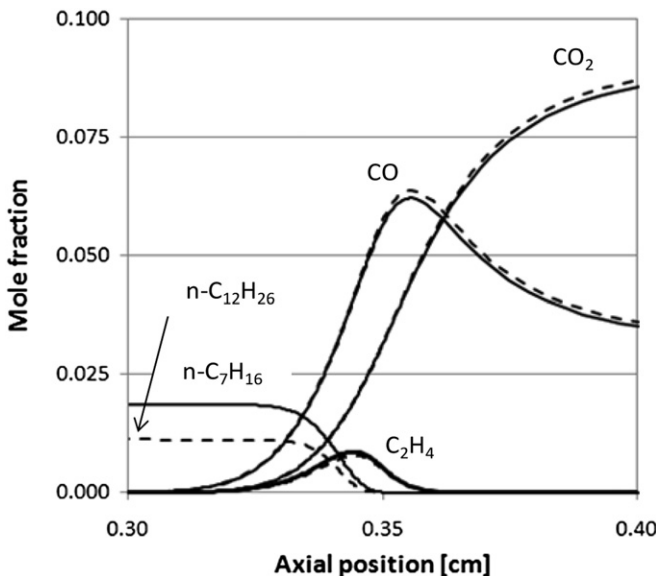


Fig. 24. Similarity of the structures of air-stoichiometric n-heptane and n-dodecane flames.

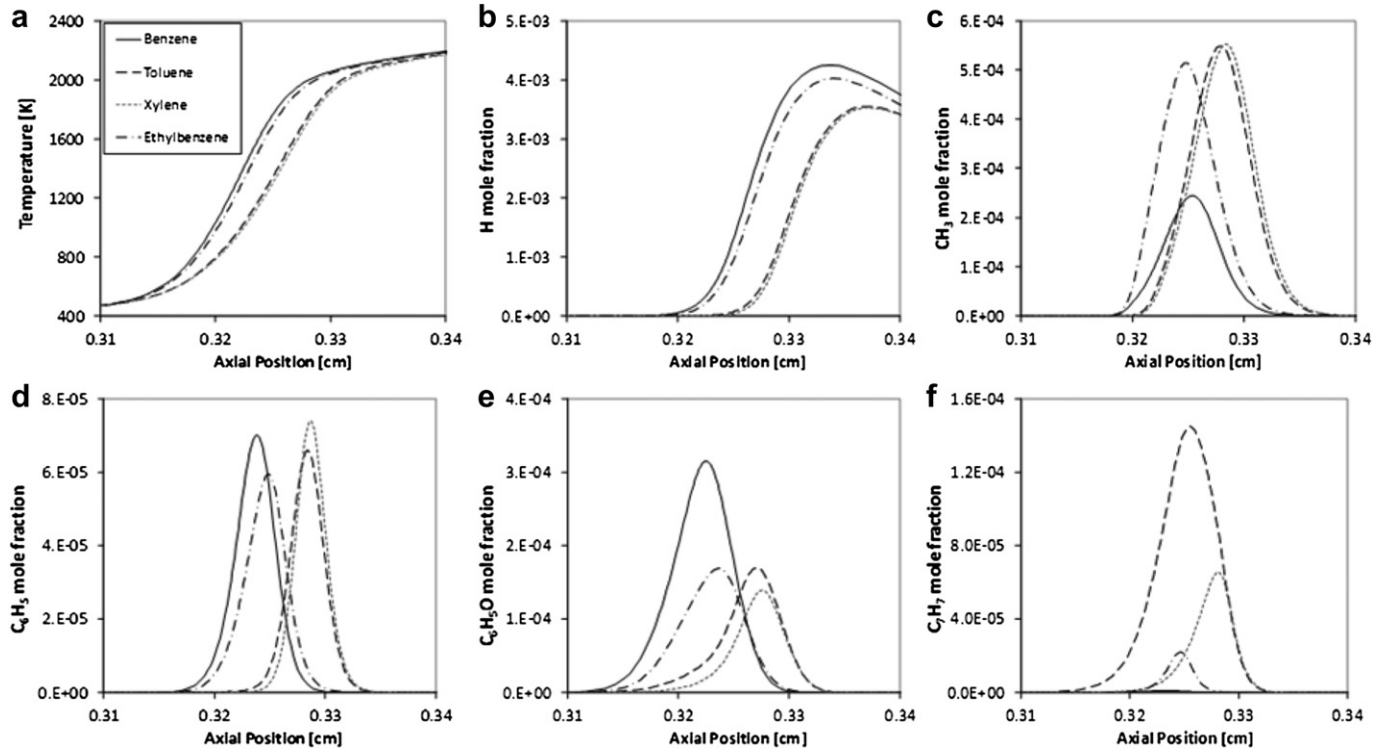


Fig. 25. Flame structure and radical profiles in the air flames of aromatics ($T_0 = 450$ K and 3 atm). Panel a: Temperature profile; Panel b–f: Profiles of H, CH₃, phenyl, phenoxy and benzyl radicals.

3.2.3. Heavy normal-alkanes (*n*-decane and *n*-dodecane)

Heavy *n*-alkane flames have received considerable attention in recent studies [76,86,89–91]. Fig. 23 compares the laminar flame speeds of *n*-decane and *n*-dodecane at different initial temperatures. The predictions agree well with the data of Ji et al. [76], while the results of Kumar and Sung [89] are again consistently higher, as noted earlier. Furthermore, the values of these heavy alkanes are very close to those of *n*-heptane, at the same temperature, which further confirm the similarity in the laminar flame speeds [14,76] and the extinction strain rates [76] of the higher *n*-alkanes, from C₅ to C₁₂. These similarities also support the extensive kinetic analysis of Ranzi et al. [92], which demonstrated that the same kinetic parameters can be used for all the heavy *n*-alkanes, from *n*-heptane up to *n*-hexadecane. Specifically, these results suggest that heavy *n*-alkanes exhibit the same kinetic and oxidation behavior, not only at high temperatures, where decomposition reactions are similar for the combustion of different fuels, but also in the low temperature range. Mechanistically, since the hydrocarbon is mainly consumed by unimolecular decomposition and H-abstraction reactions with the formation of alkyl radicals, which rapidly transform into smaller species via β -decomposition reactions, reactions involving fuel decomposition are too fast to be rate limiting. Consequently the laminar flame speeds of the heavy *n*-alkanes are mainly sensitive to the oxidation kinetics of the small species. This fact is well confirmed by sensitivity analysis in that the dominant chemistry is almost identical for the different *n*-alkanes.

Furthermore, Kelley et al. [14] have demonstrated that the structures of the flames from *n*-pentane up to the heavier *n*-alkanes are very similar and sensitivity analysis always identifies the same key reactions in the reaction mechanisms. The temperature and heat release profiles for the different fuels are basically identical; therefore the flame speeds are also almost the same for the different systems. Fig. 24 shows the profiles of the concentrations of

the fuels, ethylene, CO and CO₂, for the *n*-heptane and *n*-dodecane flames. The differences in the initial fuel decomposition pathways lead to very similar concentrations of the smaller species and radicals and then to similar successive oxidation reactions. This lends support to the observed fuel similarity in the laminar flame speeds.

Recognizing that the laminar flame speeds of *n*-alkanes are similar for all fuels over the entire range of ϕ , it is nevertheless noted that the laminar flame speeds for the lighter fuels, such as *n*-C₅H₁₂, tend to be 1–2 cm/s higher than those of the heavier fuels. Although these differences can be attributed to data uncertainty, it can also be argued that fuel diffusivity could be responsible for all or part of the observed variations. The model predictions confirm

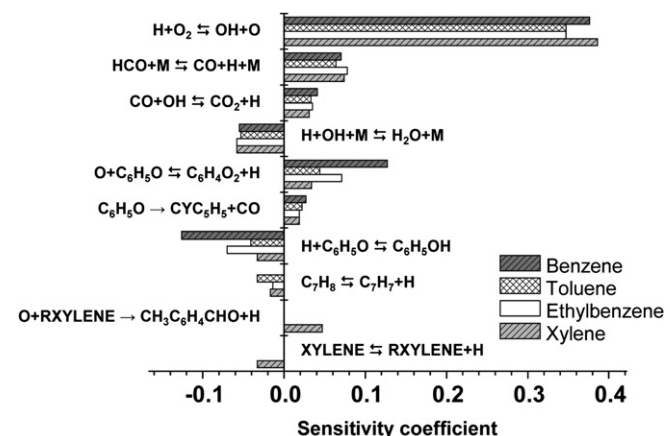


Fig. 26. Sensitivity coefficients of laminar flame speed on reaction rate coefficients, for aromatic/air flames at $\phi = 1$ and atmospheric pressure.

these small reductions for the larger hydrocarbons with decreased fuel diffusivity. In general, the somewhat larger diffusivity of the lighter fuels could lead to a small increase in the flame speed as compared to the heavier fuels. The small influence is confirmed by sensitivity analysis which shows that the laminar flame speed is not strongly affected by fuel diffusivity. This result also agrees with the work of Smallbone et al. [11], who observed that an increase of the n-heptane diffusivity by 50% leads to negligible changes in the flame speeds. Ji et al. [76] in addition showed that flame propagation is not very sensitive to the binary diffusion coefficient of fuel-N₂, whilst it is affected by that of O₂-N₂.

3.2.4. Aromatics

As discussed in Brezinsky [93], the oxidation of aromatics is quite different from that of the aliphatics. The aromatic ring provides a site for electrophilic addition reactions that compete with the abstraction of H from the ring itself or from the side chain [75]. High temperature benzene oxidation shows the sequence of phenol, cyclopentadiene, vinyl acetylene, and butadiene together with ethylene and acetylene. The high temperature oxidation and combustion of aromatic species was discussed in [94], highlighting the relevant analogies and similarities among the different reactions progressing from benzene and toluene towards the heavier aromatics. The definition of the different reaction classes of growth and oxidation is an important step in the characterization of radicals and aromatics that recursively contribute to PAH formation and the subsequent soot inception. More recently, a consistent chemical mechanism to predict the high temperature combustion

characteristics of several aromatic species was presented and discussed by Narayanaswamy et al. [26].

Farrell et al. [95] and Johnston and Farrell [7] determined the laminar flame speeds of benzene, toluene (C₆H₅), ethylbenzene (C₆H₅C₂H₅), and xylene (C₈H₁₀) at high temperature (450 K) and 3 atm pressure over a wide range of equivalence ratios, and discussed the kinetic factors affecting their values upon alkyl substitution of the aromatic ring. These experimental data, corrected for flame stretch, showed the flame speed of benzene to be the fastest, followed by ethylbenzene > toluene > m-xylene. At stoichiometric conditions, the model correctly predicts the same trend, with the fastest speed of benzene flames being 66.5 cm/s and the slowest one of 50.3 cm/s for m-xylene. The adiabatic flame temperature follows a similar order, bracketed by 2468 K for benzene and 2442 K for m-xylene, with 2448 and 2452 K for ethylbenzene and toluene in between.

Fig. 25 compares the flame structure and radical profiles of the different aromatic/air flames. Furthermore, Fig. 26 shows that the fuel-specific reactions are mainly related to the phenoxy as well as the resonantly stabilized benzyl-like radicals (C₇H₇ and C₈H₉). The role of the phenoxy radical, which is more prominent for benzene and ethylbenzene, is mainly based on the competition between the following reactions:

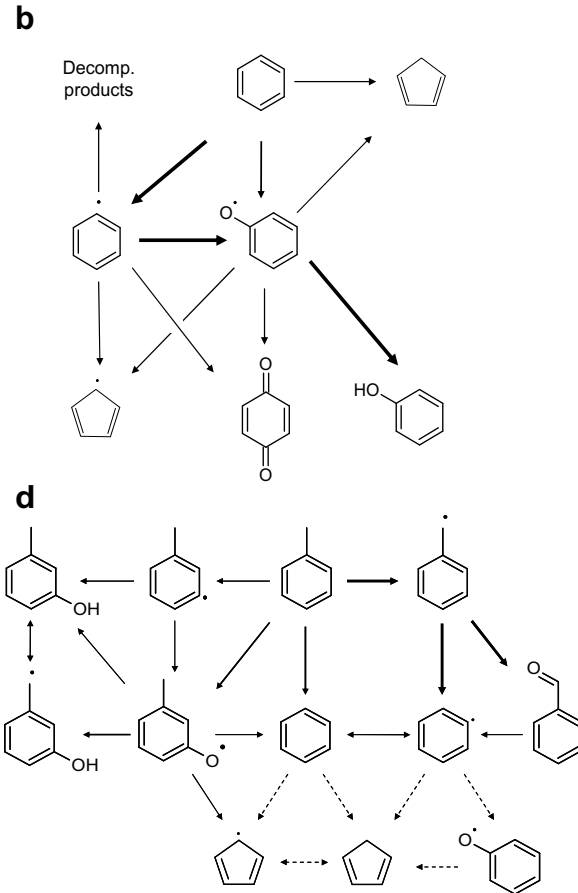
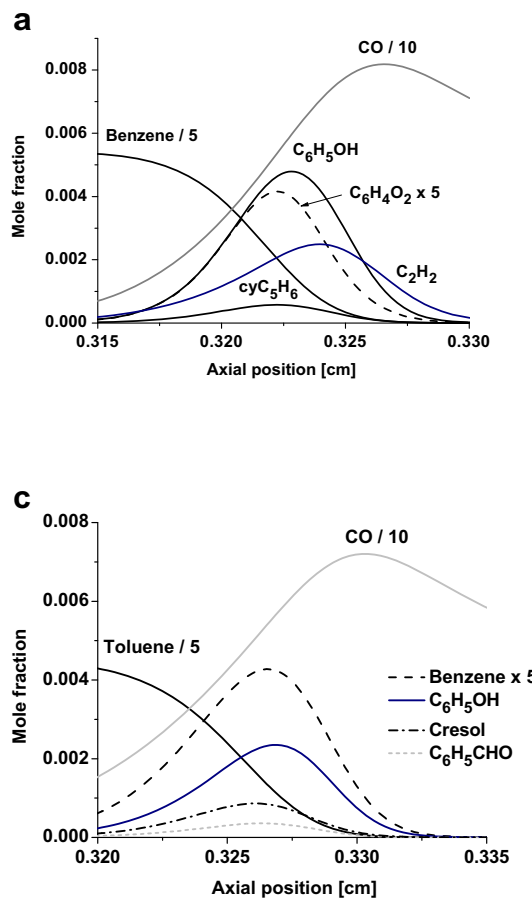
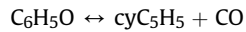


Fig. 27. Flame structure and main reaction paths in air-stoichiometric benzene and toluene flames ($T_0 = 450$ K and 3 atm). Panel a and b: Benzene flame; Panel c and d: Toluene flame.



(R34)



(R37)

It is seen that phenoxy and H radical recombine to form phenol, thereby reducing the laminar flame speeds of all aromatics, while the reverse occurs for the remaining reactions. The H radical profiles in different flames show a clear distinction between two pairs of flames: benzene and ethylbenzene flames with higher flame speeds, as compared to the toluene and xylene flames with lower H concentrations and flame speeds. This distinction is consistent and is further supported by the concentration profiles of the resonantly stabilized benzyl (C_7H_7) and methyl-benzyl (C_8H_9) radicals, as indicated in Panel f of Fig. 25. The benzyl radical concentration is very low in the ethylbenzene flames and is practically zero in the benzene flames, while it is relevant in the toluene and xylene flames. Fig. 26 shows that both the unimolecular decomposition reactions:



act as radical recombination reactions with negative sensitivity coefficients, thus reducing the H concentrations and flame speeds. The methyl radical concentration in the ethylbenzene flame mainly comes from the favored initiation reaction with the pyrolytic cleavage of the C-C bond on the ethyl group:

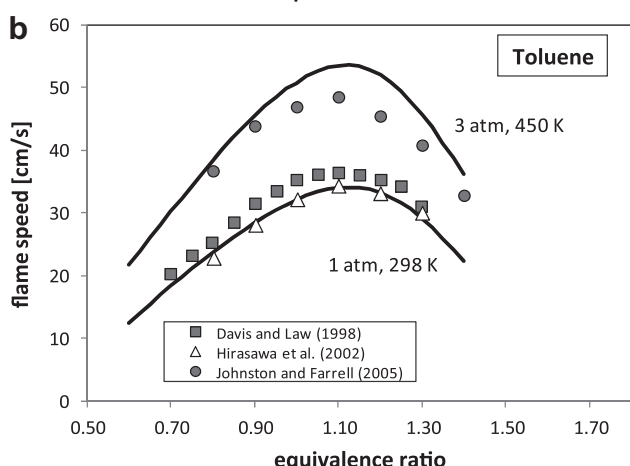
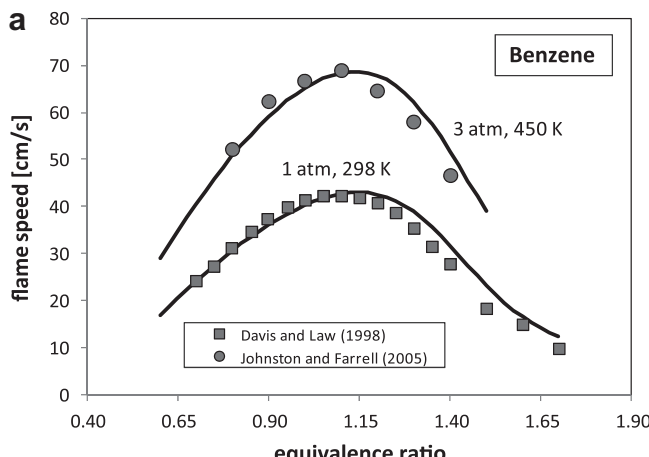


Fig. 28. Laminar flame speeds of benzene (panel a) and toluene (panel b) at 1 (Δ and ■) and 3 (●) atm and different temperatures. Experimental data from [6,7,63].

Fig. 27 shows the flame structure together with the main reaction paths in stoichiometric benzene/air and toluene/air flames, at $T_0 = 450$ K and 3 atm. As already mentioned in the sensitivity analysis, the role of the phenoxy radical, with the formation of para-benzoquinone ($\text{C}_6\text{H}_4\text{O}_2$) in reaction (R33), is very important in the benzene flame [38]. Cyclopentadiene is a minor intermediate, while the C_2H_2 profile indicates the importance of the parallel decomposition paths.

The main reaction paths in the toluene flame show the formation of benzyl radicals due to the cleavage of the weak benzyl-H bond. The subsequent reactions of the C_7H_7 radical with oxygen and the O radical lead to the formation of benzaldehyde ($\text{C}_6\text{H}_5\text{CHO}$):



In rich and fouling conditions, benzyl radicals are important precursors of PAH components, via the radical recombination reactions as well as C_2H_2 addition [96]. Parallel paths of toluene oxidation form cresol and the cresoxy radical. The subsequent oxidation and decomposition of cresol are similar to the corresponding ones of phenol, because of the OH group on the aromatic ring, and to toluene, because of the presence of the methyl group.

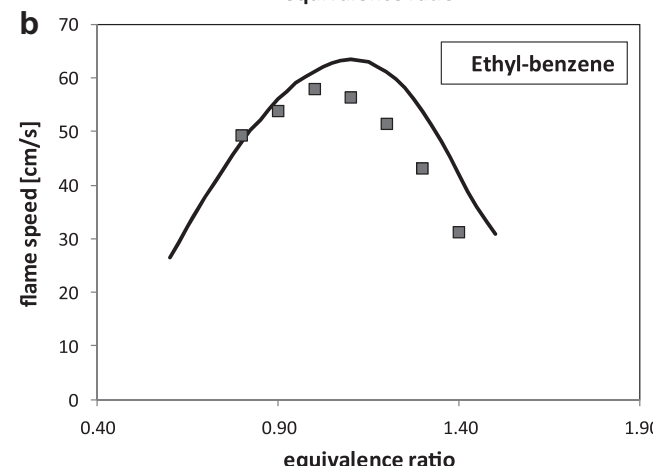
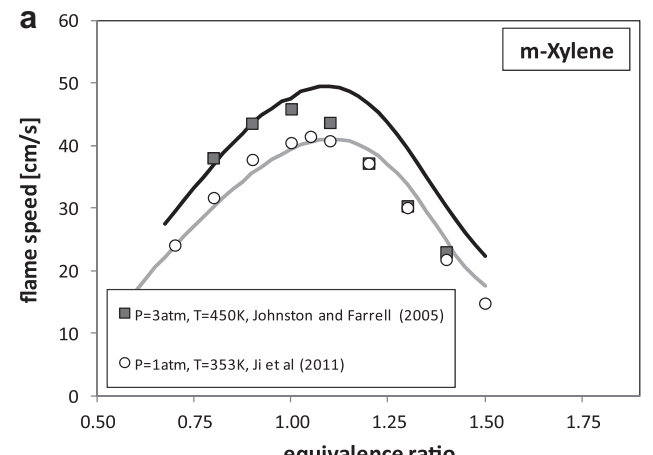


Fig. 29. Laminar flame speeds of xylene (panel a) and ethylbenzene (panel b) at $T_0 = 450$ K and 3 atm. Experimental data from [7] and [159].

The de-methylation reaction of toluene forms benzene and the phenyl radical with their subsequent paths already discussed in the benzene oxidation.

Fig. 28 compares the laminar flame speeds of benzene and toluene at 1 and 3 atm and different temperatures [6,7,63]. The increase of the flame speed here is primarily due to the temperature increase. It is seen that the calculation properly captures the lower reactivity of toluene, due to the resonantly stabilized benzyl radicals.

Fig. 29 shows the laminar flame speeds of m-xylene and ethylbenzene flames. Here two different phenyl-ethyl radicals ($C_6H_5C_2H_4$) are formed from H-abstraction reactions on the ethyl group of ethylbenzene. The aromatic ring strongly influences the selectivity of the H-abstraction reactions on the side chain, due to the weaker C-H bond. Thus, the abstraction reaction of the secondary H atoms is favored, with the subsequent phenyl-ethyl radical dehydrogenation to form styrene:



As already mentioned, the decrease in reactivity of methylbenzenes is simply due to the formation of resonantly stabilized benzyl radicals. Xylene reactions are mainly derived from the corresponding ones of toluene, as was validated in predictions of the extinction limits of jet fuel surrogates [97]. The present mechanism accounts for a single lumped species for the three different xylenes. Rigorous, stretch-corrected, flame speeds have only been reported for m-xylene, as shown in Fig. 29. The work of Farrell et al. [95] also shows that while o-xylene has a higher propagation speed than m-xylene for rich mixtures, they behave almost identically for lean mixtures. The different reactivity of the three xylene isomers, both at low and high temperatures, has been thoroughly discussed in the literature [98–102]. New experimental data on laminar flame speeds of pure isomers could be useful to clarify the role of different molecular structures.

3.3. Alcohols and oxygenated species

3.3.1. Alcohols

The kinetic mechanism of alcohols, from ethanol to the butanol isomers, was recently discussed for a wide range of conditions [43,103,104]. Laminar flame speeds and extinction strain rates of methanol, ethanol and n-butanol flames at atmospheric pressure were also recently determined [17,68,105,106]. These results show that the laminar flame speeds of methanol are higher than those of ethanol and the heavier alcohol flames, under fuel-rich conditions. Furthermore, while the laminar flame speeds of methanol are also consistently higher than those of methane, the flame speeds of ethanol and n-butanol are similar to those of the corresponding n-alkanes. These results confirm and explain the previous data and analysis of Davis and Law [6]. The effect of hydroxyl substitution of hydrogen is to enhance the laminar flame speeds of methanol, as compared to methane, while having minor differences for ethanol as compared to ethane.

Fig. 30 shows close agreement for the C_1-C_3 alcohols. As already observed by Veloo et al. [17], the difference in the laminar flame speeds of methanol with those of the heavier alcohols is mainly due to kinetics instead of the different adiabatic flame temperatures. H-abstraction reactions on methanol form CH_2O without significant CH_3 radical formation. Higher concentrations of CH_3 and CH_4 are observed in ethanol flames and they are mainly due to the production of CH_3CHO and the subsequent decomposition of the CH_3CO radicals. Similarly, laminar flames of heavier alcohols and alkanes have higher concentrations of CH_3 and CH_4 and lower laminar flame speeds in comparison to the methanol flames. Thus,

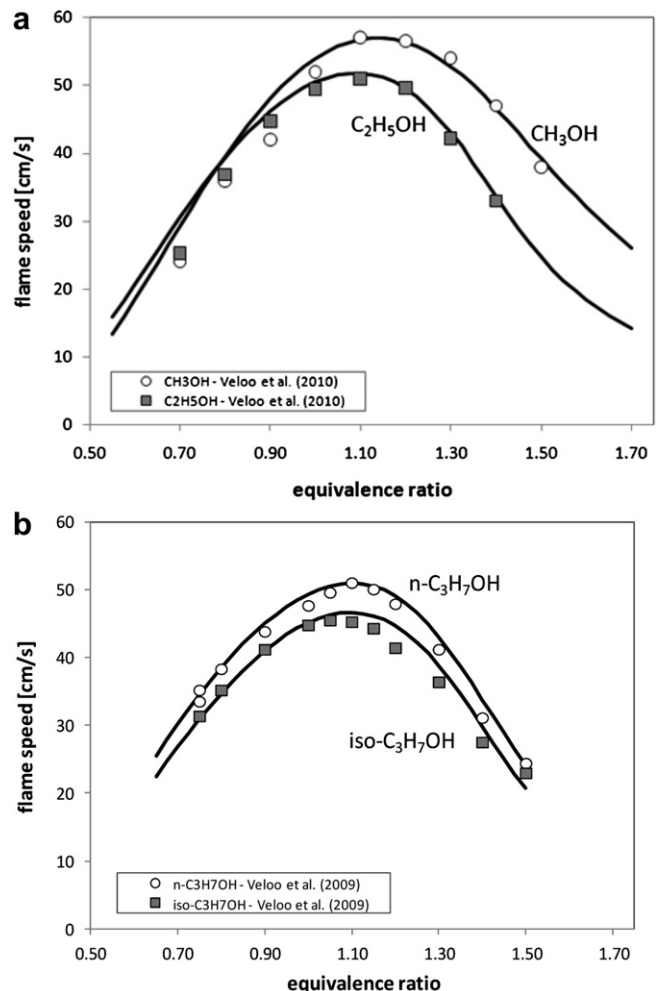


Fig. 30. Laminar flame speeds of atmospheric flames of C_1-C_3 alcohol fuels at 343 K: (a) flame velocity of methanol and ethanol [17]; (b) Flame velocity of n-propanol and iso-propanol [105].

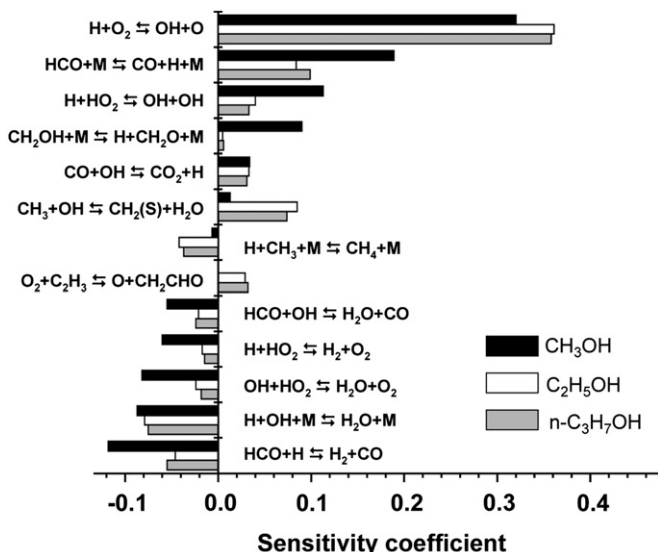


Fig. 31. Sensitivity coefficients of laminar flame speed on reaction rate coefficients, for alcohol/air flames at $\phi = 1$ and atmospheric pressure.

the uniqueness of the methanol reaction mechanism is the limited CH₃ formation with a prevailing H radical path with branching reactions. These considerations are further supported by sensitivity analysis shown in Fig. 31. Again, while ethanol and n-propanol show similar reactivity. The branched iso-propanol has a lower flame speed.

Fig. 32 shows the structure of the atmospheric flames of the four butanol isomers at 343 K in stoichiometric air. Temperature as well as H concentration profiles well confirm the lowest flame speed of the tert-butanol flame. The maximum vinyl and the lowest allyl and C₄H₇ radical concentrations explain the highest flame speed of 1-butanol. Experimentally, the flame speeds are in the order: tert-butanol < iso-butanol ≈ sec-butanol < n-butanol [106]. The model predictions, shown in Fig. 33, agree reasonably well with the measurements for the linear isomers, while the flame speed of tert-butanol is higher by a few cm/s, mainly in lean conditions. Sensitivity analysis shows the importance of the molecular dehydration reaction with the formation of isobutene:



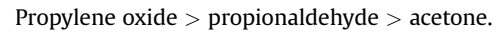
Despite the large formation of isobutene, these over-predictions cannot be attributed to the effect of isobutene whose laminar flame speed is well predicted by the model (see Fig. 11). As recently observed in [107–109], the kinetic modeling of tert-butanol pyrolysis and combustion requires further investigation.

Other recent experimental measurements of the laminar flame speeds of n-butanol and iso-butanol at $T = 353$ K [16] are shown in Fig. 34. The model is again seen to accurately predict the flame speeds at elevated pressures.

We finally note the recent works of Liao et al. [110], Gu et al. [111,112] and Togbé et al. [113] which extended the kinetic analysis of alcohol fuels to 1-pentanol by measuring the laminar flame speed in spherical bombs.

3.3.2. Oxygenated species

3.3.2.1. $\text{C}_3\text{H}_6\text{O}$ isomers (1,3-propylene oxide, propionaldehyde and acetone). The laminar flame speeds of three $\text{C}_3\text{H}_6\text{O}$ isomers (1,3-propylene oxide, propionaldehyde and acetone), representative of cyclic ether, aldehyde and ketone species, were measured in a nearly spherical combustion vessel by Burluka et al. [114]. Their measured values are very different, following the order:



This order corresponds to their enthalpies of formation, i.e. to their adiabatic flame temperatures, recognizing that the adiabatic flame temperature of propylene oxide (~ 2360 K) is 80–90 K higher than that of the lowest one, acetone. Flame speeds at 298 K and 1 atm of pure acetone in air were measured in a spherical bomb by Pichon et al. [115], while the effect of acetone on the laminar flame speed of methane/air mixtures was also investigated by [116].

The kinetics of these $\text{C}_3\text{H}_6\text{O}$ isomers were already described in the kinetic model of propane and butane combustion [117] because of their role in the different steps of oxidation and autoignition of hydrocarbon fuels. While acetone and propionaldehyde are chemically distinct species, propylene oxide is considered as a lumped species indicative of a mixture of 1,2- and 1,3-propylene oxide (or oxetane). Both these oxides are cyclic ethers obtained from the decomposition of propyl-hydroperoxide radicals.

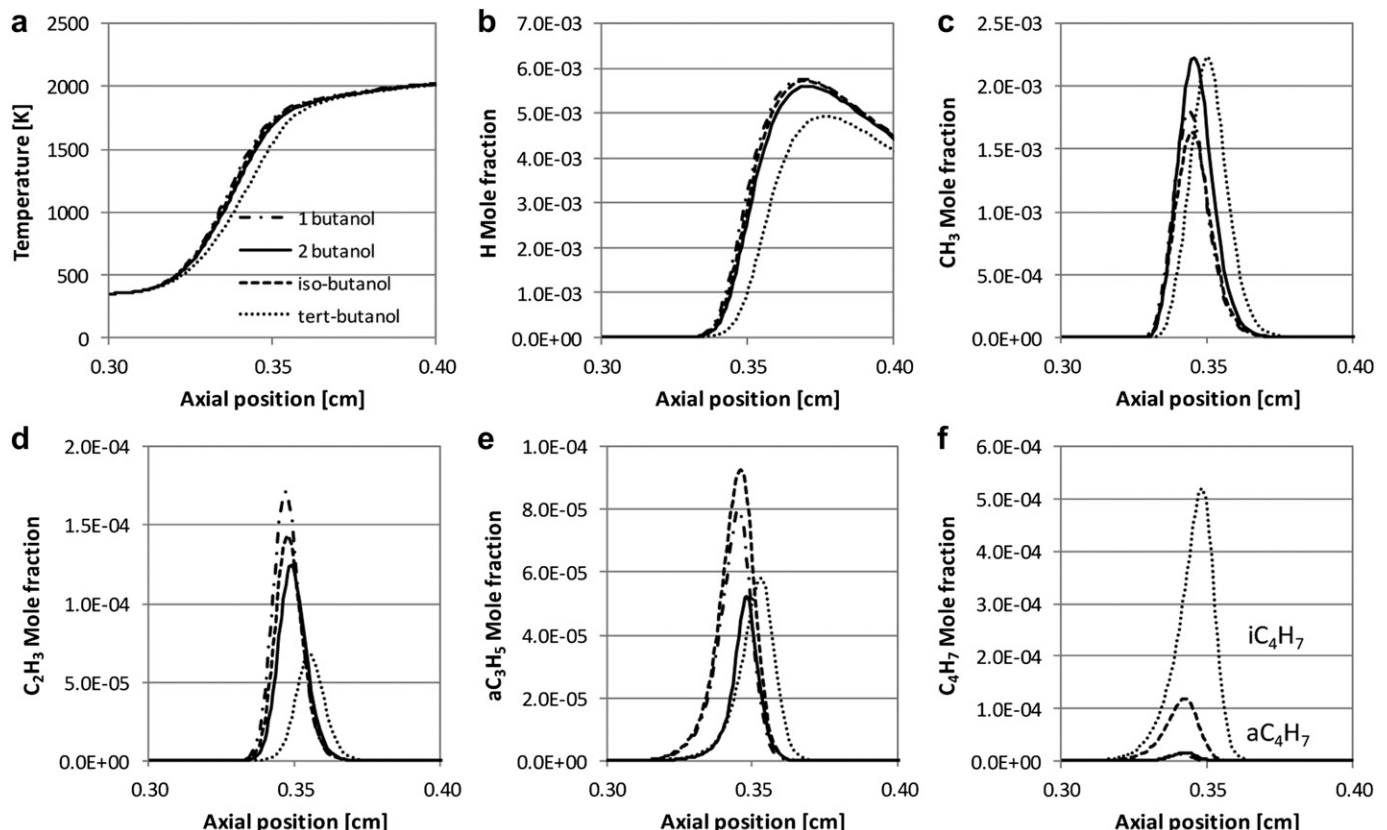


Fig. 32. Structure of the air-stoichiometric flames of the four butanol isomers at $T_0 = 343$ K. Panel a: Temperature profiles. Panels b–f: Profiles of relevant radicals: H, CH₃, Vinyl, Allyl and C₄H₇ radicals.

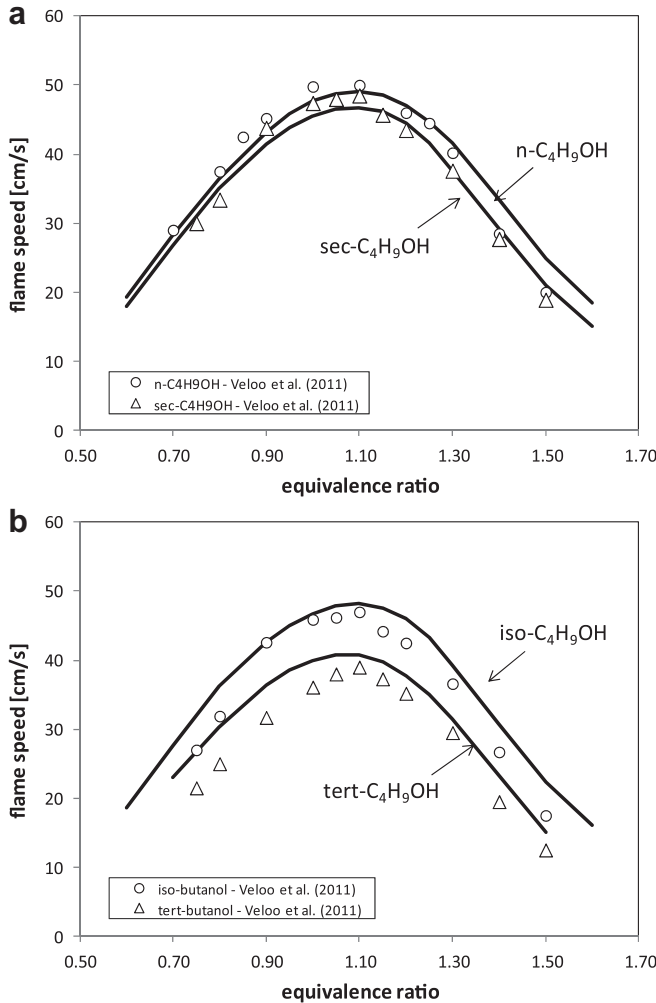


Fig. 33. Laminar flame speeds of butanol isomers at 343 K in air at $P = 1$ atm. Experimental data from [106].

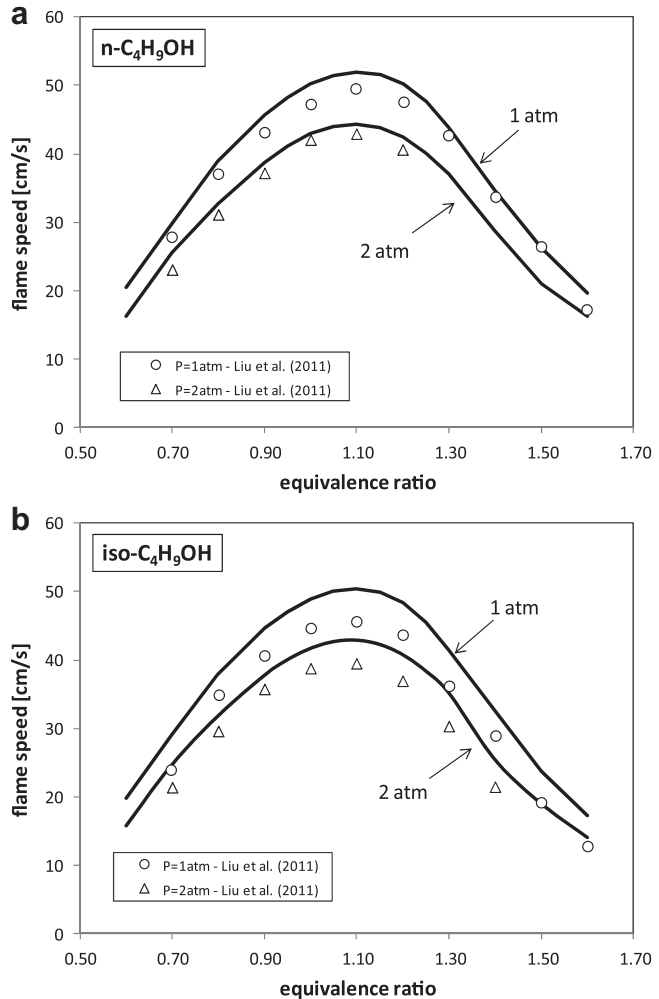


Fig. 34. Laminar flame speeds of n-butanol (panel a) and iso-butanol (panel b) flames in air at 1 and 2 atm and 353 K [16].

Fig. 35 compares the flame speeds of these three isomers. The agreement is satisfactory for acetone and propanal, while the under-prediction of propylene oxide is partially due to the assumption of the enthalpy of formation of the lumped propylene oxide. The enthalpy of formation of oxetane is -80.54 kJ/mol, while we have assumed the value of -94.68 kJ/mol for 1,2-propylene oxide. Accordingly, sensitivity analysis of these flames indicates that the predicted laminar flame speeds are weakly dependent on the fuel-specific reaction rates.

3.3.2.2. Ethers (dimethyl and ethyl tertiary butyl ether). The laminar flame speeds of dimethyl ether (DME) and air at atmospheric and elevated pressures up to 10 atm were measured by Qin and Ju [118], complementing those at atmospheric pressure [5,119]. These data were already critically discussed by Zhao et al. [120] in the development of a comprehensive kinetic model used to simulate experimental results obtained in flow and jet-stirred reactors, shock tubes, and burner-stabilized flames. **Fig. 36** compares predicted and experimental laminar flame speeds of DME at different pressures.

The laminar flame speeds of ethyl tertiary butyl ether (ETBE) were measured in a spherical bomb by Yahyaoui et al. [121] over a wide range of equivalence ratios. **Fig. 37** compares the model predictions and experimental measurements, recognizing that the kinetics of ETBE and different oxygenated octane improvers was

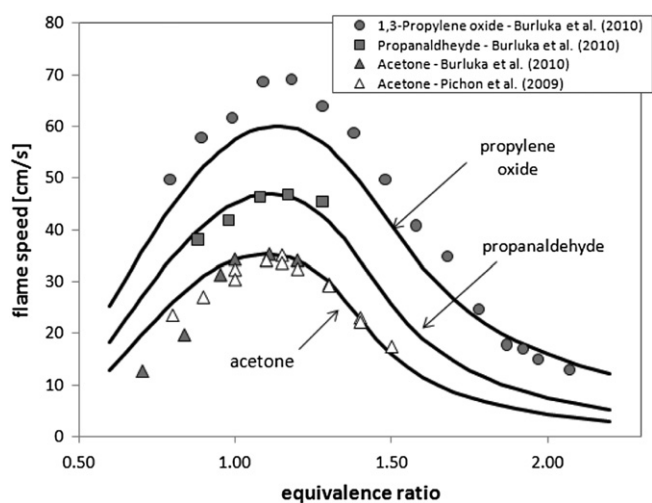


Fig. 35. Laminar flame speeds of C_3H_6O isomers. Experimental data from [115] and [114].

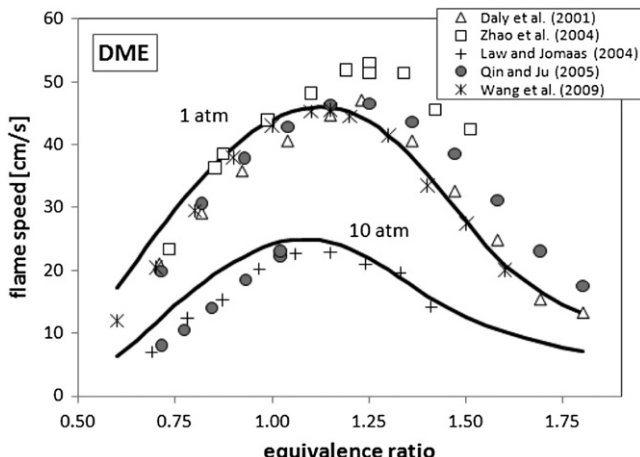


Fig. 36. Laminar flame speeds of DME at 1 and 10 atm: [5,118,119,160]. Data of Law and Jomaas are taken from paper [160].

studied in [122]. It is seen that the agreement is satisfactory and sensitivity analysis indicates the importance of reactions involving the small reactive radicals, without significant effect of fuel-specific reactions. ETBE exhibits a lower laminar flame speed than DME due to the effect of the tertiary butyl radical and of isobutene.

Additional measurements of the laminar flame speeds of DME, ETBE and diethyl ether, especially at elevated pressures, were recently reported in [123–126].

3.3.2.3. Fatty acid methyl esters. In order to understand the combustion behavior of biodiesel fuels, which consist of fatty acid methyl ester (FAME) mixtures, chemical mechanisms of simple methyl esters such as methyl formate (MF), methyl crotonate (MC) and methyl butanoate (MB) are analyzed. Panel a of Fig. 38 compares the laminar flame speeds of MF with the experimental measurements of MF [127] and methanol [17]. Panel b shows the predicted laminar flame speeds of methyl crotonate with the experimental measurements of Wang et al. [128]. Finally, Panels c and d show the experimental and calculated results for methyl butanoate/air mixtures at 403 K and 353 K and initial pressures of 1 and 2 atm [16,128]. Model predictions agree well with the data of Liu et al. [16], while a slight under-prediction is observed with the data of Wang et al. [128]. According to the experimental data

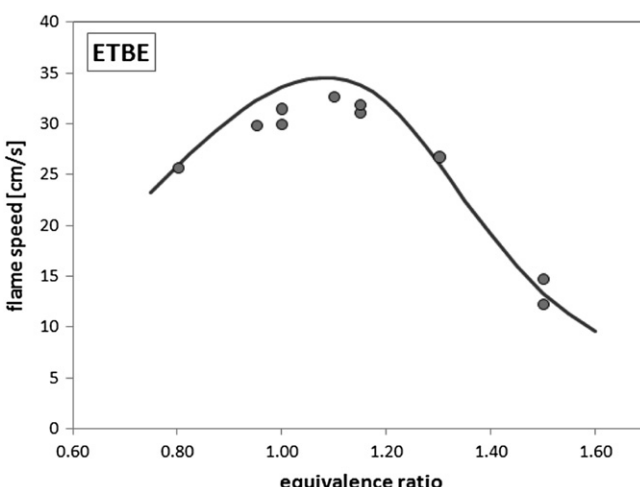


Fig. 37. Laminar flame speed of ETBE in air at 298 K [121].

[16,128], the predicted laminar flame speeds for methyl butanoate are uniformly lower than those of n-butane and n-butanol. Based on the reliability of these model predictions, Fig. 39 directly compares the predicted laminar flame speeds of the small methyl esters in air, for the same flame conditions ($T_0 = 403$ K and 1 atm). Panel b of the figure shows the corresponding maximum flame temperatures, while Panels c and d report the peak concentrations of the H, CH_3 , OH and C_2H_3 radicals.

This analysis shows several interesting features. First, the laminar flame speeds of unsaturated esters are higher than that of methyl butanoate. The lowest speed of MB is well explained on the basis of the lower adiabatic flame temperatures. This behavior is the same as that already observed for alkanes and alkenes. With similar flame temperatures, the flame speed of methyl acrylate (MA) is higher than that of crotonate. Again there is a clear similarity to the behavior of ethylene and propylene. The MA flame shows a C_2H_3 radical peak concentration which is about twice that of the MC (and MB) flame. Sensitivity analysis on the MA flame speed confirms the importance of the branching reaction (R9), thus explaining the highest reactivity of MA in these conditions. Furthermore, the MC flame shows the highest methyl radical concentration with its corresponding inhibiting effect on the flame speed.

Second, the laminar flame speed of methyl formate exhibits a different shape with a maximum at $\phi \sim 1.2$, while the remaining esters peak at ~ 1.1 . The laminar flame speeds of MF in rich conditions approach those of methyl acrylate, despite the lower adiabatic flame temperatures. The peak concentrations of the H and CH_3 radicals (Panel c) confirm this behavior. Methyl formate mostly forms methanol, via the molecular path:



and partially forms formaldehyde, both via the H-abstraction reactions and with the molecular path:



For this reason the peak concentrations of the CH_3 radical are the lowest in the MF flame. On the contrary, the peak concentrations of the hydrogen radical, mainly formed via subsequent HCO dehydrogenation, are the highest in rich conditions. Both the high H and the low CH_3 concentrations promote system reactivity and higher flame speed.

It is also of interest to analyze the location of the maximum laminar flame speed of different fuels vs. the equivalence ratio. There is an obvious correlation between the maximum flame speed and maximum flame temperature, i.e. flame speed and adiabatic temperature profiles vs. the equivalent ratio are expected to be largely similar, with a moderate shift, except for the highly-diffusive hydrogen/air flames [73]. The maximum flame speed of MF peaks at an equivalence ratio of ~ 1.2 , while methane and the saturated fuels mostly peak at ~ 1.1 . The MF flame peaks in between the maximum flame temperature and the maximum H radical concentration (see Fig. 40). The peak location corresponds to the maximum rate of (R1). The release of H atoms via the formyl radical with reaction (R2) in rich conditions explains the shift of the maximum flame speed towards higher equivalence ratios, despite the lower flame temperatures. A similar situation is also present in methanol and formaldehyde flames.

A different explanation is required for acetylene flames. The maximum laminar flame speed of acetylene peaks at equivalent ratios higher than 1.30–1.40 (see Panel a of Fig. 15). In this case, the adiabatic flame temperature also maintains a behavior similar to the flame speed profile, with the maximum temperature at the

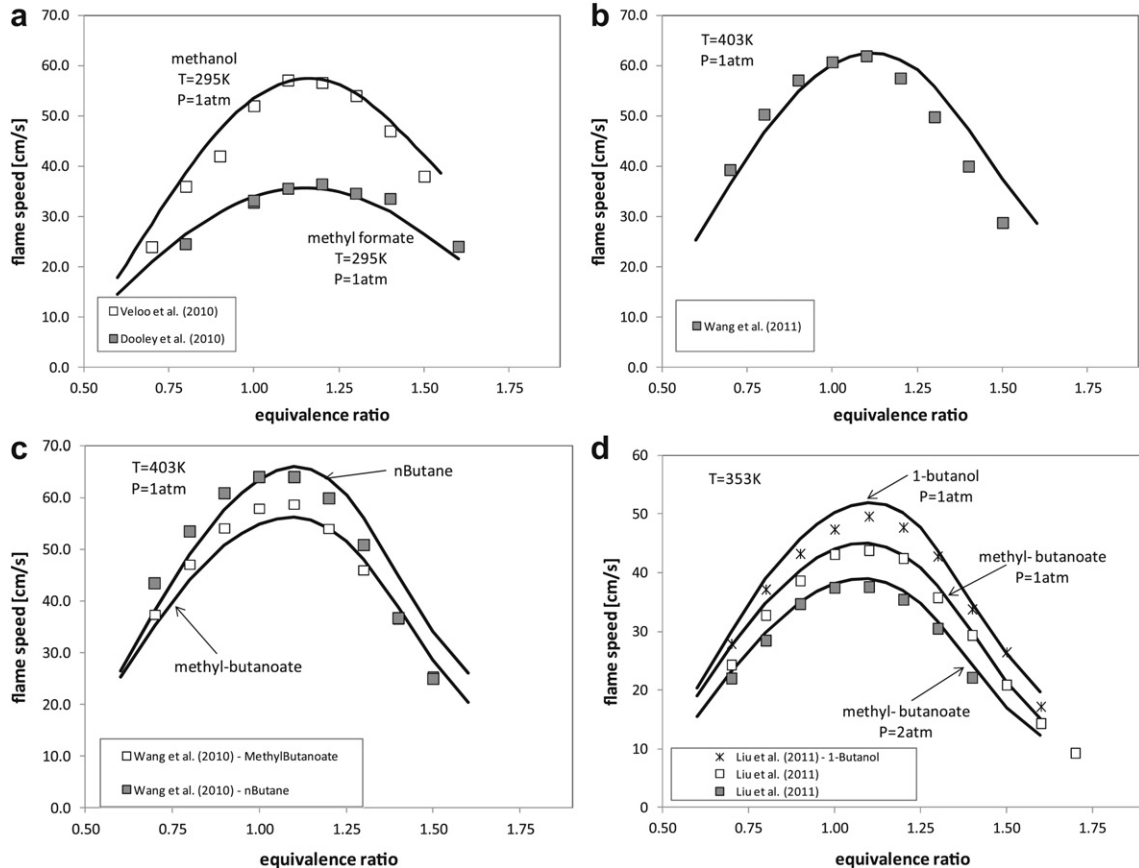


Fig. 38. Premixed laminar flame speeds in air. Panel a: methyl formate at 295 K and 1 atm [127]; methanol at 343 K and 1 atm [17]. Panel b: methyl crotonate at 403 K and 1 atm [128]. Panel c: methyl butanoate and n-butane at 403 K and 1 atm [128]. Panel d: 1-butanol and methyl butanoate at 353 K [16].

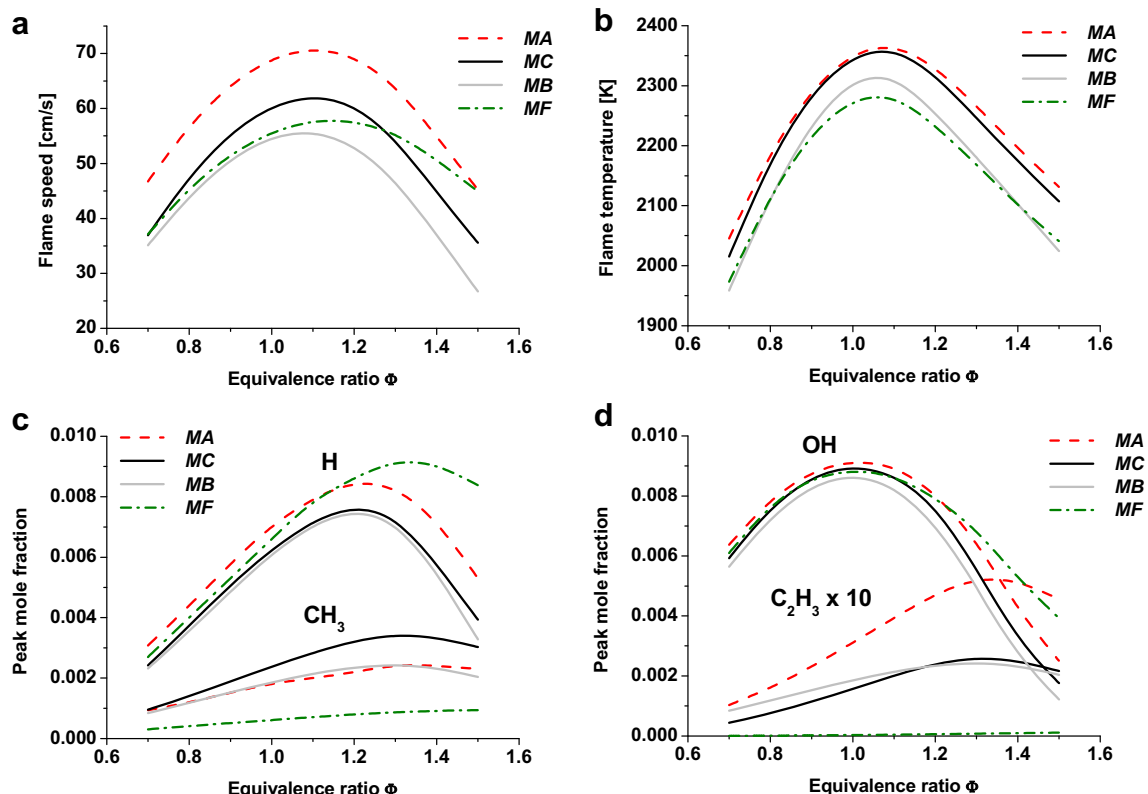


Fig. 39. Predicted laminar flame of small methyl esters in air, at $T_0 = 403\text{ K}$ and 1 atm . Panel a: Flame speeds. Panel b: Flame temperatures. Panel c: Peak mole fractions of H and CH_3 radicals. Panel d: peak mole fractions of OH and C_2H_3 radicals.

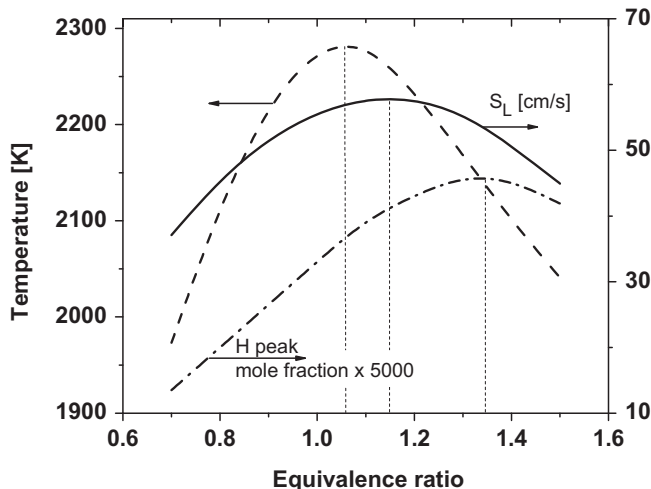


Fig. 40. Laminar flame of methyl formate in air, at $T_0 = 403$ K and 1 atm. Flame speed, adiabatic flame temperature and peak mole fractions of H vs the equivalence ratio.

similar equivalence ratio, more than 60 K higher than the temperature of the stoichiometric flame. This temperature increase is mainly due to the exothermic condensation and dehydrogenation reactions in rich conditions. As a consequence, the higher

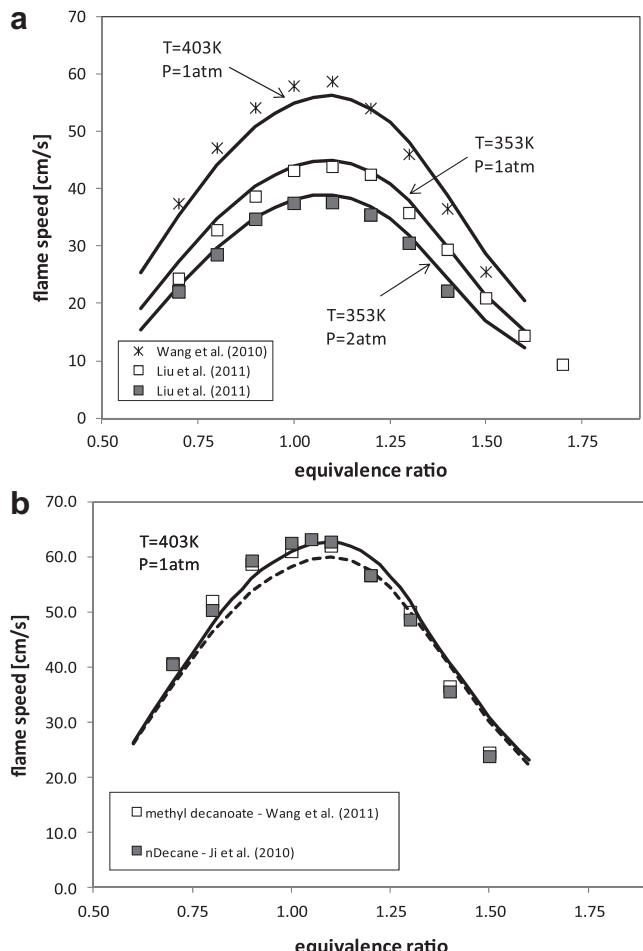


Fig. 41. Panel a) Laminar flame speeds of methyl butanoate in air. Panel b) comparison between air flames of n-decane (■ and continuous line) and methyl decanoate (□ and dotted line). Experimental data from [16,128] and [76].

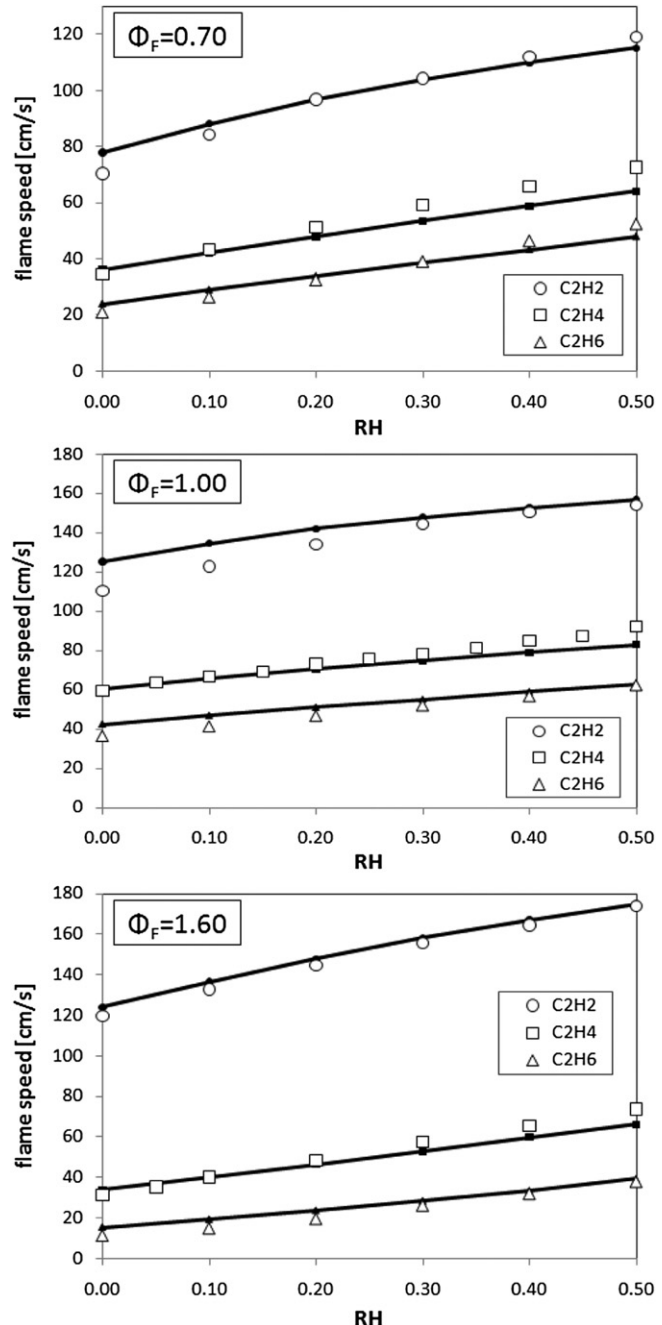


Fig. 42. Laminar flame speeds of C_2 -fuel-air mixtures with hydrogen addition at atmospheric pressure (initial temperature: 293 ± 2 K). Experimental data from [161]. See text for RH and Φ_F .

adiabatic flame temperature in rich conditions explains the peak of the flame speed at high equivalence ratios. Similarly, ethylene, butadiene and unsaturated species have the tendency to shift the maximum flame speed towards equivalence ratios higher than 1.1.

Fig. 41 compares the predicted laminar flame speed of methyl butanoate and methyl decanoate with the experimental measurements of Wang et al. [128]. It is seen that the laminar flame speeds of methyl decanoate are very similar to those of the large n-alkanes. A recent shock tube study of the autoignition of methyl decanoate [129] confirms this similarity. The ignition delay times of methyl decanoate and n-decane are very similar at high temperatures, while methyl decanoate shows somewhat longer ignition delay

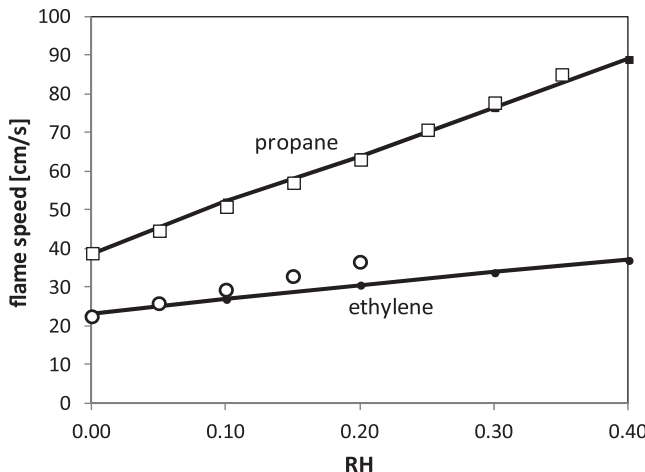


Fig. 43. Laminar flame speeds of ethylene-air mixtures with hydrogen addition at $\Phi_F = 0.7$ and $P = 5$ atm (initial temperature: 293 ± 2 K) and propane-oxygen-helium mixtures with hydrogen addition at $\Phi_F = 0.6$ and $P = 20$ atm ($O_2:He = 21:79$ vol.%; initial temperature: 293 ± 2 K). Experimental data from [161]. See text for RH and Φ_F .

times at low temperatures. The comparison of experimental ignition delay times of the two fuels confirms the importance of the long alkyl chain in controlling the reactivity of methyl decanoate at high temperatures and the partial inhibiting role of the methyl ester group at low temperatures.

Laminar flame speeds of practical fuels including Jet-A1, diesel, palm methyl esters and their blends with diesel and Jet-A1 fuels were determined using the jet-wall stagnation flame configuration in [130].

3.4. Hydrocarbon mixtures

Since most of practical hydrocarbon fuels are mixtures of different chemicals, and since the various fuels and fuel fragments may have chemical interactions not typical of the single-component fuels, it is important to analyze the kinetic mechanisms of fuel mixtures. Since the present reference kinetic mechanism already includes the kinetic interactions among the primary radicals formed from the different fuels of the mixture, it is expected to reliably identify the flame structures and consequently predict the laminar flame speeds of different mixtures as well.

3.4.1. Hydrogen addition to C₁–C₃ fuel-Air mixtures

Laminar flame speeds of C₁–C₃ hydrocarbons with hydrogen addition have been measured [131–133], with the results interpreted on the bases of enhanced thermal, kinetic and transport effects due to the corresponding increases in the adiabatic flame temperature, reaction kinetics, and diffusivity. These studies also showed that the laminar flame speeds can be approximately linearly correlated with a hydrogen addition parameter R_H defined as:

$$R_H = \frac{C_H + \frac{C_H}{(C_H/C_A)_{st}}}{C_F + \left[C_A - \frac{C_H}{(C_H/C_A)_{st}} \right]}$$

where C_F , C_H and C_A are the mole concentrations of the hydrocarbon fuel, hydrogen and air respectively; and the subscript "st" designates the value at the stoichiometric condition.

Fig. 42 shows the comparison between measured and predicted laminar flame speeds of ethane-air, ethylene-air and acetylene-air mixtures with hydrogen addition at atmospheric pressure, at three

different values of Φ_F (0.7, 1.0 and 1.6), while Fig. 43 compares the laminar flame speeds of the ethylene-air mixtures at 5 atm and propane/oxygen/helium mixtures at 20 atm with hydrogen addition. Here Φ_F is defined as an effective equivalence ratio of the hydrocarbon fuel [133]. The definitions of R_H and Φ_F imply that there is always enough oxygen to complete the hydrogen oxidation and only then the remaining oxygen would react with the remaining fuel. It is seen that the measured and calculated laminar flame speeds agree reasonably well for all the fuels.

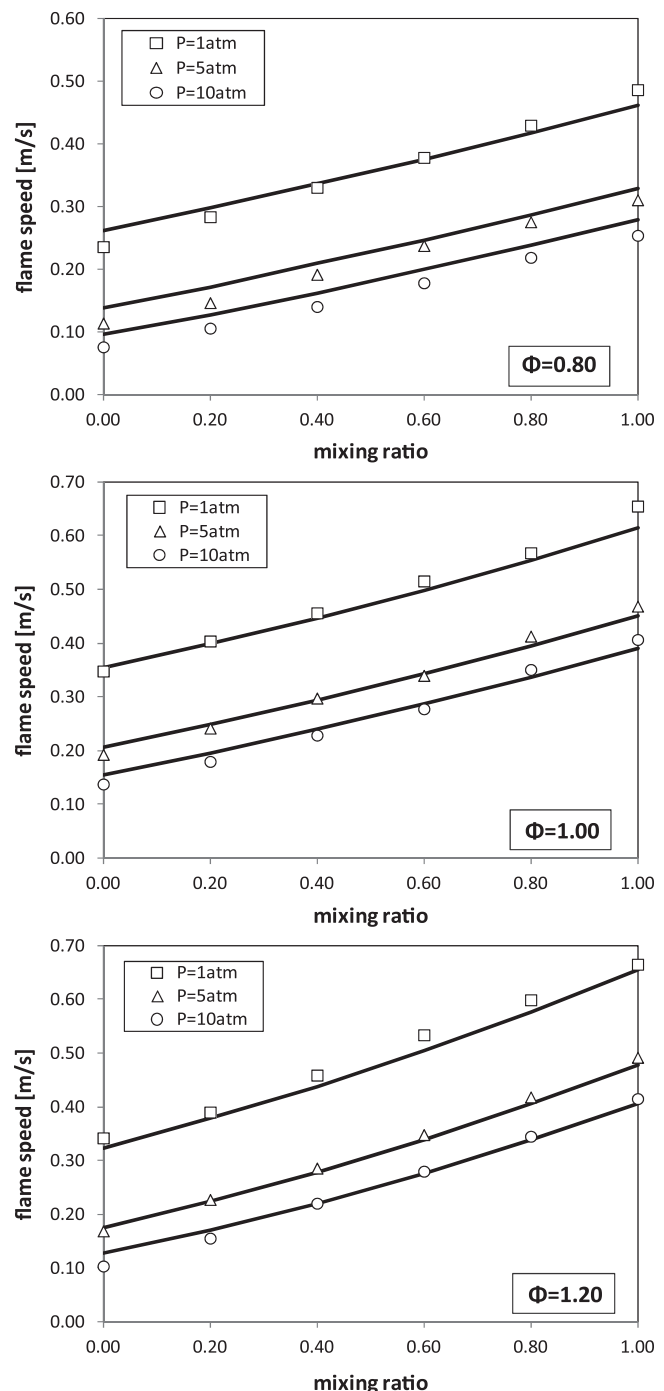


Fig. 44. Laminar flame speeds of CH₄/C₂H₄/air mixtures versus mixing ratio at 300 K, 1, 5 and 10 atm and different equivalence ratios [12].

Additional data on H₂ addition to small hydrocarbons are reported in [67,134–139].

3.4.2. Methane/ethylene mixtures

Measurements of the laminar flame speeds of CH₄/C₂H₄/air mixtures at atmospheric and elevated pressures up to 10 atm, with different equivalence ratios, were reported in Liu et al. [12]. The stoichiometrically-weighted mixing ratio varied from 0 to 1, from pure methane to pure ethylene. Predicted laminar flame speeds with different mixing ratios are compared with the experimental measurements in Fig. 44, at equivalence ratios of 0.8, 1.0 and 1.2. It is seen that the predictions and measurements agree well, showing that ethylene addition results in faster flame propagation in an approximately linear manner in terms of the mixing ratio as defined.

3.4.3. Primary reference fuel mixtures

The laminar flame speed data for the Primary Reference Fuel mixture PRF87 are reported in [10]. Fig. 45 shows satisfactory agreement with the model calculations, including pressure effects. It is seen that the laminar flame speed decreases with a pressure power of about –0.3, implying that the laminar burning flux increases with a 0.7 pressure power. Furthermore, because of the high concentration of iso-octane, the flame speed of PRF87 is very close to that of iso-octane.

Bradley et al. [140] measured the laminar flame speeds of mixtures of PRF90 between 358 K and 450 K, at pressures between 1 and 10 bar, and equivalence ratios of 0.8 and 1.0. Fig. 46 again shows a power dependence of –0.3 for the laminar flame speeds, in agreement with that of [10].

Data for mixtures of PRF with alcohol fuels [141,142] and with reformer gas [84] have also been reported.

3.4.4. Other hydrocarbon mixtures

Aiming at studying the non-linearity effect of different fuels, Hirasawa et al. [63] measured the laminar flame speeds of three binary fuel mixtures consisting of ethylene, n-butane and toluene in air. The use of semi-empirical temperature-based mixing rules in order to estimate the flame speeds of binary fuel mixtures on the basis of those of the individual components was also discussed. In order to account for the effects of thermal and kinetic interactions, non-linear temperature-based mixing rules were obtained to predict the flame speeds of binary mixtures. This approach can be applied if the kinetic coupling between the two components of the fuel blend is limited, i.e. when the two different fuels interact predominantly through reactions with generic flame radical species, such as H, O, and OH. Furthermore, it was observed that for Primary Reference Fuels and other mixtures, for which the flame temperatures and transport properties are very similar, the difference in the laminar flame speeds requires kinetic interpretation.

Fig. 47 shows that the kinetic mechanism is able to correctly predict the different behavior of the laminar flame speeds of ethylene/butane mixtures, with different compositions. A similar agreement is also observed in Fig. 48, where equi-molar mixtures of toluene/ethylene and n-butane/toluene are considered. A non-linear effect is present in the case of the toluene mixtures, when considered on molar basis. Fig. 49 shows the sensitivity analysis performed for the pure fuels and binary ethylene/toluene mixtures. The blending modifies the sensitivity coefficients in a non-linear way. As expected, the role of the vinyl radical reactions is higher for the pure ethylene flame, while that of the resonantly stabilized benzyl and phenoxyl radicals is almost the same as that for pure toluene and also for the toluene/ethylene mixtures. This result clearly shows that the non-linear behavior observed for the toluene mixtures, which is characterized by a lower flame speed, should be

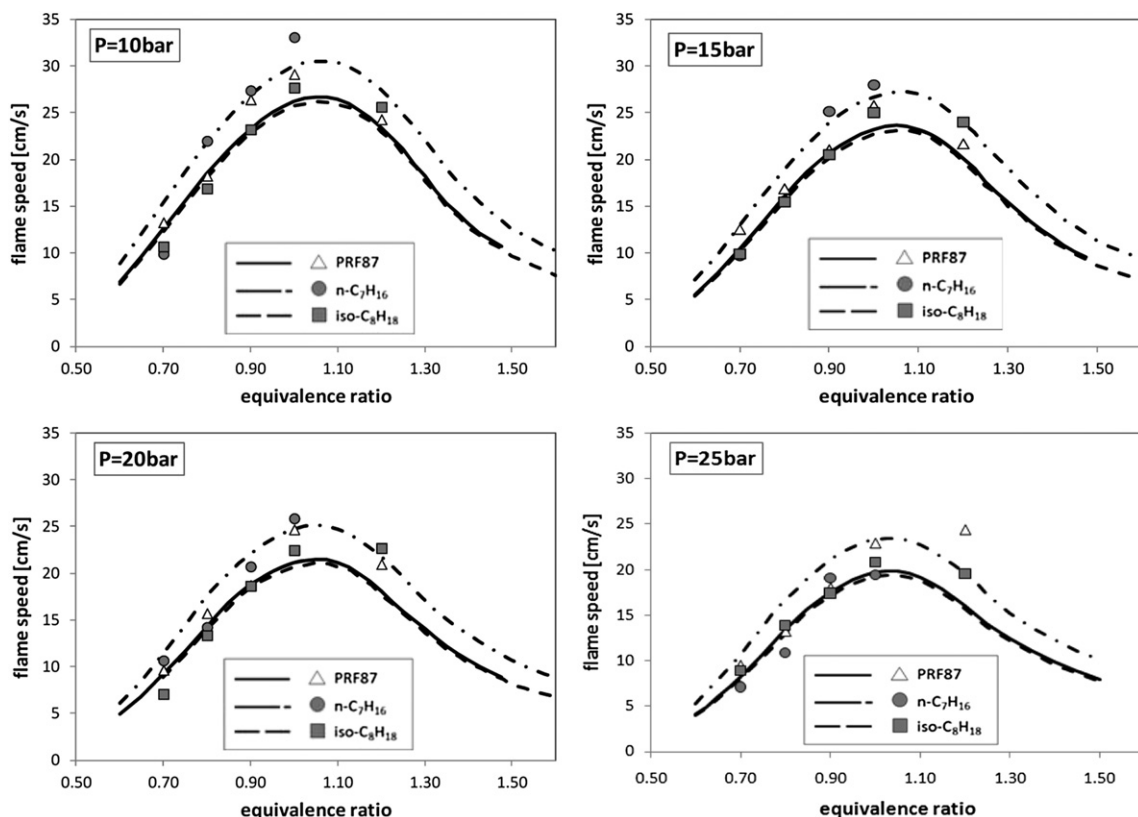


Fig. 45. Laminar flame speeds of PRF/air ($O_2 = 0.205$) and PRF87/air ($O_2 = 20.5\% \text{ vol.}$) at 10, 15, 20 and 25 bar and 373 K. Experimental data from [10].

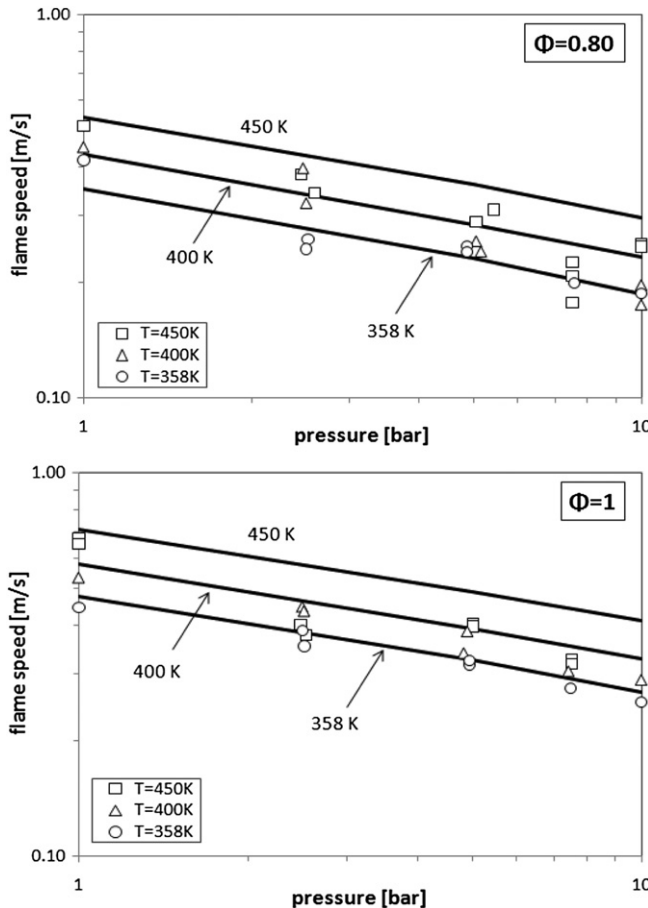


Fig. 46. Laminar speeds of air/PRF90 flames between 358 K and 450 K, at pressures between 1 and 10 bar and equivalence ratios of 0.8 and 1.0. Experimental data from [140].

correlated to the H-radical scavenging effect of the benzyl and phenoxy radicals.

Additional data on binary mixtures of n-dodecane with toluene and methyl-cyclohexane obtained in the counterflow configuration were recently reported in Ji and Egolfopoulos [143].

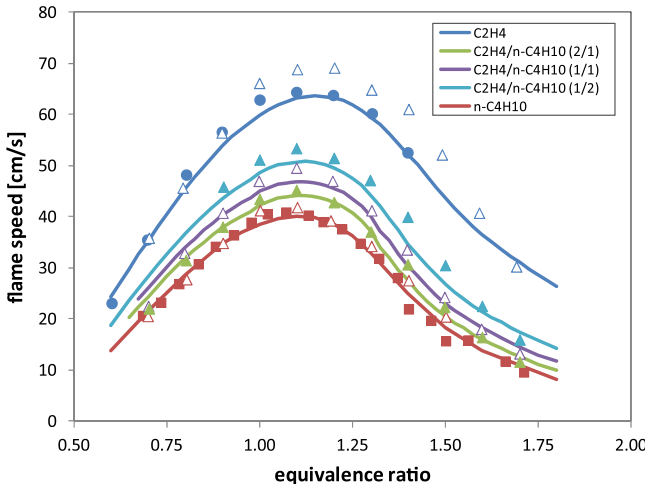


Fig. 47. Flame speeds of ethylene/n-butane mixtures. Experimental data: ▲ Δ [63], ● [65], ■ [6].

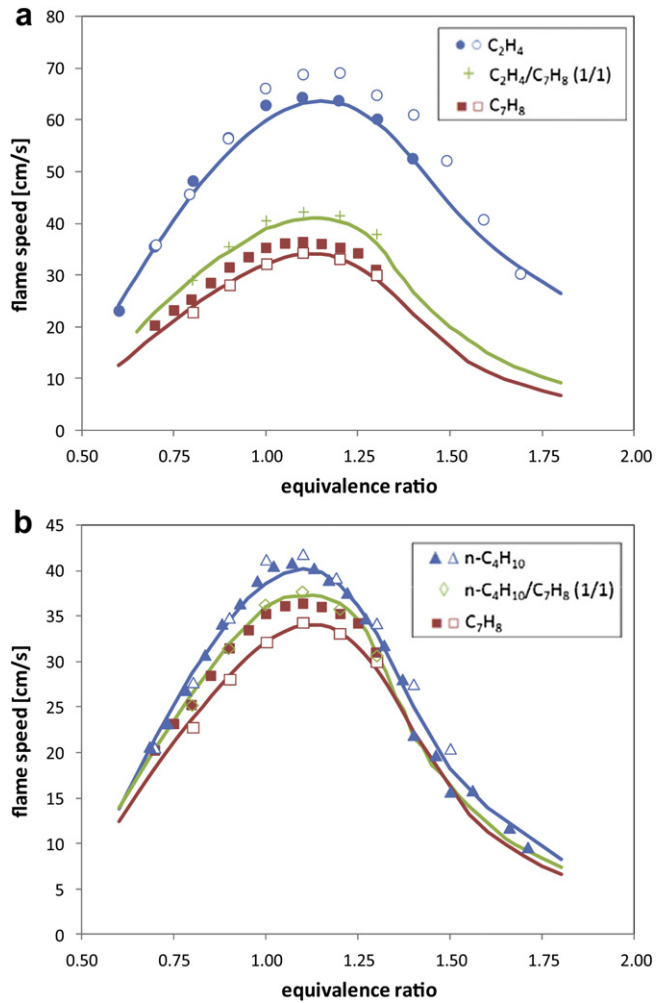


Fig. 48. Laminar flame speeds of Toluene/Ethylene (panel a) and toluene/n-butane mixtures in air at 298 K and 1 atm (panel b). Experimental data: ○ + △ □ [63], ● ■ [65].

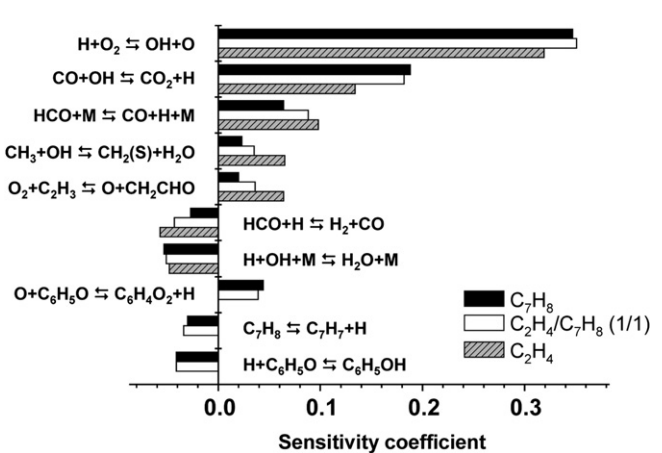


Fig. 49. Sensitivity coefficients of laminar flame speed on reaction rate coefficients, for the toluene/ethylene mixture and pure fuels at $\Phi = 1$ and atmospheric pressure (see Fig. 48).

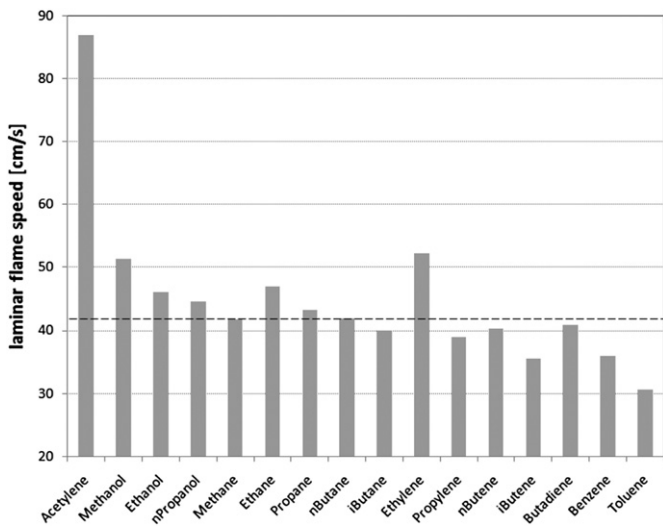


Fig. 50. Laminar speeds of atmospheric and stoichiometric flames of various fuels at $T_{\text{flame}} = 2300$ K, calculated by modifying heat capacity of N_2 .

4. Laminar flame speeds at constant flame temperature

In order to verify and to highlight the pure kinetic effect from those due to different adiabatic temperatures, laminar flame speeds of several fuel species were studied at the same flame temperature. Zhu et al. [144] first experimentally studied the effect of equivalence ratio on CH_4 flames, while Law [73] analyzed the laminar flame speeds of C_2 species at the same flame temperature by modifying the N_2 dilution. Fig. 50 shows the laminar flame speeds of atmospheric and stoichiometric flames of several species at $T = 298$ K, calculated by modifying the specific heat of N_2 to such an extent that the adiabatic flame temperature matches 2300 K for all the fuels, without altering the transport properties of the reacting mixture. This figure and comparison isolate the pure kinetic effects:

- Only flame speeds of the C_2 species maintain and confirm the original order: alkanes < alkenes < alkynes. This order changes for the flame speeds of C_3 , C_4 and the heavier species, where it becomes alkenes < alkanes.
- The laminar flame speed of methanol is the fastest among the alcohol fuels. This fact has been already well explained on the basis of the successive dehydrogenations of methoxyl radical [17]. The laminar flame speeds of propanol and butanol isomers are close to those of the corresponding alkanes.
- The laminar flame speeds of the alcohols and alkanes approach an asymptotic value (~ 42 cm/s at stoichiometric composition) by increasing the molecular weight, due to the relevant role of pyrolysis reactions. The laminar flame speed of methane is also close to this value.
- Both C_4 alkanes and alkenes confirm the negative effect of methyl substitutions on the flame speed. Pyrolysis reactions of branched hydrocarbons not only favor methyl (and methane) formation but also reduce ethylene formation, which in turn reduces the laminar flame speed. The same effect of methyl substitutions is observed for the alcohol fuels.
- The laminar flame speeds of propene and butenes are lower than those of the corresponding alkanes, due to the increasing role of the resonant allyl and methyl-allyl radicals.
- The laminar flame speeds of the aromatics are definitely lower for the formation of the resonantly stabilized radicals, such as the phenoxyl radical from benzene, benzyl radical from toluene, methyl-benzyl radicals from xylene and so on.

5. Conclusions

By using the same kinetic model to simulate a large variety of experimental laminar flame speeds data of different fuels under different conditions, the present study integrates the understanding of the high temperature kinetics of hydrocarbon fuels into the interpretation and determination of laminar flame speeds. Notable unifying concepts include: small radical and molecular species created from high temperature decomposition processes are the active species in all cases; hydrogen radical is the most effective flame speed enhancer because of its branching activation; the methyl radical significantly reduces the flame speed, especially in removing H from the system through the recombination reaction to form CH_4 .

Laminar flame speeds of various hydrocarbon species, including alkanes, alkenes, alkynes, aromatics and alcohols are compared over an extensive range of equivalence ratios, temperatures and pressures. They show that the laminar flame speeds of normal alkanes are nearly identical for C_4 and larger molecules, while those of cyclo-alkanes are similar to the values of their corresponding alkanes. For fuels with the same carbon number, unsaturated species have higher flame speeds in the following order: alkanes < alkenes < alkynes. Branched species show lower flame speeds than the corresponding linear components. Methyl substitution reduces the laminar flame speeds not only for alkanes and alkenes but also for alcohols and oxygenated species. This is due to the increase of methyl and the decreasing importance of hydrogen radicals as branching agents.

Two major understandings are acquired:

- Methyl substitution reduces the laminar flame speed, mainly at stoichiometric conditions. Since the adiabatic flame temperatures of iso- and normal alkanes are very similar, the reduction in the laminar flame speed due to methyl substitutions has to be explained on kinetic basis.
- The effect of unsaturation of the molecules is to increase the laminar flame speed. The higher flame speed due to unsaturation is demonstrated in Fig. 15, in which flames of ethane, ethylene and acetylene are compared. This is further emphasized for the C_4 species where the effect of unsaturation is shown by analyzing the laminar flame speeds of n-butane, n-butene and 1,3-butadiene. The effect of unsaturation appears to be the largest for smaller hydrocarbons, and decreases as the carbon number increases. It is emphasized that the thermal and dynamic structures of the laminar flame are largely dependent on the adiabatic flame temperatures. These considerations further support the importance of accurate thermodynamic properties for the estimation of laminar flame speeds [9].

Acknowledgments

The authors gratefully acknowledge Prof. F. N. Egolfopoulos of the University of Southern California for his input in the preparation of the Appendix and for providing his database of laminar flame speeds for hydrocarbons and oxygenated fuels, as well as the xylene data of Fig. 29, prior to publication. The authors also gratefully acknowledge the very useful comments of the reviewers. The work at Politecnico di Milano was supported by the European Community (Emicopter Project: CS-GA-2009-251798) and by the Italian Government MSE/CNR (Biofuel Project). The work at Princeton University was supported by the Combustion Energy Frontier Research Center, an Energy Frontier Research Center funded by the U.S. Department of Energy, Office of Basic Energy

Sciences under Award Number DE-SC0001198, and by the Air Force Office of Scientific Research.

Appendix. Experimental methods for the determination of laminar flame speeds

Since the laminar flame speed of a given mixture is defined on the idealized but unattainable situation of the adiabatic, steady, one-dimensional propagation of a planar flame through this mixture in the doubly infinite domain, the key criteria in the development and adoption of an experimental method for its determination must be: (1) closeness to the idealized limit; and (2) a procedure through which the remaining nonideal effects can be systematically subtracted from the experimental data.

The dominant parameter controlling laminar flame propagation is the (adiabatic) flame temperature, which in turn is affected primarily by heat loss as well as aerodynamic stretch in the presence of mixture nonequidiffusion [73]. In fact, both of these nonideal processes can be considered from the unified viewpoint of loss (or gain) of the mixture's total enthalpy as the mixture traverses the diffusive-convective zone of the flame ahead of the active reaction zone [145]. Consequently, substantial and systematic errors can result if these leading-order effects are overlooked, as demonstrated by the wide data scatter in Fig. 1.

At present, the determination of laminar flame speeds is moderately accurate in that the leading-order effects are mostly recognized and accounted for in data gathering and processing. Second-order effects, however, can still be substantial and are also harder to recognize and correct. Experimental efforts have mostly employed four flame configurations, namely the 1D burner-stabilized flame, the counterflow flame, the expanding spherical flame, and the Bunsen flame. The principles and intricacies of these methods are briefly discussed in the following.

A1. The 1D burner-stabilized flame

Botha and Spalding [146] first proposed this method, in which a flat flame is stabilized over a water-cooled flat porous plug through heat loss to the surface. The flame speed, which is just the flow rate through the porous plug, is determined as a function of the heat loss rate. Linear extrapolation of the measured flame speed to zero heat loss rate then yields the (adiabatic) flame speed. This method is limited by the potential surface deactivation of the back-diffusing radical species at the burner surface, the nonadiabatic and divergent downstream flow, and the tendency of the flame to become wrinkled for high flow rates especially for near-adiabatic conditions. To circumvent the difficulty to obtain a near-adiabatic flame, Bosschaart and de Goeij [147] heated the upstream flow by an amount equal to the heat loss to the burner surface, thereby creating an adiabatic flame.

Eng et al. [148] proposed a completely different concept in 1D flame stabilization by using a cylindrical (which can also be spherical) burner through which the combustible mixture is issued. By continuously increasing the flow rate the flame recedes from the burner surface until eventually it is stabilized by flow divergence instead of heat loss to the burner surface, and as such can absorb further increase in the flow velocity by moving to a large radial location. The burner surface then ceases to affect the flame speed, which can be readily determined by noting the flame radius and hence the local flow velocity. Furthermore, being 1D and steady, the flame is not subjected to flame stretch effects [73]. The primary limitation of this method is the need for radial symmetry, and hence can only be conducted in microgravity, as was done in [148].

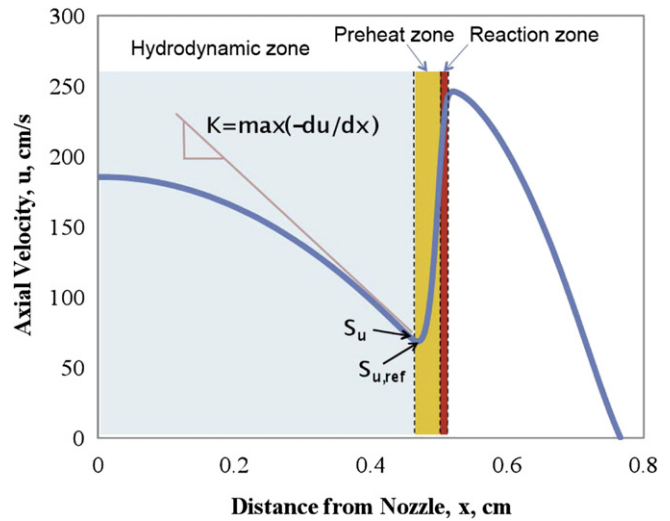


Fig. A1. Theoretical axial velocity profile along the system centerline of the counterflow. The stretch rate, K , is determined from the velocity gradient on the upstream side of the preheat zone. The reference upstream flame speed, $S_{u,\text{ref}}$, is determined from the minimum speed upstream of the reaction zone.

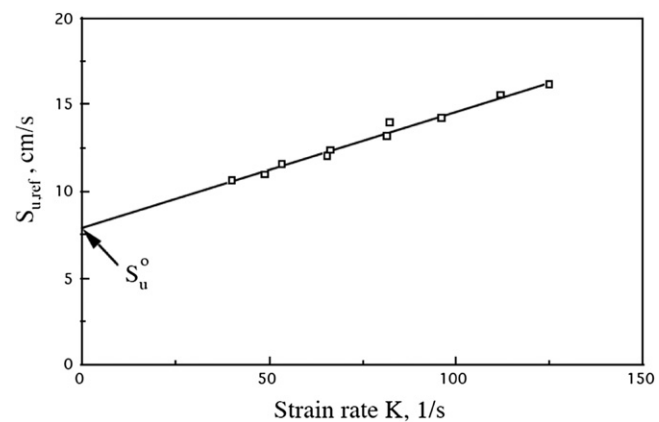


Fig. A2. Demonstration of the concept of linear extrapolation of the reference, stretched flame speed data to zero strain rate to yield the unstrained laminar flame speed (for a $\text{Le} < 1$ mixture).

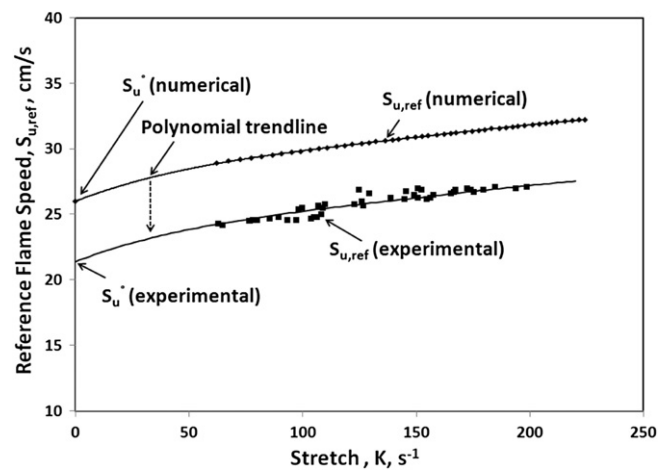


Fig. A3. Representative non-linear behavior of the reference upstream flame speed as a function of stretch rate. Reference experimental flame speeds, $S_{u,\text{ref}}$ are extrapolated to zero stretch rate using a polynomial trendline. The reference speed at zero stretch rate, S_u^0 , is the unstretched flame speed. The polynomial trendline is determined from numerical simulations using a starting reaction mechanism [5].

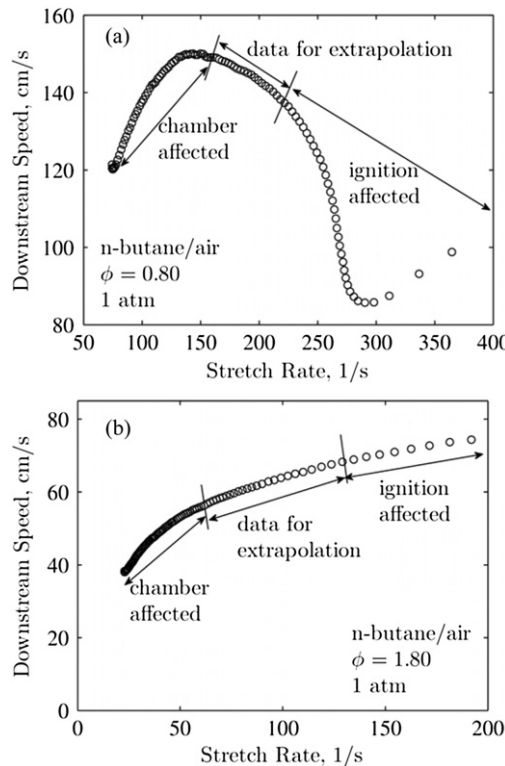


Fig. A4. Downstream stretched-flame speed as a function of stretch rate for a typical (a) lean and (b) rich n-butane outwardly propagating flame experiment. The experiment is influenced by ignition and wall confinement and care must be taken to determine data that are uninfluenced by these effects.

A2. The counterflow flame

Wu and Law [2] first recognized the leading-order effect of stretch on the determination of laminar flame speeds and, based on the theory of stretched flames [149,150], suggested that the laminar flame speed can be determined by linearly extrapolating the propagation speeds of stretched flames to zero stretch rate. For the symmetrical counterflow twin-flame configuration, for which the downstream heat loss is eliminated such that the flames can be considered to be adiabatic, a reference, stretched flame speed can be identified as the minimum velocity of the velocity profile upstream of the reaction zone (Fig. A1) and the velocity gradient ahead of the flame as the corresponding stretch rate. The flow velocity can be varied to produce a range of stretch rates and stretched flame speeds, which can then be extrapolated to zero stretch rate to determine the unstretched flame speed. Fig. A2 shows a representative extrapolation for a mixture with Lewis numbers smaller than unity.

Subsequently, Tien and Matalon [151] noted that thermal expansion across the flame leads to an apparent forward displacement of the stagnation surface based on potential flow consideration, and hence yields a correspondingly higher laminar flame speed. The effect is non-linear and is most significant at small strain rates. Consequently a linear extrapolation would yield a slightly higher, incorrect laminar flame speed. Chao et al. [152] and Vagelopoulos et al. [153] subsequently showed that the extent of the over-estimation increases with the ratio of the flame thickness to the nozzle separation distance, and as such can be reduced for sufficiently large separation distances. For usual hydrocarbon fuels and a nozzle diameter of say 1 cm, a separation

distance of about 2 cm appears to be adequate to reduce the error below other uncertainties in the experiment such as those in the LDV determination of the velocity.

Recently Wang et al. [5] proposed an approach to account for the non-linearity in the extrapolation. The method involves first numerically calculating the reference velocity as a function of the local strain rate down to very small strain rates, using a given, starting reaction mechanism. The non-linear trend for the small strain rate so identified is then used to extrapolate the experimental data to zero strain rate to yield the laminar flame speed (Fig. A3). The primary assumption of this method is that the starting mechanism should be close to the correct one, which is frequently the case.

A3. The expanding spherical flame

A widely used configuration in the determination of laminar flame speeds is the expanding spherical flame, initiated by a spark discharge in a combustible mixture [73]. The mixture can be either confined by an expandable barrier such as a soap bubble, or even a plastic bag, or a rigid chamber. When the flame propagates in a rigid chamber, the pressure and thereby the chamber temperature continuously increase, hence imparting a continuously varying environment within which the flame propagates. Consequently either these changes have to be accounted for or only the early part of the flame propagation can be used before the environment is substantially changed.

If the expanding flame can be imaged, say through high-speed Schlieren photography, then the velocity of the flame front can be identified and used for extrapolation to the unstretched flame speed. However, optical windows cannot be installed for very high pressure experiments because they cannot withstand the severe pressure and temperature rise. Consequently the flame speed is indirectly determined by measuring the pressure rise within the chamber. This approach however is rarely adopted nowadays because, lacking direct imaging, the potential influence of the flame surface morphology such as spherical symmetry and the development of surface wrinkles due to flame front instability cannot be assessed.

A dual-chamber design has been advanced [154] in order to realize constant- and high-pressure flame propagation with imaging capability. In this design, an inner, working chamber is filled with the test mixture, and an outer chamber with a much larger volume is filled with an inert of the same density. The two chambers are connected by overlapping holes that are closed before the experiment and are opened at the instant of ignition. Consequently the expanding flame is automatically quenched as it reaches the boundary between the chambers before substantial pressure builds up. Using this apparatus laminar flame speeds at pressures as high as 60 atm have been acquired [64]. It is noted that, because of the potential pressure buildup, the maximum initial pressure experimented with single chamber designs is about 10 atm.

In view of the capability to provide high-pressure data, considerable investigation has been recently conducted on the expanding spherical flame, particularly on the accuracy in the extrapolation to eliminate stretch effects. Fig. A4a and b [4] respectively show the data of the (downstream) flame speed as a function of the instantaneous strain rate for lean and rich butane/air mixtures, whose Lewis numbers are respectively greater and smaller than unity. It was found that flame propagation is affected respectively by the ignition transient and wall effects during the early and latter parts of the lifetime, with the lean mixture exhibiting a particularly non-monotonic response because of the excess energy needed to initiate the strongly stretch-affected propagation

subsequent to ignition. These data clearly demonstrate the non-linear trend of the range of useable data, and as such the need for non-linear extrapolation.

Studies [155–158] have been performed to systematically assess these effects as well as any residual, nonideal chamber effects such as the cylindrical vs. spherical configuration as well as the weak pressure rise during propagation. In particular, [158] identified the regime of flame propagation over which the geometry effect is negligible, and derived the following high-order non-linear relation suitable for extrapolation:

$$s_u \left[1 + \frac{1}{R_f} + \frac{1}{R_f^2} + \frac{2}{3} \frac{1}{R_f^3} + o\left(\frac{1}{R_f^4}\right) \right] = 1$$

where s_u and R_f are the instantaneous scaled flame speed and radius respectively. The above equation has been found to be highly accurate in reproducing the numerically obtained solution, and is recommended for the extrapolation.

A4. The bunsen flame

The Bunsen flame is easy to set up and was extensively used in earlier investigations. The flame in the cylindrical configuration is subjected to stretch, whose effect must also be subtracted, as was done in [2]. Stretch, however, is absent in the 2D, slot configuration (apart from the base and tip regions) and holds the potential for further development as this is the only flame configuration that closely mimics the 1D freely propagating flame. Such slot flames, however, have been found to be quite susceptible to exhibit oscillations, ostensibly caused by some form of flow instability at the slot exit.

Another novel arrangement involving Bunsen flames is to impinge two identical Bunsen flames onto each other, in the manner of the counterflow, such that the negative strain experienced by the Bunsen flame is approximated canceled by the positive strain of the counterflow, yielding a stabilized flame segment that is largely stretch free [61].

A5. Concluding remarks

The state of the determination of laminar flame speeds mirrors that of combustion science in that, supported by advances in combustion theory, it is becoming more quantitatively reliable. The specific method adopted for measurement depends on the use of the data. If the use is only for a rough, order-of-magnitude estimation, then simple methods such as that of the Bunsen flame could suffice. In fact, since the laminar flame speed is largely controlled by the adiabatic flame temperature of the mixture, and since the high temperature chemistry of the hydrocarbons is similar anyway, a simple scaling referenced to some well-established results would probably be adequate.

Recent interest in the data on laminar flame speeds is however motivated by their use in the development and validation of reaction mechanisms. Consequently, the demand for fidelity and accuracy is much more stringent, requiring more elaborate apparatuses such as the counterflow and chambered expanding flames. Furthermore, the need for high-pressure data for the development of high-pressure kinetics, and for data on large, high-boiling-point liquid fuels for their practical relevance, further restrict the option in the methods. Specifically, the dual-chamber design appears to be the only viable apparatus for pressures above say 10 atm. For lower pressures the single chamber, counterflow burner, and flat flame burner can be used. Studies of high-boiling-point fuels require pre-vaporization and heating of the apparatus and/or the flow circuit to

prevent re-condensation. This is a challenging task as any unaccounted condensation could greatly affect the fuel concentration in the test mixture, leading to a shift in the concentration coordinate of the usual flame speed plots. This in turn could result in substantial error in reporting the laminar flame speed as it varies quite sensitively with the fuel equivalence ratio.

In summary, while approximate values of the laminar flame speeds can sometimes be acquired with moderate effort, the determination of high-precision data needed for kinetics studies requires a good understanding of the phenomena at hand and great care in the experimentation and the subsequent data analysis.

Appendix A. Supplementary material

Supplementary material associated with this article can be found, in the online version, at doi:10.1016/j.pecs.2012.03.004.

References

- [1] Gibbs GJ, Calcolte HF. Effect of molecular structure on burning velocity. *Journal of Chemical and Engineering Data* 1959;4:226.
- [2] Wu CK, Law CK. On the determination of laminar flame speeds from stretched flames. *Symposium (International) on Combustion* 1985;20: 1941–9.
- [3] Law CK. The 2011 Dryden Lecture: fuel options for next generation chemical propulsion. *AIAA Journal* 2011;50:1–18.
- [4] Kelley AP, Law CK. Nonlinear effects in the extraction of laminar flame speeds from expanding spherical flames. *Combustion and Flame* 2009;156: 1844–51.
- [5] Wang YL, Holley AT, Ji C, Egolfopoulos FN, Tsotsis TT, Curran HJ. Propagation and extinction of premixed dimethyl-ether/air flames. *Proceedings of the Combustion Institute* 2009;32:1035–42.
- [6] Davis SG, Law CK. Determination of and fuel structure effects on laminar flame speeds of C1 to C8 hydrocarbons. *Combustion Science and Technology* 1998;140:427–49.
- [7] Johnston RJ, Farrell JT. Laminar burning velocities and Markstein lengths of aromatics at elevated temperature and pressure. *Proceedings of the Combustion Institute* 2005;30:217–24.
- [8] Bosschaart KJ, De Goey LPH. The laminar burning velocity of flames propagating in mixtures of hydrocarbons and air measured with the heat flux method. *Combustion and Flame* 2004;136:261–9.
- [9] Blanquet G, Pepiot-Desjardins P, Pitsch H. Chemical mechanism for high temperature combustion of engine relevant fuels with emphasis on soot precursors. *Combustion and Flame* 2009;156:588–607.
- [10] Jerzembeck S, Peters N, Pepiot-Desjardins P, Pitsch H. Laminar burning velocities at high pressure for primary reference fuels and gasoline: experimental and numerical investigation. *Combustion and Flame* 2009;156: 292–301.
- [11] Smallbone AJ, Liu W, Law CK, You XQ, Wang H. Experimental and modeling study of laminar flame speed and non-premixed counterflowignition of n-heptane. *Proceedings of the Combustion Institute* 2009;32:1245–52.
- [12] Liu W, Kelley AP, Law CK. Flame propagation and counterflow nonpremixed ignition of mixtures of methane and ethylene. *Combustion and Flame* 2010; 157:1027–36.
- [13] Kelley AP, Liu W, Xin YX, Smallbone AJ, Law CK. Laminar flame speeds, nonpremixed stagnation ignition, and reduced mechanisms in the oxidation of iso-octane. *Proceedings of the Combustion Institute* 2011;33:501–8.
- [14] Kelley AP, Smallbone AJ, Zhu DL, Law CK. Laminar flame speeds of C5 to C8 n-alkanes at elevated pressures: experimental determination, fuel similarity, and stretch sensitivity. *Proceedings of the Combustion Institute* 2011;33: 963–70.
- [15] Konnon AA, Meuwissen RJ, De Goey LPH. The temperature dependence of the laminar burning velocity of ethanol flames. *Proceedings of the Combustion Institute* 2011;33:1011–9.
- [16] Liu W, Kelley AP, Law CK. Non-premixed ignition, laminar flame propagation and mechanism reduction of n-butanol, iso-butanol and methyl butanoate. *Proceedings of the Combustion Institute* 2011;33:995–1002.
- [17] Veloo PS, Wang YL, Egolfopoulos FN, Westbrook CK. A comparative experimental and computational study of methanol, ethanol, and n-butanol flames. *Combustion and Flame* 2010;157:1989–2004.
- [18] Law CK. A compilation of experimental data on laminar burning velocities. In: Peters N, Rogg B, editors. *Reduced kinetic mechanisms for application in combustion*. Springer-Verlag; 1993. p. 15–26.
- [19] Pitz WJ, Mueller CJ. Recent progress in the development of diesel surrogate fuels. *Progress in Energy and Combustion Science* 2011;37:330–50.
- [20] Battin-Leclerc F. Detailed chemical kinetic models for the low-temperature combustion of hydrocarbons with application to gasoline and diesel fuel surrogates. *Progress in Energy and Combustion Science* 2008;34:440–98.

- [21] Simmie JM. Detailed chemical kinetic models for the combustion of hydrocarbon fuels. *Progress in Energy and Combustion Science* 2003;29:599–634.
- [22] Harper MR, Van Geem KM, Pyl SP, Marin GB, Green WH. Comprehensive reaction mechanism for n-butanol pyrolysis and combustion. *Combustion and Flame* 2011;158:16–41.
- [23] Tian Z, Pitz WJ, Fournet R, Glaude PA, Battin-Leclerc F. A detailed kinetic modeling study of toluene oxidation in a premixed laminar flame. *Proceedings of the Combustion Institute* 2011;33:233–41.
- [24] Herbinet O, Pitz WJ, Westbrook CK. Detailed chemical kinetic mechanism for the oxidation of biodiesel fuels blend surrogate. *Combustion and Flame* 2010;157:893–908.
- [25] Mzé-Ahmed A, Hadj-Ali K, Diévert P, Dagaut P. Kinetics of oxidation of a synthetic jet fuel in a jet-stirred reactor: experimental and modeling study. *Energy and Fuels* 2010;24:4904–11.
- [26] Narayanaswamy K, Blanquart G, Pitsch H. A consistent chemical mechanism for oxidation of substituted aromatic species. *Combustion and Flame* 2010;157:1879–98.
- [27] Honnet S, Seshadri K, Niemann U, Peters N. A surrogate fuel for kerosene. *Proceedings of the Combustion Institute* 2009;32:485–92.
- [28] Westbrook CK, Pitz WJ, Herbinet O, Curran HJ, Silke EJ. A comprehensive detailed chemical kinetic reaction mechanism for combustion of n-alkane hydrocarbons from n-octane to n-hexadecane. *Combustion and Flame* 2009;156:181–99.
- [29] Dooley S, Curran HJ, Simmie JM. Autoignition measurements and a validated kinetic model for the biodiesel surrogate, methyl butanoate. *Combustion and Flame* 2008;153:2–32.
- [30] Rasmussen CL, Rasmussen AE, Glarborg P. Sensitizing effects of NO_x on CH₄ oxidation at high pressure. *Combustion and Flame* 2008;154:529–45.
- [31] Chaos M, Kazakov A, Zhao Z, Dryer FL. A high-temperature chemical kinetic model for primary reference fuels. *International Journal of Chemical Kinetics* 2007;39:399–414.
- [32] Coppens FHV, De Ruyck J, Konnov AA. The effects of composition on the burning velocity and nitric oxide formation in laminar premixed flames of CH₄+H₂+O₂+N₂. *Combustion and Flame* 2007;149:409–17.
- [33] Muhamar Y, Warnatz J. Kinetic modelling of the oxidation of large aliphatic hydrocarbons using an automatic mechanism generation. *Physical Chemistry Chemical Physics* 2007;9:4218–29.
- [34] Saxena P, Williams FA. Numerical and experimental studies of ethanol flames. *Proceedings of the Combustion Institute* 2007;31:1149–56.
- [35] Wang H, You X, Joshi AV, Davis SG, Laskin A, Egolfopoulos FN, et al. USC mech version II. High-temperature combustion reaction model of H₂/CO/C₁–C₄ compounds. http://ignis.usc.edu/USC_Mech_II.htm; 2007.
- [36] Lindstedt RP, Rizos KA. The formation and oxidation of aromatics in cyclopentene and methyl-cyclopentadiene mixtures. *Proceedings of the Combustion Institute* 2002;29:2291–8.
- [37] Richter H, Howard JB. Formation and consumption of single-ring aromatic hydrocarbons and their precursors in premixed acetylene, ethylene and benzene flames. *Physical Chemistry Chemical Physics* 2002;4:2038–55.
- [38] Alzueta MU, Glarborg P, Dam-Johansen K. Experimental and kinetic modeling study of the oxidation of benzene. *International Journal of Chemical Kinetics* 2000;32:498–522.
- [39] Smith GP, Golden DM, Frenklach M, Moriarty NW, Eiteneer B, Goldenberg M, et al. GRI-Mech 3.0. http://www.me.berkeley.edu/gri_mech/.
- [40] Wang H, Dames E, Sirjean B, Sheen DA, Tangko R, Violi A, et al. A high-temperature chemical kinetic model of n-alkane (up to n-dodecane), cyclohexane, and methyl-, ethyl-, n-propyl and n-butyl-cyclohexane oxidation at high temperatures. JetSurF version 2.0, <http://melchior.usc.edu/JetSurF/JetSurF.2.0>; September 19, 2010.
- [41] Ranzi E, Sogaro A, Gaffuri P, Pennati G, Westbrook CK, Pitz WJ. A new comprehensive reaction mechanism for combustion of hydrocarbon fuels. *Combustion and Flame* 1994;99:201–11.
- [42] Ranzi E, Dente M, Goldaniga A, Bozzano G, Faravelli T. Lumping procedures in detailed kinetic modeling of gasification, pyrolysis, partial oxidation and combustion of hydrocarbon mixtures. *Progress in Energy and Combustion Science* 2001;27:99–139.
- [43] Grana R, Frassoldati A, Faravelli T, Niemann U, Ranzi E, Seiser R, et al. An experimental and kinetic modeling study of combustion of isomers of butanol. *Combustion and Flame* 2010;157:2137–54.
- [44] Ranzi E. A wide range kinetic modeling study of oxidation and combustion of transportation fuels and surrogate mixtures. *Energy and Fuels* 2006;20:1024–32.
- [45] Kee RJ, Rupley F, Miller JA. Chemkin II: a Fortran chemical kinetics package for the analysis of gas-phase chemical kinetics. Sandia report SAND89-8009. Sandia National Laboratories; 1989.
- [46] Goos E, Burcat A, Rusic B. Third millennium thermodynamic database for combustion and air pollution use, <http://garfield.chem.elte.hu/Burcat/BURCAT.THR>; 2009.
- [47] Benson SW. Thermochemical kinetics. 2nd ed. New York: Wiley; 1976.
- [48] Smooke MD, Rabitz H, Reuven Y, Dryer FL. Application of sensitivity analysis to premixed hydrogen-air flames. *Combustion Science and Technology* 1983;59:295–319.
- [49] Kee RJ, Grcar JF, Smooke MD, Miller JA. Premix: a Fortran program for modeling steady laminar one-dimensional premixed flames. Sandia report SAND85-8240. Sandia National Laboratories; 1985.
- [50] Cuoci A, Frassoldati A, Faravelli T, Ranzi E. Open SMOKE: numerical modeling of reacting systems with detailed kinetic mechanisms. XXXIV meeting of the Italian Section of the Combustion Institute; 2011. doi:10.4405/34proci2011.II23. Rome (Italy).
- [51] Manca D, Buzzi Ferraris G, Faravelli T, Ranzi E. Numerical modeling of oxidation and combustion processes. *Combustion Theory and Modeling* 2001;5:185–99.
- [52] Buzzi-Ferraris G. Scientific C++: building numerical libraries the object-oriented way. Addison-Wesley; 1993.
- [53] Buzzi-Ferraris G, Manca D. BzzOde: a new C++ class for the solution of stiff and non-stiff ordinary differential equation systems. *Computers and Chemical Engineering* 1998;22:1595–621.
- [54] Buzzi-Ferraris G. BzzMath 6.0 numerical libraries. Available: <http://homes.chem.polimi.it/gbzui/index.htm>; 2010.
- [55] Burke MP, Chaos M, Dryer FL, Ju Y. Negative pressure dependence of mass burning rates of H₂/CO/O₂/diluent flames at low flame temperatures. *Combustion and Flame* 2010;157:618–31.
- [56] Das AK, Kumar K, Sung CJ. Laminar flame speeds of moist syngas mixtures. *Combustion and Flame* 2011;158:345–53.
- [57] Hermanns RTE, Konnov AA, Bastiaans RJM, de Goey LPH. Laminar burning velocities of diluted hydrogen-oxygen-nitrogen mixtures. *Energy and Fuels* 2007;21:1977–81.
- [58] Frassoldati A, Faravelli T, Ranzi E. The ignition, combustion and flame structure of carbon monoxide/hydrogen mixtures. Note 1: detailed kinetic modeling of syngas combustion also in presence of nitrogen compounds. *International Journal of Hydrogen Energy* 2007;32:3471–85.
- [59] Egolfopoulos FN, Zhu DL, Law CK. Experimental and numerical determination of laminar flame speeds: mixtures of C₂-hydrocarbons with oxygen and nitrogen. *Symposium (International) on Combustion* 1990;23:471–8.
- [60] Hassan MI, Aung KT, Kwon OC, Faeth GM. Properties of laminar premixed hydrocarbon-air flames at various pressures. *Journal of Propulsion and Power* 1998;14:479–88.
- [61] Vagelopoulos CM, Egolfopoulos FN. Direct experimental determination of laminar flame speeds. *Symposium (International) on Combustion* 1998;27:513–9.
- [62] Gu XJ, Haq MZ, Lawes M, Woolley R. Laminar burning velocity and Markstein lengths of methane-air mixtures. *Combustion and Flame* 2000;121:41–58.
- [63] Hirasawa T, Sung CJ, Joshi A, Yang Z, Wang H, Law CK. Determination of laminar flame speeds using digital particle image velocimetry: binary fuel blends of ethylene, n-butane, and toluene. *Proceedings of the Combustion Institute* 2002;29:1427–33.
- [64] Rozenhan G, Zhu DL, Law CK, Tse SD. Outward propagation, burning velocities, and chemical effects of methane flames up to 60 atm. *Proceedings of the Combustion Institute* 2002;29:1461–9.
- [65] Jomaas G, Zheng XL, Zhu DL, Law CK. Experimental determination of counterflow ignition temperatures and laminar flame speeds of C₂–C₃ hydrocarbons at atmospheric and elevated pressures. *Proceedings of the Combustion Institute* 2005;30:193–200.
- [66] Halter F, Tahtouh T, Mounaim-Rousselle C. Nonlinear effects of stretch on the flame front propagation. *Combustion and Flame* 2010;157:1825–32.
- [67] Park O, Veloo PS, Liu N, Egolfopoulos FN. Combustion characteristics of alternative gaseous fuels. *Proceedings of the Combustion Institute* 2011;33:887–94.
- [68] Veloo PS, Egolfopoulos FN. Studies of n-propanol, iso-propanol, and propane flames. *Combustion and Flame* 2011;158:501–10.
- [69] Babushok VI, Tsang W. Kinetic modeling of heptane combustion and PAH formation. *Journal of Propulsion and Power* 2004;20:403–14.
- [70] Westbrook CK. Chemical kinetics of hydrocarbon ignition in practical combustion systems. *Proceedings of the Combustion Institute* 2000;28:1563–77.
- [71] Burcat A, Scheller K, Lifshitz A. Shock-tube investigation of comparative ignition delay times for C₁–C₅ alkanes. *Combustion and Flame* 1971;16:29–33.
- [72] Warnatz J. Chemistry of stationary and non stationary combustion. In: Herbert PDKH, Jager W, editors. *Modelling of chemical reaction systems*. Berlin: Springer-Verlag; 1981. p. 162–88.
- [73] Law CK. *Combustion physics*. New York: Cambridge University Press; 2006.
- [74] Westbrook CK, Dryer FL. Prediction of laminar flame properties of methanol-air mixtures. *Combustion and Flame* 1980;37:171–92.
- [75] Glassman I, Yetter RA. *Combustion*. Academic Press; 2008.
- [76] Ji C, Dames E, Wang YL, Wang H, Egolfopoulos FN. Propagation and extinction of premixed C₅–C₁₂ n-alkane flames. *Combustion and Flame* 2010;157:277–87.
- [77] Lowry W, De Vries J, Krejci M, Petersen E, Serinyel Z, Metcalfe W, et al. Laminar flame speed measurements and modeling of pure alkanes and alkane blends at elevated pressures. *Journal of Engineering for Gas Turbines and Power* 2011;133.
- [78] Marshall SP, Stone R, Heghes C, Davies TJ, Cracknell RF. High pressure laminar burning velocity measurements and modelling of methane and n-butane. *Combustion Theory and Modeling* 2010;14:519–40.
- [79] Kumar K, Mittal G, Sung CJ, Law CK. An experimental investigation of ethylene/O₂/diluent mixtures: laminar flame speeds with preheat and ignition delays at high pressures. *Combustion and Flame* 2008;153:343–54.
- [80] Davis SG, Law CK, Wang H. Propene pyrolysis and oxidation kinetics in a flow reactor and laminar flames. *Combustion and Flame* 1999;119:375–99.
- [81] Ranzi E, Faravelli T, Gaffuri P, Sogaro A, D'Anna A, Caijolo A. A wide-range modeling study of iso-octane oxidation. *Combustion and Flame* 1997;108:24–42.
- [82] Curran HJ, Gaffuri P, Pitz WJ, Westbrook CK. A comprehensive modeling study of iso-octane oxidation. *Combustion and Flame* 2002;129:253–80.

- [83] Kumar K, Freeh JE, Sung CJ, Huang Y. Laminar flame speeds of preheated iso-octane/O₂/N₂ and n-heptane/O₂/N₂ mixtures. *Journal of Propulsion and Power* 2007;23:428–36.
- [84] Huang Y, Sung CJ, Eng JA. Laminar flame speeds of primary reference fuels and reformer gas mixtures. *Combustion and Flame* 2004;139:239–51.
- [85] Ji C, Dames E, Wang YL, Sirjean B, Wang H, Egolfopoulos FN. An experimental and modeling study of the propagation of cyclohexane and mono-alkylated cyclohexane flames. *Proceedings of the Combustion Institute* 2011;33:971–8.
- [86] Wang H, Dames E, Sirjean B, Sheen DA, Tangko R, Violi A, et al. JetSurF version 2.0: a high-temperature chemical kinetic model of n-alkane (up to n-dodecane), cyclohexane, and methyl-, ethyl-, n-propyl and n-butyl-cyclohexane oxidation at high temperatures. <http://melchior.usc.edu/JetSurF/JetSurF2.0/>; 2010.
- [87] Wu F, Kelley AP, Law CK. Laminar flame speeds of cyclohexane and mono-alkylated cyclohexanes at elevated pressures. *Combustion and Flame* 2012;159(4):1417–25.
- [88] Dubois T, Chaumeix N, Paillard CE. Experimental and modeling study of n-propylcyclohexane oxidation under engine-relevant conditions. *Energy and Fuels* 2009;23:2453–66.
- [89] Kumar K, Sung CJ. Laminar flame speeds and extinction limits of preheated n-decane/O₂/N₂ and n-dodecane/O₂/N₂ mixtures. *Combustion and Flame* 2007;151:209–24.
- [90] Singh D, Nishiie T, Qiao L. Experimental and kinetic modeling study of the combustion of n-decane, Jet-A, and S-8 in laminar premixed flames. *Combustion Science and Technology* 2011;183:1002–26.
- [91] Zhao Z, Juan LI, Kazakov A, Dryer FL, Zeppieri SP. Burning velocities and a high-temperature skeletal kinetic model for n-decane. *Combustion Science and Technology* 2005;177:89–106.
- [92] Ranzi E, Frassoldati A, Granata S, Faravelli T. Wide-range kinetic modeling study of the pyrolysis, partial oxidation, and combustion of heavy n-alkanes. *Industrial and Engineering Chemistry Research* 2005;44:5170–83.
- [93] Brezinsky K. The high-temperature oxidation of aromatic-hydrocarbons. *Progress in Energy and Combustion Science* 1986;12:1–24.
- [94] Granata S, Cambianica F, Zinesi S, Faravelli T, Ranzi E. Detailed kinetics of PAH and soot formation in combustion processes: analogies and similarities in reaction classes. *European Combustion Meeting* 2005;35:1–6. Paper.
- [95] Farrell JT, Johnston RJ, Androulakis IP. Molecular structure effects on laminar burning velocities at elevated temperature and pressure. SAE paper # 2004-01-2936; 2004.
- [96] Da Silva G, Bozzelli JW. Indene formation from alkylated aromatics: kinetics and products of the fulvenallene + acetylene reaction. *Journal of Physical Chemistry A* 2009;113:8971–8.
- [97] Seshadri K, Frassoldati A, Cuoci A, Faravelli T, Niemann U, Weydert P, et al. Experimental and kinetic modeling study of combustion of JP-8, its surrogates and components in laminar premixed flows. *Combustion Theory and Modeling* 2011;15:569–83.
- [98] Emdee JL, Brezinsky K, Glassman I. High-temperature oxidation mechanisms of m- and p-xylene. *Journal of Physical Chemistry* 1991;95:1626–35.
- [99] Roubaud A, Minetti R, Sochet LR. Oxidation and combustion of low alkylbenzenes at high pressure: comparative reactivity and auto-ignition. *Combustion and Flame* 2000;121:535–41.
- [100] Da Silva G, Bozzelli JW. On the reactivity of methylbenzenes. *Combustion and Flame* 2010;157:2175–83.
- [101] Battin-Leclerc F, Bounacour R, Belmekki N, Glaude PA. Experimental and modeling study of the oxidation of xylenes. *International Journal of Chemical Kinetics* 2006;38:284–302.
- [102] Gail S, Dagaout P, Black G, Simmie JM. Kinetics of 1,2-dimethylbenzene oxidation and ignition: experimental and detailed chemical kinetic modeling. *Combustion Science and Technology* 2008;180:1748–71.
- [103] Frassoldati A, Cuoci A, Faravelli T, Niemann U, Ranzi E, Seiser R, et al. An experimental and kinetic modeling study of n-propanol and iso-propanol combustion. *Combustion and Flame* 2010;157:2–16.
- [104] Frassoldati A, Cuoci A, Faravelli T, Ranzi E. Kinetic modeling of the oxidation of ethanol and gasoline surrogate mixtures. *Combustion Science and Technology* 2010;182:653–67.
- [105] Veloo PS, Egolfopoulos FN, Westbrook CK. Studies of n-propanol/air and iso-propanol/air premixed flames. Fall meeting of WSS/CI - paper # 09F-44; 2009.
- [106] Veloo PS, Egolfopoulos FN. Flame propagation of butanol isomers/air mixtures. *Proceedings of the Combustion Institute* 2011;33:987–93.
- [107] Lefkowitz JK, Heyne JS, Hee Won S, Dooley S, Kim HH, Haas FM, et al. A chemical kinetic study of tertiary-butanol in a flow reactor and a counterflow diffusion flame. *Combustion and Flame*; 2011 [Available online 28 October 2011].
- [108] Stranic I, Chase DP, Harmon JT, Yang S, Davidson DF, Hanson RK. Shock tube measurements of ignition delay times for the butanol isomers. *Combustion and Flame* 2012;159(2):516–27.
- [109] Frassoldati A, Grana R, Faravelli T, Ranzi E, Oßwald P, Kohse-Höinghaus K. Detailed kinetic modeling of the combustion of the four butanol isomers in premixed low-pressure flames, submitted to *Combustion and Flame* 2011.
- [110] Liao SY, Jiang DM, Huang ZH, Zeng K, Cheng Q. Determination of the laminar burning velocities for mixtures of ethanol and air at elevated temperatures. *Applied Thermal Engineering* 2007;27:374–80.
- [111] Gu X, Huang Z, Li Q, Tang C. Measurements of laminar burning velocities and markstein lengths of n-butanol-air premixed mixtures at elevated temperatures and pressures. *Energy and Fuels* 2009;23:4900–7.
- [112] Gu X, Huang Z, Wu S, Li Q. Laminar burning velocities and flame instabilities of butanol isomers-air mixtures. *Combustion and Flame* 2010;157:2318–25.
- [113] Togbé C, Halter F, Foucher F, Mounaim-Rousselle C, Dagaut P. Experimental and detailed kinetic modeling study of 1-pentanol oxidation in a JSR and combustion in a bomb. *Proceedings of the Combustion Institute*; 2011:367–74.
- [114] Burluka AA, Harker M, Osman H, Sheppard CGW, Konnov AA. Laminar burning velocities of three C₃H₆O isomers at atmospheric pressure. *Fuel* 2010;89:2864–72.
- [115] Pichon S, Black G, Chaumeix N, Yahyaoui M, Simmie JM, Curran HJ, et al. The combustion chemistry of a fuel tracer: measured flame speeds and ignition delays and a detailed chemical kinetic model for the oxidation of acetone. *Combustion and Flame* 2009;156:494–504.
- [116] Chong CT, Hochgreb S. Measurements of laminar flame speeds of acetone/methane/air mixtures. *Combustion and Flame* 2011;158:490–500.
- [117] Ranzi E, Faravelli T, Sogaro A, Gaffuri P, Pennati G. A wide range modeling study of propane and n-butane oxidation. *Combustion Science and Technology* 1994;100:299–320.
- [118] Qin X, Ju Y. Measurements of burning velocities of dimethyl ether and air premixed flames at elevated pressures. *Proceedings of the Combustion Institute* 2005;30:233–40.
- [119] Daly CA, Simmie JM, Würmel J, Djeballi N, Paillard C. Burning velocities of dimethyl ether and air. *Combustion and Flame* 2001;125:1329–40.
- [120] Zhao Z, Chaos M, Kazakov A, Dryer FL. Thermal decomposition reaction and a comprehensive kinetic model of dimethyl ether. *International Journal of Chemical Kinetics* 2008;40:1–18.
- [121] Yahyaoui M, Djeballi-Chaumeix N, Dagaout P, Paillard CE. Ethyl tertiary butyl ether ignition and combustion using a shock tube and spherical bomb. *Energy and Fuels* 2008;22:3701–8.
- [122] Goldaniga A, Faravelli T, Ranzi E, Dagaout P, Cathonet M. Oxidation of oxygenated octane improvers: MTBE, ETBE, DIPE, and TAME. *Symposium (International) on Combustion* 1998;27:353–60.
- [123] Chen Z, Wei L, Huang Z, Miao H, Wang X, Jiang D. Measurement of laminar burning velocities of dimethyl ether-air premixed mixtures with N₂ and CO₂ dilution. *Energy and Fuels* 2009;23:735–9.
- [124] De Vries J, Lowry WB, Serinyel Z, Curran HJ, Petersen EL. Laminar flame speed measurements of dimethyl ether in air at pressures up to 10 atm. *Fuel* 2011;90:331–8.
- [125] Gong J, Jin C, Huang Z, Wu X. Study on laminar burning characteristics of premixed high-octane fuel-air mixtures at elevated pressures and temperatures. *Energy and Fuels* 2010;24:965–72.
- [126] Di Y, Huang Z, Zhang N, Zheng B, Wu X, Zhang Z. Measurement of laminar burning velocities and markstein lengths for diethyl ether-air mixtures at different initial pressure and temperature. *Energy and Fuels* 2009;23:2490–7.
- [127] Dooley S, Burke MP, Chaos M, Stein Y, Dryer FL, Zhukov VP, et al. Methyl formate oxidation: speciation data, laminar burning velocities, ignition delay times, and validated chemical kinetic model. *International Journal of Chemical Kinetics* 2010;42:527–49.
- [128] Wang YL, Feng Q, Egolfopoulos FN, Tsotsis TT. Studies of C₄ and C₁₀ methyl ester flames. *Combustion and Flame* 2011;158:1507–19.
- [129] Wang W, Oehlschlaeger MA. A shock tube study of methyl decanoate autoignition at elevated pressures. *Combustion and Flame* 2012;159(2):476–81.
- [130] Chong CT, Hochgreb S. Measurements of laminar flame speeds of liquid fuels: jet-A1, diesel, palm methyl esters and blends using particle imaging velocimetry (PIV). *Proceedings of the Combustion Institute* 2011;33:979–86.
- [131] Wu FJ, Kelley AP, Tang CL, Zhu DL, Law CK. Measurements and correlation of laminar flame speeds of CO and C₂-hydrocarbons with hydrogen addition at atmospheric and elevated pressures. *International Journal of Hydrogen Energy* 2011;36:13171–80.
- [132] Tang CL, Huang Z, Law CK. Determination, correlation, and mechanistic interpretation of effects of hydrogen addition on laminar flame speeds of hydrocarbon-air mixtures. *Proceedings of the Combustion Institute* 2011;33:921–8.
- [133] Yu G, Law CK, Wu CK. Laminar flame speeds of hydrocarbon + air mixtures with hydrogen addition. *Combustion and Flame* 1986;63:339–47.
- [134] Dong Y, Vagelopoulos CM, Spedding GR, Egolfopoulos FN. Measurement of laminar flame speeds through digital particle image velocimetry: mixtures of methane and ethane with hydrogen, oxygen, nitrogen, and helium. *Proceedings of the Combustion Institute*; 2002:1419–26.
- [135] Hu E, Huang Z, He J, Jin C, Zheng J. Experimental and numerical study on laminar burning characteristics of premixed methane-hydrogen-air flames. *International Journal of Hydrogen Energy* 2009;34:4876–88.
- [136] Huang Z, Zhang Y, Zeng K, Liu B, Wang Q, Jiang D. Measurements of laminar burning velocities for natural gas-hydrogen-air mixtures. *Combustion and Flame* 2006;146:302–11.
- [137] Konnov AA, Riemeijer R, de Goey LPH. Adiabatic laminar burning velocities of CH₄ + H₂ + air flames at low pressures. *Fuel* 2010;89:1392–6.
- [138] Tahtouh T, Halter F, Samson E, Mounaim-Rousselle C. Effects of hydrogen addition and nitrogen dilution on the laminar flame characteristics of premixed methane-air flames. *International Journal of Hydrogen Energy* 2009;34(19):8329–38.

- [139] Tang C, He J, Huang Z, Jin C, Wang J, Wang X, et al. Measurements of laminar burning velocities and Markstein lengths of propane-hydrogen-air mixtures at elevated pressures and temperatures. *International Journal of Hydrogen Energy* 2008;33:7274–85.
- [140] Bradley D, Hicks RA, Lawes M, Sheppard CGW, Woolley R. The measurement of laminar burning velocities and Markstein numbers for iso-octane-air and iso-octane-n-heptane-air mixtures at elevated temperatures and pressures in an explosion bomb. *Combustion and Flame* 1998;115:126–44.
- [141] Holley AT, Dong Y, Andac MG, Egolfopoulos FN. Extinction of premixed flames of practical liquid fuels: experiments and simulations. *Combustion and Flame* 2006;144:448–60.
- [142] Van Lipzig JPJ, Nilsson EJK, De Goey LPH, Konnov AA. Laminar burning velocities of n-heptane, iso-octane, ethanol and their binary and tertiary mixtures. *Fuel* 2011;90:2773–81.
- [143] Ji C, Egolfopoulos FN. Flame propagation of mixtures of air with binary liquid fuel mixtures. *Proceedings of the Combustion Institute*; 2011:955–61.
- [144] Zhu DL, Egolfopoulos FN, Law CK. Experimental and numerical determination of laminar flame speeds of methane/(Ar, N₂, CO₂)-air mixtures as function of stoichiometry, pressure, and flame temperature. *Symposium (International) on Combustion* 1989;22:1537–45.
- [145] Law CK. Combustion at a crossroads: status and prospects. *Proceedings of the Combustion Institute* 2007;31:1–29.
- [146] Botha JP, Spalding DB. The laminar flame speed of propane-air mixtures with heat extraction from the flame. *Proceedings of the Royal Society of London A* 1954;225:71–96.
- [147] Bosschaart KJ, De Goey LPH. Detailed analysis of the heat flux method for measuring burning velocities. *Combustion and Flame* 2003;132(1–2):170–80.
- [148] Eng JA, Law CK, Zhu DL. On burner-stabilized cylindrical premixed flames in microgravity. *Proceedings of Combustion Institute* 1994;25:1711–8.
- [149] Clavin P, Williams FA. Effects of molecular diffusion and of thermal-expansion on the structure and dynamics of premixed flames in turbulent flows of large-scale and low intensity. *Journal of Fluid Mechanics* 1982;116:251–82.
- [150] Matalon M, Matkowsky BJ. Flames as gas-dynamic discontinuity. *Journal of Fluid Mechanics* 1982;124:239–59.
- [151] Tien JH, Matalon M. On the burning velocity of stretched flames. *Combustion and Flame* 1991;84:238–48.
- [152] Chao BH, Egolfopoulos FN, Law CK. Structure and propagation of premixed flame in nozzle-generated counterflow. *Combustion and Flame* 1997;109:620–38.
- [153] Vagelopoulos CM, Egolfopoulos FN, Law CK. Further considerations on the determination of laminar flame speeds with the counterflow twin-flame technique. *Symposium (International) on Combustion* 1994;25:1341–7.
- [154] Tse SD, Zhu DL, Law CK. An optically accessible high-pressure combustion apparatus. *Review of Scientific Instruments* 2004;75:233–9.
- [155] Burke MP, Chen Z, Ju Y, Dryer FL. Effect of cylindrical confinement on the determination of laminar flame speeds using outwardly propagating flames. *Combustion and Flame* 2009;156:771–9.
- [156] Chen Z, Burke MP, Ju Y. Effects of compression and stretch on the determination of laminar flame speeds using propagating spherical flames. *Combustion Theory and Modeling* 2009;13:343–64.
- [157] Chen Z. On the extraction of laminar flame speed and Markstein length from outwardly propagating spherical flames. *Combustion and Flame* 2011;158:291–300.
- [158] Kelley AP, Bechtold JK, Law CK. Premixed flame propagation in a confining vessel with weak pressure rise. *Journal of Fluid Mechanics* 2012;691:26–51.
- [159] Ji C, Dames E, Wang H, Egolfopoulos FN. Propagation and extinction of benzene and alkylated benzene flames. Submitted to *Combustion and Flame* 2011.
- [160] Zhao Z, Kazakov A, Dryer FL. Measurements of dimethyl ether/air mixture burning velocities by using particle image velocimetry. *Combustion and Flame* 2004;139:52–60.
- [161] Wu F, Kelley AP, Zhu DL, Law CK. "Further Study on Effects of Hydrogen Addition on Laminar Flame Speeds of Fuel-Air Mixtures" presented at the 7th US National Combustion Meeting, Atlanta, GA., 2011.